TUDelft

Delft University of Technology

The impact of sewer condition on the performance of sewer systems

van Bijnen, Marco

The impact of sewer condition on the performance of sewer systems

NETWORK ON THE TABLE

Marco van Bijnen

Propositions

accompanying the PhD thesis

The impact of sewer condition on the performance of sewer systems

by

Johannes Adrianus Cornelis van Bijnen

1. Writing a PhD thesis in a foreign language is a risk in itself.

2. It is not the quality of the teachers but the use of their laptops and smartphones during lectures that prohibits the personal development of students.

3. Being on a slippery slope and learning through trial and error is a perfect manner to learn something, however, it is disturbing that nowadays there is no time left anymore to make errors.

4. Writing a PhD thesis next to a full-time job and a family can be compared to walking a tight rope while eating spaghetti and trying to enjoy the scenery.

5. Application of increasingly complicated models in urban drainage masks a lack of knowledge.

6. The method of 'hydraulic fingerprinting' as presented in this thesis provides more and better information for sewer asset management than e.g. CCTV inspection results.

7. The added value of model calibration in urban drainage is mainly found in the increase of the modeller's general mistrust in models.

8. The recent attention to 'fat in sewers' by the public media should apply the slogan 'clean out your own mess' as a general message to the users of the sewer system.

These propositions are regarded as opposable and defendable, and have been approved as such by the promotors prof. dr. ir. F.H.L.R. Clemens and dr. ir. J.G. Langeveld.

Stellingen

behorende bij het proefschrift

The impact of sewer condition on the performance of sewer systems

door

Johannes Adrianus Cornelis van Bijnen

1. Een proefschrift schrijven in een andere taal dan je moederstaal vormt een risico op zichzelf.

2. Niet de kwaliteit van de docenten, maar het gebruik van hun laptops en smartphones tijdens de les belemmert de persoonlijke ontwikkeling van leerlingen.

3. Je kunt je best op glad ijs begeven en met vallen en opstaan leren, maar de tijd om te vallen is er niet meer.

4. Een proefschrift schrijven naast een volledige baan en een gezin, kan worden vergeleken met het jongleren op een dunne draad terwijl je spaghetti eet en probeert te genieten van het landschap.

5. Het gebruik van geavanceerde rekenmodellen binnen gebruiksvriendelijke software maskeert een gebrek aan kennis.

6. De methode 'hydraulic fingerprinting' van een rioolstelsel, zoals gepresenteerd in dit proefschrift geeft meer en beter bruikbare informatie voor het beheer van rioolsystemen dan bijvoorbeeld CCTV-inspectie.

7. De meerwaarde van het toepassen van modelkalibratie in het geval van rioolsystemen is vooral gelegen in een toename van het wantrouwen van de modelleur in modellen in zijn algemeenheid.

8. De recente aandacht in de publieke media voor het probleem van 'vet in het riool', zou de slogan 'ruim je eigen rotzooi op' kunnen gebruiken als algemeen appel aan de gebruiker van het rioolsysteem.

Deze stellingen worden opponeerbaar en verdedigbaar geacht en zijn als zodanig goedgekeurd door de promotoren prof. dr. ir. F.H.L.R. Clemens en dr. ir. J.G. Langeveld.

THE IMPACT OF SEWER CONDITION ON THE PERFORMANCE OF SEWER SYSTEMS

Marco van Bijnen

THE IMPACT OF SEWER CONDITION ON THE PERFORMANCE OF SEWER SYSTEMS

Proefschrift

ter verkrijging van de graad van doctor
aan de Technische Universiteit Delft,
op gezag van de Rector Magnificus prof.dr.ir. T.H.J.J. van der Hagen,
voorzitter van het College van Promoties
in het openbaar te verdedigen
op vrijdag 22 juni 2018 om 12:30 uur

door

Johannes Adrianus Cornelis VAN BIJNEN

ingenieur in de weg- en waterbouwkunde, Hogeschool 's-Hertogenbosch
geboren te Drunen, Nederland.

Dit proefschrift is goedgekeurd door
          promotor: prof. dr. ir. F.H.L.R. Clemens
          promotor: dr. ir. J.G. Langeveld

Samenstelling promotiecommissie:
          Rector Magnificus   voorzitter
          Prof. dr. ir. F.H.L.R. Clemens   Technische Universiteit Delft, promotor
          Dr. ir. J.G. Langeveld   Technische Universiteit Delft, promotor

Onafhankelijke leden:
          Prof. dr. dipl-ing. D. Muschalla   Technische Universität Graz
          Prof. dr. S.J. Tait   University of Sheffield
          Prof. dr. J-L. Bertrand-Krajewski   INSA de Lyon
          Prof. dr. ir. M. Kok   Technische Universiteit Delft
          Prof. dr. dipl-ing. T. Ertl   Universität fur Bodenkultur Vienna
          Prof. dr. ir. J.B. van Lier   Technische Universiteit Delft, reservelid

An electronic version of this document is available free of charge in the Delft University Repository at http://repository.tudelft.nl/.

Now I've reached the age
I've tried to do all those things the best I can
No matter how I try
I find my way to the same old jam

Led Zeppelin, Good times bad times (1969)

Back to life, back to reality…

Soul II Soul, Back to life (1989)

Voorwoord

Sommige dingen in het leven duren langer dan gepland en dit promotieonderzoek is er daar één van. Het valt niet mee om gedurende lange tijd serieus onderzoek te doen naast een volledige baan. Ik begon mijn onderzoek tijdens mijn dienstverband bij de gemeente Utrecht. Sinds ik in januari 2015 startte als zelfstandig ondernemer werd het er niet makkelijker van om het te combineren met mijn werk en privéleven. Het vraagt niet alleen tijd en energie van jezelf, maar ook van andere personen die je na staan. Michelle, Kay en Lièn, dank voor het toestaan van deze egoïstische inbreuk op ons gezinsleven en jullie onvoorwaardelijke steun. Wim en Riet Leeferink, dank voor de relativerende gesprekken op de juiste momenten gedurende de afgelopen jaren. Deze hebben mij enorm geholpen en niet alleen om mijn onderzoek af te ronden. Bertha en Jan Heesters bedankt voor jullie bijdrage wanneer de situatie daarom vroeg.

Veel dank ben ik verschuldigd aan Hans Korving, Jeroen Langeveld en François Clemens. Jullie hebben mijn promotie mogelijk gemaakt en jullie bijdrage aan mijn onderzoek is enorm geweest. Hans zonder jouw input en geweldige kennis van statistiek was er nooit een proefschrift gekomen. Onze telefoongesprekken duurde vaak lang en we dwaalden van het ene onderwerp in het andere en aan het eind van elk gesprek waren we ook weer volledig op de hoogte van wat ons op dat moment bezig hield in het dagelijkse leven. Ik heb echt genoten van deze gesprekken en sta versteld van de wijze waarop jij praktijkproblemen kunt vertalen naar beschrijvende statistiek.

Jeroen jij hebt je roeping als modeontwerper gemist. Je hebt het vermogen om wetenschap te passen in een "rioolbeheerders jasje". Vraag en aanbod is geen match fixing, maar een kwaliteit. Je hebt de trein voor mij de afgelopen twee jaar zowel op de rails als op snelheid gehouden. Op de momenten dat het tegen zat en ik echt een boost nodig had, wist je altijd de juiste snaar te raken. Je bent een druk baasje, maar op die momenten nam je de tijd en hoe vaak ik ook de prioriteit niet bij de promotie maar bij mijn projecten legde, geen woord daarover en altijd lag er een uur later weer een concreet plan en dacht ik: ik ben er eigenlijk bijna.

François voor jou lijkt geen probleem te veel. Een van de meest lastige zaken in de afgelopen jaren vond ik persoonlijk het verwerken van opmerkingen van reviewers op onze artikelen. Met name opmerkingen die omlijst waren met persoonlijke meningen over de materie. Tot in de laatste week voordat ik dit boekje liet drukken liet je me weer zien hoe je de meest lastige vragen en opmerkingen aanpakt en weerlegt. Mijn complimenten voor de wijze waarop jij in staat bent om oplossingen te bedenken.

Naast een enorme inspanning en een focus op de juiste tijden, vraagt een promotieonderzoek ook ontspanning, een relativerende kijk en zeker ook een gezonde dosis slappe klets en onzin. Het antwoord daarop zijn Johan Post en Wouter van Riel. Naast jullie inhoudelijke hulp kijk ik met jullie terug op een bijzondere periode met een dosis gezonde humor en waarin ik naast de onderhoudstoestand van riolen ook mijn eigen onderhoudstoestand heb leren kennen. Ik vraag me nog steeds af hoeveel de kans, om volledig geïnfecteerd te raken met complete onzin, is toegenomen sinds mijn kennismaking met jullie. We hebben samen veel 'praktijkkennis' gedeeld. Jullie waren altijd bereikbaar en behulpzaam op welke tijdstippen dan ook. Dank voor jullie ondersteuning, lol en enthousiasme. Daarnaast wil ik alle collega's van de sectie Gezondheidstechniek, die ik tijdens mijn onderzoek in Delft heb leren kennen, bedanken voor de gezellige uren op de TU. Ik was niet elke week op de TU aanwezig, maar dat mocht de pret niet drukken op de dagen dat ik er wel was.

Zonder de financiële steun van de gemeente Utrecht en medewerking van oud collega's was dit allemaal niet mogelijk geweest. Ik wil de gemeente Utrecht bedanken voor deze financiële steun en iedereen binnen de gemeente Utrecht die mij, op welke manier dan ook, heeft geholpen tijdens mijn onderzoek. Een aantal van deze personen vragen speciale aandacht. Michiel Rijsdijk jij bent een inspirator voor je omgeving. Arjen Kruithof, ik vraag me nog steeds af wie jou het beste kent. Maar wie iets in een kluis wil bewaren moet het jou vertellen. Han van Ringelenstein, onbevooroordeeld als altijd en een voorbeeld voor iedereen die sociale vaardigheden wil leren. Nico Vos, samen met Han de Wikipedia van de Utrechtse "onderwereld". Erwin Rebergen, ik zou willen dat ik ook iets van het geduld zou bezitten dat jij bezit. En last but not least Arjan van der Steen. Voor jou zijn er geen geheimen in Matlab, kennis waar ik altijd gebruik van heb mogen maken. Dank aan jullie allen. Naast de gemeente Utrecht ben ik ook mijn dank verschuldigd aan het Kennisprogramma Urban Drainage voor de financiële bijdrage tijdens de laatste jaren.

Voorwoord

Een aantal personen hebben een bijzondere rol gespeeld in mijn onderzoek, omdat zij het min of meer praktisch mogelijk hebben gemaakt dat ik mijn onderzoek heb kunnen uitvoeren zoals ik dat heb gedaan. Arie de Niet bedankt voor het optuigen van het rekencluster aan pc's waarmee ik de vele simulaties in de Monte Carlo procedure kon doorrekenen. Daan Dwarswaard, voormalig medewerker van de gemeente Utrecht, bedankt voor het jarenlang verzamelen van gegevens met betrekking tot sediment in het rioolstelsel van Utrecht. Mijn complimenten aan Daniëlle Jansma voor het screenen van een groot deel van dit proefschrift op de Engelse taal. In mijn geval een niet te onderschatten klus. De les 'het gebruik van bijvoeglijke naamwoorden in het Engels' blijft me zeker bij. Bram Stegeman bedankt voor het mogen gebruiken van de gegevens die je in het veld hebt geïnventariseerd. Deze gegevens hebben een cruciale bijdrage geleverd aan de kwaliteit van het rioleringsmodel. Didrik Meijer, dank voor al je tijd en energie die je gestopt hebt in het testen van de grafentheorie op het rioleringsmodel van 'Tuindorp'. Petra van Daal-Rombouts, bij tijden zou ik willen dat je een soort van bibliotheek was. Dan kwam ik op gezette tijden wat van je 'discipline' lenen om mezelf wat meer aan de regels te kunnen houden. Je hulp bij de datavalidatie stel ik erg op prijs. Rémy Schilperoort, gezelligheid kent geen tijd. Vanaf het begin van mijn onderzoek hebben we elkaar op willekeurige momenten getroffen. Signor, voor mij was het elke keer een welkome afleiding. Kristian van der Lek, student aan de Hogeschool Utrecht, je enthousiasme en gretigheid heeft me een extra stimulans gegeven voor het verdedigen van mijn proefschrift. Jij bent een aanwinst voor het vak en een "outlier" in het onderbouwen van stelling 2 van dit proefschrift.

Als laatste wil ik ook nog mijn speciale dank uitbrengen aan Anton Reijnders om het kunstwerk 'Netwerk op tafel' van Netty van den Heuvel te mogen gebruiken op de omslag van mijn proefschrift. En niet te vergeten Rick Chaudron van de gemeente Leiden. Rick je geduld het afgelopen jaar, en de ruimte die je me daarmee op de juiste momenten hebt gegeven om aan mijn promotie te werken, stel ik erg op prijs.

Rest mij enkel nog mijn 'raadgever' te bedanken, die mij gedurende bijna elke minuut van de tijd die ik aan het schrijven van dit proefschrift heb besteed heeft bijgestaan: het boek 'Righting English that's gone Dutch'. Vertrouwen spreek je uit, maar deze keer volstaat het op papier.

Michelle, Kay en Lièn: we gaan back to life, back to reality!

Marco van Bijnen, mei 2018

Summary

Sewer systems are underground infrastructure networks, comprising pipes, manholes and ancillary works, that collect and transport rainfall runoff and sewage to wastewater treatment plants. These systems protect society from exposure to faecal contamination and flooding of urban areas due to heavy storm events to a predefined service level. Protection of the environment (surface water and groundwater) is a main prerequisite as well. Due to deterioration the performance of sewer systems may decrease over time. Consequently, it is important to maintain the defined service level over time. General activities to achieve this goal are sewer cleaning, sewer replacement and the prioritization of strategies. In the Netherlands, 1,5 billion euro is spent annually to maintain and operate sewer systems. Increasingly, risk-based sewer asset management is being advocated to balance the required budget and the provided service to society. A prerequisite for risk-based sewer asset management is to be able to relate the condition of the infrastructure with infrastructure performance and consequently, the provided service level.

The assessment of sewer performance is divided into three different parts: hydraulic, environmental and structural performance. The assessments consist of simulations, inspections and process monitoring. Sewer performance (including pluvial flooding and emissions) is generally assessed by hydrodynamic models, which assume the absence of in-sewer defects (e.g. root intrusion, surface damage, attached and settled deposits). Visual inspections (CCTV) are carried out to collect information on the internal condition of sewers. The operational condition of a sewer system's assets affects hydraulic performance of the sewer system and may cause increased pluvial flooding. In addition, visual inspections obtain information on sewer objects and it is generally not known how this affects hydraulic performance of the sewer system. Exposure to urban pluvial flooding may pose a health risk to humans, since the flooded sewage contains a variety of pathogens depending on its origin.

Nowadays, the maintenance activities to provide the required system performance are mainly based on the observed condition of individual assets and simulation results of calculations using as-built data. Assessing the actual sewer hydraulic performance for directing maintenance actions requires more information on the relation between the actual condition of an asset versus the influence it has on sewer network level. Therefore, the objective of this thesis is to develop methods to assess and quantify the effect of in-sewer defects on sewer performance. In order to meet this objective, the influence of sewer condition on hydraulic performance is studied and model calibration is applied to identify in-sewer defects affecting hydraulic performance. Furthermore, the impact of in-sewer defects on urban pluvial flooding and, subsequently, on infection probabilities for humans is addressed.

The impact of in-sewer defects on urban pluvial flooding on network level is studied in two research catchments in the Netherlands ('Tuindorp' and 'Loenen'). Impacts are assessed using Monte Carlo simulations with a full hydrodynamic model of the sewer system. The studied defects include root intrusion, surface damage, attached deposits and settled deposits and sedimentation. These defects are based on the results of field observations and are translated to two model parameters (roughness and sedimentation). The calculation results demonstrate that the return period of flooding, number of flooded locations and flooded volumes are substantially affected by in-sewer defects. The impact of in-sewer defects is larger in the flat 'Tuindorp' area with the looped sewer system than in the mildly-sloping 'Loenen' area with the partly-branched sewer system. This mainly results from the flatness of the catchment. In the partly-branched sewer system, especially for sedimentation, the variance of all flooding characteristics is larger than in the looped system.

The concept of 'hydraulic fingerprinting' based on model calibration is introduced to identify in-sewer defects which affect hydraulic performance. Model calibration enables detection of changes in hydraulic properties of the sewer system. Each model calibration results in a set of model parameter values, their uncertainties and residuals. The model parameter values also incorporate the antecedent condition of the catchment of the calibrated event and are therefore less suitable for the identification of in-sewer defects. The residuals on the other hand, and more specifically their absolute values, statistical properties and the correlation between residuals at different monitoring locations, are suitable as indicators of the occurrence of in-sewer defects. This allows the application of 'hydraulic fingerprinting' based on model calibration, where the 'fingerprint' is defined by the model parameters and the residuals. The concept of 'fingerprinting' is demonstrated for the combined sewer system 'Tuindorp'. The results show that 'hydraulic fingerprinting' can be a powerful tool for directing sewer asset management actions.

Summary

Sewer systems are networks consisting of many elements. Not all individual elements are equally important for the hydraulic performance of sewers systems. The importance of an element for the network depends on the characteristics of the element and its position in the network. In case of detecting changes in hydraulic properties of a sewer system by means of model calibration, the choice of the monitoring locations is important for the results of the calibration and, consequently, for prioritising sewer asset management actions. Therefore, it is necessary to identify the critical sewer pipes in a sewer network. Those pipes are important assets in the hydraulic performance of the sewer system and the monitoring locations can be chosen based on those critical elements. The Graph-theory is presented as a means to identify the most critical elements in a network with respect to the malfunctioning of the total system. As opposed to conventional methods, the proposed method does not rely on iterative hydraulic calculations, instead the structure of the network is taken as a starting point. In contrast to methods applied in practise, the results are independent of the selected storm events. As the method is not computationally demanding, the method allows the analysis of large networks that are now, for practical reasons, beyond the scope of methods applied so far.

Due to high levels of pathogens in floodwater, exposure to urban pluvial flooding may pose a health risk to humans. In-sewer defects may cause increased pluvial flooding, possibly enlarging health risks. The impact of in-sewer defects on urban pluvial flooding and, subsequently, on infection probabilities for humans has been addressed. The sewer systems 'Tuindorp' and 'Loenen' are studied. As such, this thesis provides necessary input for risk-informed sewer maintenance strategies in order to preserve the hydraulic performance of a sewer system. The catchment-wide average infection probability was calculated using Quantitative Microbial Risk Assessment (QMRA) and flooding frequencies from Monte Carlo simulations with a hydrodynamic model. For the studied catchments, it is concluded that the occurrence of flooding is significantly increased by sediment deposits and, consequently, the infection probability is enlarged as well. The impact of sediment deposits on infection probabilities depends on sewer systems characteristics. The results also demonstrate that flood duration may vary considerably over the catchment, possibly affecting infection probabilities.

The application of the proposed model calibration methodology shows very promising results when applied to the 'Tuindorp' sewer system. Given the background of the methodology, i.e. detecting changes in system behaviour based on changes in characteristics of residuals, it is expected that it will also be applicable to other systems. This is supported by results of earlier work on the calibration of hydrodynamic models. Therefore, it is recommended to apply this method in other sewer catchments as well. The Graph-theory method is applicable to determine the critical pipes in sewer networks. In addition, the monitoring locations can be chosen based on those critical elements.

Visual inspections are generally applied for assessing the condition of sewers. Currently, in the Netherlands, visual inspection of all sewers within a municipality is done repeatedly approximately every 10 years. The hydraulic condition of a sewer system changes over time in a much shorter period (6 months) in comparison with the structural condition (10 years). Therefore, to maintain the defined service of sewer systems regarding hydraulic performance, an inspection frequency of once every 2 years is recommended. To this end, other different, rapid and cost-effective inspection methods are available instead of CCTV, e.g. the manhole-zoom camera and the SewerBatt™ instrument.

In this thesis, a new method has been developed to identify in sewer defects by using advanced model calibration. In addition, it is demonstrated that currently, there is a big gap between theoretical system performance and system performance in reality due to the condition of the sewers. Consequently, the return period for urban flooding can decrease from 2 years to 1 year on average with as a negative side effect an increase in the infection probability. Improved sewer maintenance or more robust sewer design could be applied to circumvent this issue. The results show that risk-based sewer asset management should focus more on risks and performance rather than on cost savings.

Samenvatting

Rioolstelsels zijn ondergrondse infrastructurele netwerken, bestaande uit leidingen, putten en overige voorzieningen (o.a. gemalen en overstorten), voor het inzamelen en transporteren van afval- en hemelwater. Goed functionerende rioolstelsels vormen een essentiële voorwaarde voor een gezond leefklimaat in steden en dorpen. Rioolstelsels leveren ten eerste een bijdrage aan de volksgezondheid door het zorgen voor de afvoer van afvalwater, waardoor het contactrisico met pathogenen wordt beperkt. Ten tweede zorgen rioolstelsels voor 'droge voeten', door het verwerken van hemelwater, waarbij de oppervlaktewaterkwaliteit zo veel mogelijk wordt ontzien. Jaarlijks wordt in Nederland 1,5 miljard euro besteed aan het in standhouden en verbeteren van de riolering. Om dit geld goed te besteden, gaan steeds meer gemeenten aan de slag met 'risicogestuurd beheer'.

Om ervoor te zorgen dat rioolstelsels conform een gewenst serviceniveau blijven functioneren, is onderhoud noodzakelijk. Inzicht in de toestand en het functioneren van een rioolsysteem is daarbij noodzakelijk. Om de (onderhouds)toestand te bepalen is het gebruikelijk om rioolinspecties uit te voeren en op basis daarvan worden vervolgens gerichte acties genomen. Om inzicht te krijgen in het functioneren van rioolsystemen (wateroverlast en emissies) worden veelal hydraulische berekeningen uitgevoerd met rekenmodellen. Ook praktijkmetingen in de riolering, gericht op het in beeld brengen van de werking van rioolsystemen, worden de laatste jaren steeds vaker toegepast.

Bij het beoordelen van rioolstelsels op wateroverlast en vuilemissie door het uitvoeren van hydraulische berekeningen, wordt ervan uitgegaan dat er geen sediment en andere belemmeringen voor het hydraulisch functioneren aanwezig zijn (wortelingroei, oppervlakteschade, obstakels, aangehechte en bezonken afzettingen, et cetera). Het inspecteren van de riolen gebeurt over het algemeen met camera-inspecties. Deze visuele camera-inspecties geven informatie over de inwendige toestand van de riolen en inspectieputten. De toestand van deze afzonderlijke onderdelen van een rioolstelsel beïnvloedt de hydraulische prestaties van het rioolstelsel en een slechte toestand kan leiden tot meer wateroverlast. In de huidige praktijk is onvoldoende bekend wat de

toestand van afzonderlijke objecten betekent voor de hydraulische prestaties op systeemniveau van een rioolstelsel. Omdat er in water op straat vanuit een gemengd rioolstelsel ziekteverwekkende organismen aanwezig zijn, vormt blootstelling aan water dat op straat staat als gevolg van hevige neerslag een gezondheidsrisico voor mensen.

Voor het beoordelen van het hydraulisch functioneren van rioolstelsels en de daarbij passende onderhoudsmaatregelen, is meer informatie nodig over de relatie tussen de onderhoudstoestand van afzonderlijke objecten (buizen en putten) en de invloed op het hydraulisch functioneren van het rioolstelsel als geheel. Het doel van dit proefschrift is dan ook het ontwikkelen van methoden voor het beoordelen en kwantificeren van het effect van de onderhoudstoestand van een rioolstelsel op het hydraulisch functioneren op systeemniveau. Om dit doel te bereiken is de invloed van de aanwezigheid van verschillende defecten en sediment in het riool op de hydraulische prestaties van het systeem bestudeerd. Modelkalibratie is toegepast om afwijkingen van het hydraulisch functioneren te kunnen identificeren. Afsluitend is ingegaan op de gevolgen van de onderhoudstoestand op gezondheidsrisico's in stedelijk gebied.

De invloed van de aanwezigheid van defecten en sediment in het riool op stedelijke wateroverlast op netwerkniveau is onderzocht in twee onderzoeksgebieden: de wijk 'Tuindorp' in de gemeente Utrecht en de wijk 'Loenen' in de gemeente Apeldoorn. De invloed is bepaald met behulp van Monte Carlo simulaties met een volledig hydrodynamisch model van de rioolsystemen. De onderzochte defecten zijn: wortelingroei, oppervlakteschade, aangehechte en bezonken afzettingen en sedimentatie. De aanwezigheid van deze aspecten en sediment in de beide systemen is gebaseerd op de resultaten van veldobservaties. De resultaten van rioolinspecties en metingen van de dikte van sediment in rioolbuizen zijn beschreven met kansverdelingen en vervolgens vertaald naar twee modelparameters (wandruwheid en sedimentatie). Er zijn berekeningen uitgevoerd met 750 verschillende systeemtoestanden voor beide rioolsystemen afzonderlijk. De berekeningsresultaten tonen aan dat de herhalingstijd van water op straat, het aantal locaties waar water op straat optreedt en de hoeveelheden water op straat (volumes), aanzienlijk worden beïnvloed door de onderhoudstoestand. De invloed van de onderhoudstoestand op het hydraulisch functioneren is in het vlakke gebied 'Tuindorp' met het vermaasde rioolsysteem groter dan in het licht hellende 'Loenen' met het gedeeltelijk vertakte rioolsysteem. Dit komt voornamelijk door het vlakke maaiveldverloop in de wijk 'Tuindorp'. In het gedeeltelijke vertakte rioolsysteem in 'Loenen' is voor sedimentatie de variantie van alle in beschouwing genomen indicatoren groter in vergelijking met het vermaasde rioolsysteem in 'Tuindorp'.

Samenvatting

De methode van 'hydraulic fingerprinting' op basis van modelkalibratie is geïntroduceerd om de invloed van de operationele onderhoudstoestand van een rioolsysteem op het hydraulisch functioneren te beoordelen. Onder kalibratie wordt hier het proces verstaan waarbij een set van modelparameters wordt gegenereerd waarmee, op basis van een gevalideerd rioleringsmodel, de gevalideerde gemeten waterstanden ter plaatse van de meetlocaties zo goed als mogelijk worden gereproduceerd in het rekenmodel. Modelkalibratie maakt detectie van veranderingen in hydraulische eigenschappen van het rioolsysteem mogelijk. Elke modelkalibratie resulteert in een reeks modelparameterwaarden en residuen. De modelparameterwaarden omvatten ook de antecedente situatie van het rioleringsgebied van de gekalibreerde neerslaggebeurtenis en zijn daarom minder geschikt om afwijkingen in hydraulische eigenschappen te identificeren. Maar de residuen, en meer specifiek hun absolute waarden, statistische eigenschappen en de correlatie tussen residuen ter plaatse van verschillende meetlocaties, zijn geschikt als indicatoren voor het optreden van afwijkingen. Dit maakt de methode 'hydraulic fingerprinting' op basis van modelkalibratie geschikt voor toepassing in rioolsystemen, waarbij de 'fingerprint' wordt bepaald door de combinatie van modelparameters en de residuen. De methode is uitgevoerd voor het gemengde rioolstelsel in de wijk 'Tuindorp'. De resultaten tonen aan dat 'hydraulic fingerprinting' een krachtig hulpmiddel kan zijn voor het aansturen van onderhoudsactiviteiten.

Rioolstelsels zijn netwerken die uit veel objecten bestaan en waarin niet alle afzonderlijke objecten even belangrijk zijn voor de prestaties van het rioolstelsel op systeemniveau. Het belang van een individueel object voor het netwerk hangt af van de kenmerken van het element en de positie in het netwerk. De grafentheorie is gepresenteerd als een middel om de meest kritische rioolstrengen in een rioolsysteem te identificeren in relatie tot het hydraulisch functioneren van het rioolsysteem als geheel. In tegenstelling tot conventionele methoden, is de voorgestelde methode niet afhankelijk van (langdurige) iteratieve hydraulische berekeningen, maar wordt de structuur van het netwerk als uitgangspunt genomen. Daarnaast zijn de resultaten onafhankelijk van de gekozen neerslagbelasting op het systeem. Vanwege de beperkte rekentijd maakt de methode de analyse van omvangrijke netwerken mogelijk die tot op heden, om praktische redenen, buiten het bereik vallen van tot nu toe toegepaste methoden. Door toepassing van de grafentheorie kunnen de 30-40% meest kritische strengen van een rioolstelsel, in relatie tot het hydraulisch functioneren van het totale rioolstelsel, worden geïdentificeerd. De meetlocaties in het meetnet riolering kunnen op basis van deze methode worden gekozen, zodat het hydraulisch functioneren van het rioolstelsel kan worden bewaakt en noodzakelijke onderhoudsactiviteiten met behulp van de 'hydraulic fingerprint' methode kunnen worden bepaald.

Vanwege de aanwezigheid van ziekteverwekkende organismen in water op straat vanuit de gemengde riolering, vormt blootstelling aan dit water een gezondheidsrisico voor mensen. Een slechte onderhoudstoestand kan leiden tot meer water op straat, wat mogelijk de kans op infecties vergroot. In dit proefschrift is nader ingegaan op de gevolgen hiervan voor de kans op infectie in de wijken 'Tuindorp' en 'Loenen'. De gemiddelde gebiedsbrede infectiekans is berekend met behulp van Quantitative Microbial Risk Assessment (QMRA) en berekende frequenties van water op straat in de Monte Carlo simulaties. In beide wijken wordt op basis van de uitkomsten geconcludeerd dat, als gevolg van sedimentafzettingen zowel de frequentie van water op straat als het volume water op straat aanzienlijk worden vergroot. Als gevolg daarvan neemt de gemiddelde gebiedsbrede infectiekans in beide wijken ook toe. De invloed van sedimentafzetting op infectiekansen hangt ook weer af van de kenmerken van rioolstelsels. Het algemene beeld voor het vlakke 'Tuindorp' met het vermaasde rioolstelsel is dat de gemiddelde infectiekans van de wijk toeneemt als gevolg van sedimentatie, zowel voor volwassenen als voor kinderen. In vergelijking met een rioolsysteem zonder sedimentafzettingen is de mediaan van de kansverdeling van het rioolsysteem met sedimentafzettingen ongeveer 1,5 keer groter. Voor het licht hellende 'Loenen' met het vertakte rioolstelsel kan worden geconcludeerd dat de mediaan van de gemiddelde infectiekans ongeveer 4 keer groter is in het systeem met sedimentatie dan in het systeem zonder sedimentafzettingen. De resultaten laten ook zien dat de duur van water op straat aanzienlijk kan variëren over het stroomgebied, wat mogelijk de infectiekansen beïnvloedt.

De besluitvorming met betrekking tot het vervangen van riolen vindt in de huidige praktijk hoofzakelijk plaats op basis van uitgevoerde visuele camera-inspecties, leeftijd van de riolering en planningen van uit te voeren wegwerkzaamheden. Visuele inspecties van riolen worden dan ook periodiek gepland en uitgevoerd in wijken en buurten die met deze uitgangspunten gekozen zijn. Een bijkomend gevolg van de resultaten van de inspecties is een overzicht en planning van kleinschalige herstelwerkzaamheden in de geïnspecteerde riolen. Het is in Nederland gebruikelijk om de riolen binnen een gemeente ongeveer elke 10 jaar te reinigen en te inspecteren. De hydraulische conditie van een rioolstelsel kan in de loop van de tijd in een veel kortere periode (6 maanden) veranderen dan de structurele conditie (10 jaar). Om inzicht te krijgen in de operationele conditie van een rioolstelsel, wordt een inspectiefrequentie aanbevolen van eens per 2 jaar. Naast het uitvoeren van visuele camera-inspecties, zijn daarvoor ook snellere en meer kosteneffectieve inspectiemethoden beschikbaar zoals de manhole-zoom camera en de SewerBatt™.

Samenvatting

Dit onderzoek heeft zich gericht op het invullen van een noodzakelijke voorwaarde voor 'risicogestuurd beheer', namelijk inzicht in de relatie tussen de toestand van de infrastructuur en het functioneren van de infrastructuur. Er is een methode ontwikkeld om met behulp van modelkalibratie inzicht te krijgen in optredende defecten in de riolering. Het hydraulisch functioneren van rioolstelsels kan in de praktijk fors achterblijven bij het theoretisch functioneren. De veiligheid voor water op straat, die in het ontwerp normaliter ligt op een herhalingstijd van 2 jaar, kan in de praktijk terugvallen naar 1 jaar. Een belangrijke consequentie hiervan is dat het contactrisico met rioolwater in de praktijk groter is dan gedacht. Dit leidt tot de aanbeveling dat gemeenten met 'risicogestuurd beheer' de nadruk meer zouden moeten leggen op de risico's en de prestaties dan op besparing van de kosten.

Contents

1 Introduction

1.1 History of urban drainage

Sewer systems are underground infrastructure networks, comprising pipes, manholes and ancillary works, that collect and transport rainfall runoff and sewage to wastewater treatment plants. These systems protect society from exposure to faecal contamination and flooding of urban areas due to heavy storm events. Furthermore, protection of the environment (surface water and groundwater) is a main prerequisite.

In the mid-19th century, removal of excreta from cities became an important issue. Snow (1854) established the relationship between wastewater and diseases, which resulted in the construction of sewer systems. In combination with the improvement of drinking water quality, the latter led to better sanitary conditions and a reduction of the occurrence of infectious diseases in the 20th century. This contributed to a higher life expectancy and a decrease of child mortality (Figure 1.1). At first, the sewer systems were small in order to discharge the wastewater to surface water as quickly as possible. Later, the systems expanded and the collected wastewater was transported out of cities and discharged onto large surface water. As the first traditional barrel-systems proved to be ineffective in preventing cholera outbreaks (Van Zon, 1986), large-scale sewer systems were constructed for the disposal of wastewater at the end of the 19th century (Preston and Van de Walle, 1978) for the protection of public health. After the second World War the construction rate of sewer systems increased, motivated by economic growth and accelerated urbanisation. Dirkzwager (1997) reported the latter as a cause for the increase in the pollution of surface waters. In order to improve the surface water quality in the Netherlands, the construction of wastewater treatment plants took place in the late 1960s and 1970s (Figure 1.2).

As no computers were available, the hydraulic capacity of pipes could only be determined manually. The development of hydraulic models as we know them today has its origin in the late 1960s (Butler and Davies, 2004; Yen, 1987). In the beginning only steady state calculations were performed on simplified geometric descriptions of drainage systems. During the 1980s modelling of time dependent behaviour of water flows became possible.
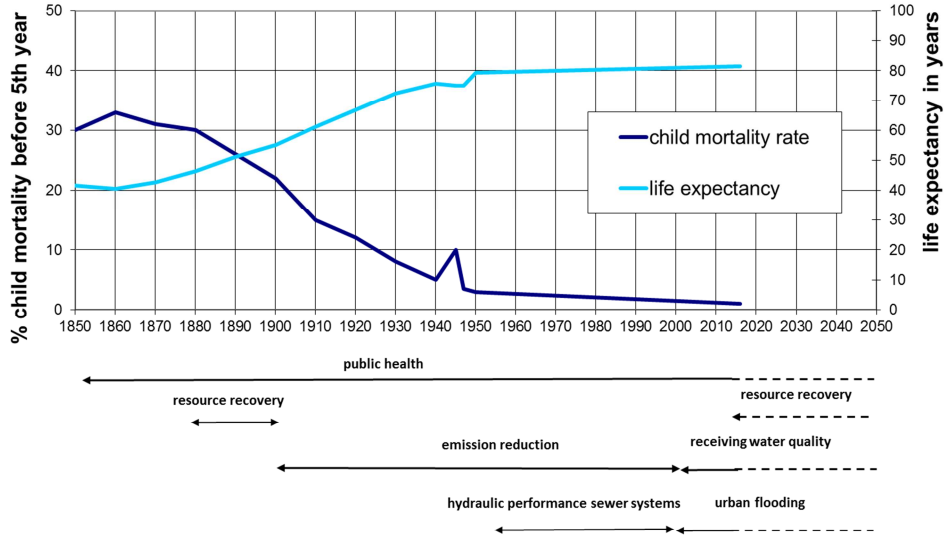

Figure 1.1:   Development of life expectancy in years of age and child mortality rate in % in the Netherlands since 1850. Information obtained from Bonneux (2010) and CBS (2016).

1.2   Sewer systems in the Netherlands

In the Netherlands municipalities are in charge to take care of a proper management of sewer systems. Water boards are regional government organisations that are responsible for the surface water bodies and the treatment of wastewater.

The predominant system type in the Netherlands is the combined sewer system, in which both wastewater and storm water are transported together in one system to the treatment plant. In 2016 there are around 13,000 combined sewer overflows (CSOs) present in combined sewers where diluted wastewater is diverted to the surface water during excessive rainfall (Stichting RIONED, 2016). The latter is a main drawback of combined sewer systems, as this causes environmental pollution of the receiving water bodies. Furthermore, the mixed wastewater often results in a loss of removal efficiency at the wastewater treatment plant (Langeveld, 2004). During the last 15 years, the number of CSOs has been reduced by 13%. As a solution to the drawbacks of combined sewer systems, most of the constructed sewer systems since the 1970s are separate sewer systems. In separate sewer systems, wastewater and storm water are transported in separate systems: the wastewater is drained to the wastewater treatment plant and the storm water is drained directly to the surface water or infiltrated in the underground. Nowadays, alternative systems are built in the Netherlands as is the case worldwide (Fletcher et al., 2015).

In the Netherlands 99.9% of the households and companies are currently connected to a sewer system (Stichting RIONED, 2016). This is shown in Figure 1.2 together with the supply of drinking water and the treatment of wastewater. The total length of sewers in the Netherlands is approximately 150,000 km and 64.9% of those sewers are gravity flow systems. The total runoff area in the Netherlands that drains to municipal sewer systems comprises 1,530 million m^2. About 57% is connected to combined sewer systems, 33% drains to separate sewer systems and 10% contains runoff area draining to alternative systems (SUDS). In order to manage urban drainage, 1.5 billion Euro is currently spent in the Netherlands every year (Stichting RIONED, 2016). This budget is covered by inhabitants and business owners by paying taxes to the municipalities. The annual inspection rate of sewers is around 10% of the total length of sewers. Pipe age is often used as a first indicator for the selection of pipes (Van Riel, 2017). In addition, visual inspection of all sewers within a municipality in the Netherlands is done repeatedly almost every 10 years.
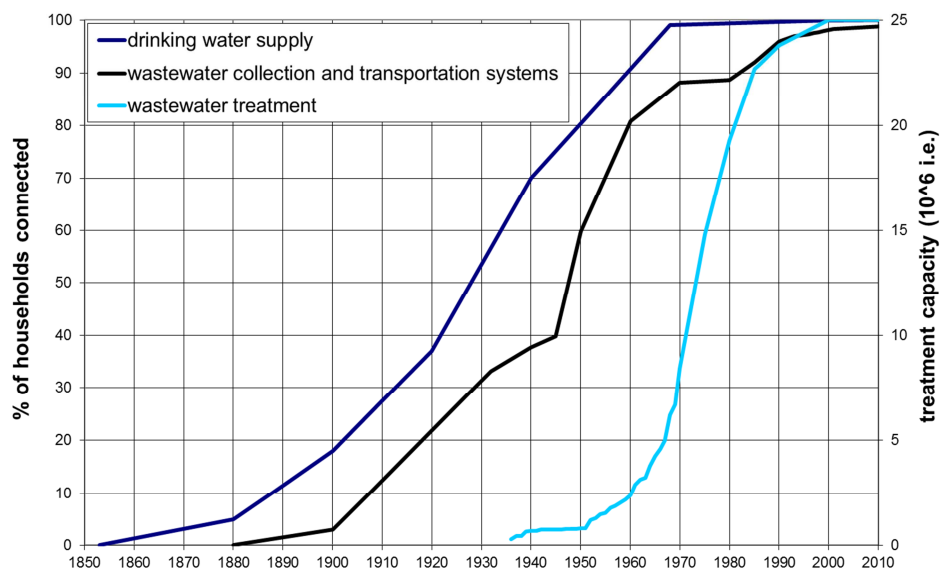
Figure 1.2: Development of the number of connected households to a sewer system, drinking water supply and wastewater treatment works in the Netherlands since 1850 (Langeveld, 2004).

1.3   Sewer asset management

Sewer systems protect society from exposure to faecal contamination and flooding of urban areas during heavy storm events. Consequently, it is important to maintain the defined service level over time. General activities to achieve this goal are sewer cleaning, sewer replacement and the prioritization of strategies. The management of sewer systems is specified in the NEN-EN 752:2017. Sewer asset management can be described as the process that starts with investigating the current sewer condition, followed by analysing the data and comparing the results with the defined performance requirements. Measures are required when system performance does not meet the requirements (see NEN-EN 752:2017, e.g. requirements regarding flooding frequencies, protecting public health, sewer surcharge frequencies, protecting receiving waters from pollution). Within this process of asset management, maintaining the same level of system performance at minimum costs is achieved when work is prioritised on components based on their impact on system performance (Wirahadikusumah et al., 2001). Performance and serviceability of sewer systems are the result of joint and individual functioning of the different objects (e.g. pipes, manholes, CSOs, pumps, gully pots) and of in-sewer processes which are unknown to a large extent (Ashley et al., 2004). In practice this hampers the development of knowledge on the relation between object and system failure (Van Riel et al., 2016).

The assessment of sewer performance is divided into three different parts: hydraulic, environmental and structural performance. The assessments consist of simulations, inspections and process monitoring. The operational condition of the assets of a sewer system affects the hydraulic performance of the sewer system and may cause increased pluvial flooding. Exposure to urban pluvial flooding may pose a health risk to humans, since the flooded sewage may contain a variety of contaminants depending on its origin (see e.g. Fewtrell et al., 2008; Lau et al., 2010; Fewtrell et al., 2011; Cann et al., 2013; De Man et al., 2014). However, sewer performance (including pluvial flooding and emissions) is generally assessed by hydrodynamic models, which assume the absence of in-sewer defects. The advantage of hydraulic simulations is that they can be done at relatively low cost once the models are built and they require limited time to obtain detailed knowledge of hydraulic system behaviour. The main drawbacks, however, are the uncertainties in the results due to data errors, the fact that several process parameters have to be estimated (Clemens, 2001a; Van Mameren and Clemens, 1997) and the absence of in-sewer defects in the model (e.g. root intrusion, surface damage, attached deposits and settled deposits). By choosing 'safe' model parameters (e.g. runoff parameters), these effects are more or less accounted for, however, the safety margin is largely unknown.

Visual inspections (CCTV) are usually carried out to collect information on the internal condition of sewers. However, alternative tools such as manhole-zoom cameras and the acoustic technology SewerBatt™ are available today (Plihal et al., 2016). The observations of in-sewer defects by carrying out CCTV are registered by the inspector using a uniform classification system. Human observations are prone to errors due to cognitive limitations in the process of addressing observed information (Dirksen et al., 2013) and also do not offer quantifying information with respect to the actual functionality. In addition, based on interviews with municipal employees in the Netherlands, Van Riel et al. (2014) emphasise that decisions regarding sewer replacement are not fully justified because they are to a large extent intuitive. This is possibly driven by the lack of knowledge in understanding the current and future condition of sewers in order to justify decision-making for sewer replacement.

Translating the effects of observed defects on object scale to quantify hydraulic performance on system scale is a very complicated task. As a result, visual inspections and hydraulic simulations, despite their drawbacks, are widely applied for assessments on structural condition of assets and hydraulic performance of sewer systems.

The results of visual inspections are the predominant source of information on which decisions on rehabilitation or replacement are based. Furthermore, the structural condition of sewers should not hamper the required hydraulic performance. Currently, in the Netherlands, visual inspection of all sewers within a municipality is done repeatedly every 10 years. One of the results based on the observed in-sewer defects, a list of 'small' maintenance actions is generated to maintain the operational performance and to extend the service life of the assets. The hydraulic condition of a sewer system changes over time in a much shorter period (6 months) in comparison with the structural condition (10 years). Stanić et al. (2014) collected data on pipe geometry and material properties of deteriorated concrete sewer pipes by using laser profiling and core sampling. The research showed sewer pipes with a sufficient structural condition after 90 years, whereas the hydraulic capacity decreased up to 50%. In addition, it is questionable if the current inspection frequency is sufficient to maintain the defined service of sewer systems regarding hydraulic performance. Furthermore, visual inspections obtain information on object scale and it is generally not straightforward how this affects hydraulic performance on system scale.

1.4   Thesis objective

During the 1980s there was an increasing number of sewer failures and corresponding consequences (Hurley, 1994; Thissen and Oomens, 1991). Proactive maintenance activities became more popular. Consequently, there became a need for prioritising those activities. In order to maintain the desired level of serviceability, the infrastructure, including sewer systems, has to be maintained and rehabilitated (Le Gauffre et al., 2007; Wirahadikusumah et al., 2001). As sewer systems are part of the underground infrastructure, the condition and corresponding maintenance and rehabilitation are mainly based on the results of visual inspections (Van Riel et al., 2016). The operational condition of the assets of a sewer system (pipes, manholes, pumps, gully pots, CSOs and other ancillary works) affects hydraulic performance of the sewer system (see e.g., Saegrov, 2006; Stanić et al., 2014; Post et al., 2016). However, sewer performance, including pluvial flooding and emissions, is usually assessed by hydrodynamic models assuming absence of in-sewer defects.

Nowadays, the maintenance activities to provide the required system performance is mainly based on the observed condition of individual assets and simulation results of calculations using as-built data. Assessing the actual sewer hydraulic performance for directing maintenance actions requires more information on the relation between the actual condition of an asset versus the influence it has on sewer network level.

This thesis focusses on the impact of in-sewer defects on urban pluvial flooding. The objective is to **develop methods to assess and quantify the effect of in-sewer defects on sewer performance**. In order to meet this objective, the following sub questions have been formulated:

1.   How does sewer condition affect sewer hydraulic performance?

2   Can model calibration direct sewer asset management actions?

3   Can critical elements and locations in sewer systems be identified?

4   What is the influence of in-sewer defects on public health?

1.5   Thesis outline

The work described in this thesis is presented in Figure 1.3 and follows the four research sub questions defined in section 1.4.
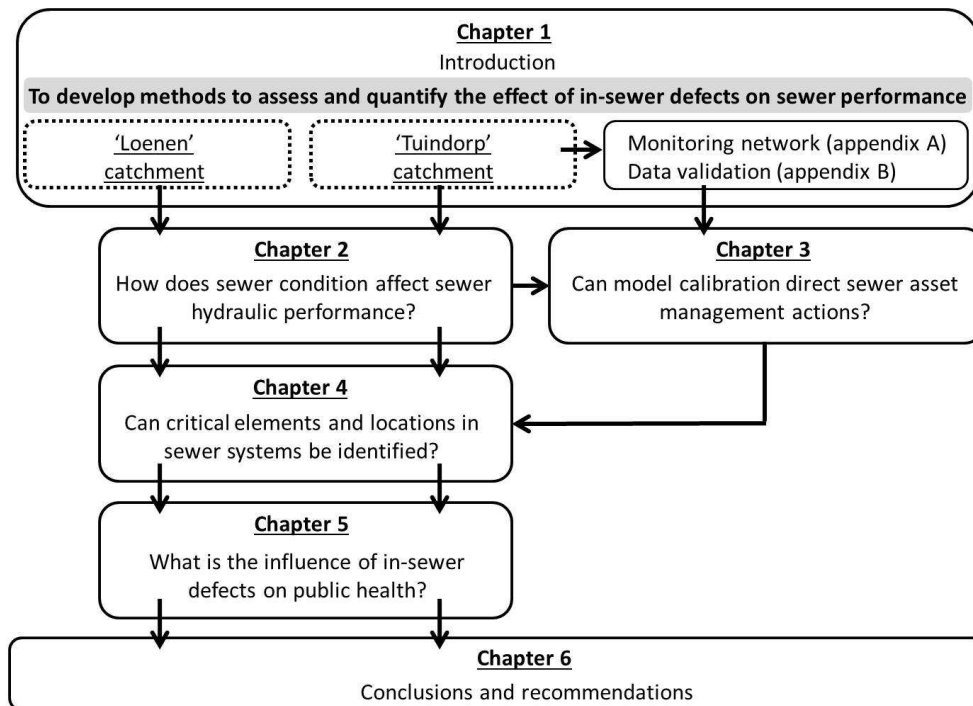
Figure 1.3:   Thesis outline.

The first chapter of this thesis deals with an overview of the history of urban drainage and sewer asset management. In addition, the studied research catchments are described and the installed monitoring network in 'Tuindorp' is presented and data validation is introduced.

The second chapter quantifies the impact of in-sewer defects on urban pluvial flooding at network level and answers the first research sub question. The studied defects are based on field observations and translated to model parameters. Impacts are assessed using Monte Carlo simulations with a full hydrodynamic model of the sewer system.

The third chapter demonstrates the concept of 'hydraulic fingerprinting' for the combined sewer system 'Tuindorp' to direct sewer asset management actions. The application of 'hydraulic fingerprinting' is based on model calibration, where 'fingerprinting' is defined by the model parameters and the residuals.

Chapter 4 describes a methodology to identify the most critical elements in a sewer system with respect to malfunctioning of the system at network level.

Chapter 5 addresses the impact of in-sewer defects on urban pluvial flooding and, subsequently, on health risks to humans. The analysis is based on flooding frequencies from the Monte Carlo simulations as presented in chapter 2 and infection probabilities due to ingestion of urban pluvial flooding as presented by De Man et al. (2014).

Finally, in chapter 6 conclusions are drawn and recommendations for further research are presented.

1.6 Research catchments

Throughout this thesis two Dutch sewer systems with different characteristics have been used as case studies: 'Tuindorp' (city of Utrecht) and 'Loenen' (city of Apeldoorn). Both sewer catchments are located in the centre part of the Netherlands, see Figure 1.4. This section gives a general overview of the two sewer catchments. Some aspects will be recalled, or more details will be added, in the respective sections when needed.

Both sewer catchments were selected to investigate the impact of sewer condition on urban flooding and health risk in chapters 2 and 5 and to determine critical elements in piped systems in chapter 4. For studying the applicability of model calibration to improve the prediction of sewer maintenance requirements, only the 'Tuindorp' catchment has been selected.

Figure 1.4: Location of thesis sewer catchments 'Tuindorp' (City of Utrecht) and 'Loenen' (City of Apeldoorn) in the Netherlands.

The 'Tuindorp' catchment area is a (predominantly) combined sewer system constructed in the 1970s as a looped gravity flow system. The catchment is relatively flat and can be considered as a residential area (Figure 1.5). The catchment area comprises a range of contributing areas in terms of roof types and pavement types. The collected sewage in this area is transported to the pumping station in the southern part of the catchment area. The sewer system comprises five combined sewer overflow (CSO) structures, see Figure 1.6. One of the CSOs discharges into a storage-settling tank. There are no discharges and inflows from adjacent systems in the catchment. The characteristics of this catchment are summarised in Table 1.1. The layout of the sewer system is presented in Figure 1.6.

Figure 1.5:   Area overview sewer catchments 'Tuindorp' (City of Utrecht) and 'Loenen' (City of Apeldoorn) in the Netherlands (source Google Maps).

The 'Loenen' catchment is a combined sewer system and can be considered as a residential area as well (Figure 1.5). It has been constructed as a partly-branched gravity system and the catchment is mildly-sloping. The sewer system is equipped with one pumping station and two CSO structures (Figure 1.6). One of these CSO structures discharges into a large pond. The latter drains the diluted wastewater into the surface water of the surrounding area. There is a relatively large average dry weather flow per inhabitant because of several industrial discharges and an inflow from an adjacent catchment. The characteristics of this catchment are summarised in Table 1.1. The layout of the sewer system is presented in Figure 1.6.
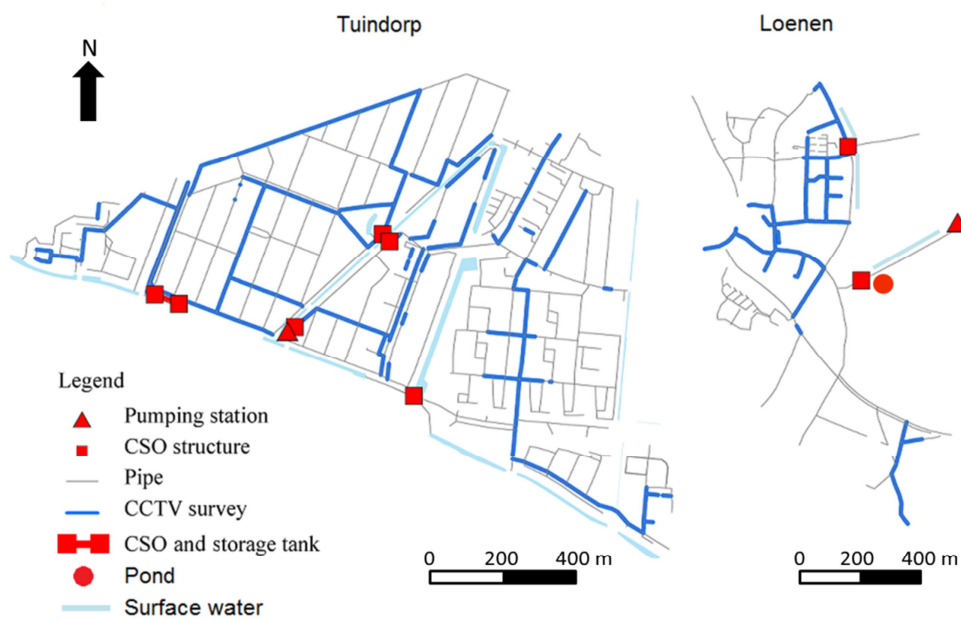
Figure 1.6: Layout 'Tuindorp' and 'Loenen' sewer catchments.

Table 1.1: Main characteristics 'Tuindorp' and 'Loenen' catchments.

Characteristics	'Tuindorp' catchment	'Loenen' catchment
area use	residential	residential
catchment area	flat	mildly-sloping
system type	combined	combined
system structure	looped	partly-branched
ground level/surface level (m AD)	0.75 – 2.25	17.8 – 28.6
average surface slope (mm/m)	3.0	8.8
average pipe slope (mm/m)	2.8	3.8
contributing area (ha)	56.9	23.4
number of CSO structures (-)	5	2
storage volume (m^3)	4,669 (= 8.2 mm)	900 (= 3.85 mm)
volume storage settling tank (m^3)	822 (= 1.4 mm)	0
number of pumping stations (-)	1	1
pumping capacity (m^3/h)	800[*]	209
number of inhabitants (-)	10,656	2,100
dry weather flow (m^3/h) (including infiltration and inflow)	157	78

[*] Based on flow measurements. According to the municipal administration the pumping capacity is 540 m^3/h.

1.7   Monitoring network and data quality

In the early 2000s, the city of Utrecht (the Netherlands) started a monitoring program comprising different types of sensors. During the period 2003 till 2008, the sewer monitoring network followed successive development stages and the number of sensors increased. The monitoring network has been installed in order to check the reliability of the computational hydrodynamic sewer model and to study the hydraulic performance of the sewer system. Flows, water levels, rainfall and turbidity are monitored at several locations in the system. The computational hydrodynamic sewer model within Utrecht comprises approximately 20,000 nodes and 21,000 conduits and the run off area estimates 1,500 ha contributing to the combined sewer system. The total combined sewer system in Utrecht is divided into 22 different sub-sewer systems (districts). The wastewater is transported between those districts by pumps. The system consists of approximately 650 km of sewers and 184 CSOs. One of the sub-sewer systems is the 'Tuindorp' sewer catchment.

Managing, analysing and presenting measured data, however, became a very extensive job for the municipality during the years due to the enormous number of measurements that were registered daily. Every day at least 55,000 data entries were stored in a database. Without data processing and validation, this results in a large inaccessible data set with unknown quality. Therefore, validation of measured data is a prerequisite. This not only provides information on the functionality of the measuring equipment, but also limits the large amount of measurement data in order to provide accessibility. Finally, validated data increase the reliability of model results and investments based on those results. Therefore, an automatic validation tool has been developed for validation of the large data sets of sewer measurements (Van Bijnen and Korving, 2008). There are several examples of (automatic) data validation in the field of sewer systems and wastewater treatment plants (e.g. Mourad and Bertrand-Krajewski, 2002; Yoo et al., 2006; Schilperoort, 2011).

This research is performed in cooperation with the city of Utrecht and the municipality of Utrecht made it possible to use the municipal monitoring network in 'Tuindorp'. For the purpose of this research, the monitoring network has been extended in 2009. To obtain data on the hydraulic performance of the sewer system and to understand the impact of in-sewer defects on hydrodynamic system behaviour, a total of 30 sensors have been installed (Figure 1.7). Flows (F1), water levels (Lev1, Lev2,…, Lev27) and rainfall (R1 and R2) are monitored at several locations in the catchment area (Figure 1.7). The monitoring

network design is based on a combination of hydrodynamic simulations, reported incidents and observed in-sewer defects. For example, several water level sensors are installed in the manholes just upstream and downstream of an observed defect. Two tipping-bucket rain gauges (R1 and R2) have been used to measure rainfall in 'Tuindorp'. At all sensors, data are registered every 5 minutes. The 'Tuindorp' system was monitored during the period January 2010 - September 2015. A full description of the monitoring network is presented in appendix A.
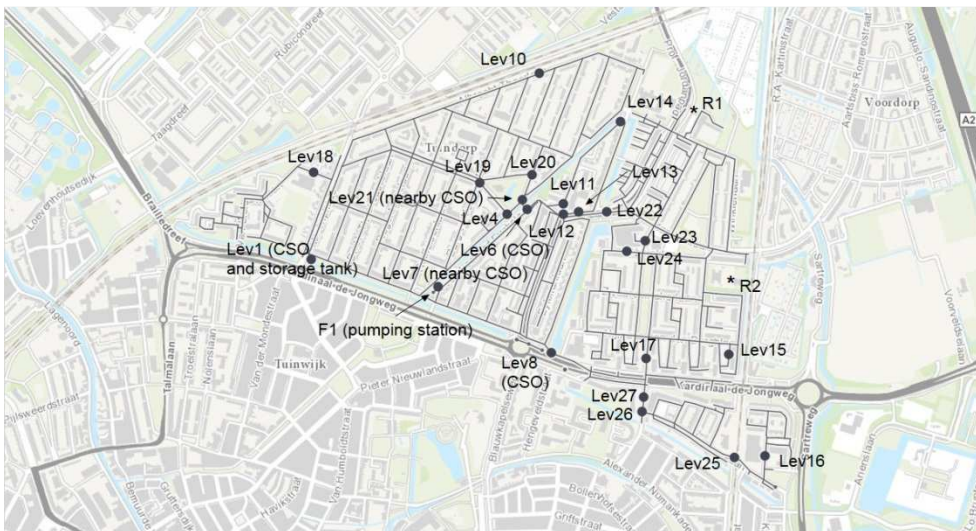
Figure 1.7:   Overview monitoring network 'Tuindorp' sewer catchment. Flows (F1), water levels (Lev1 to Lev27) and rainfall (R1 and R2).

The automatic validation procedure, as applied in the municipality of Utrecht and described in this section and in Van Bijnen and Korving (2008), has been carried out to assess the monitoring data used in this research. The validation procedure comprises several general standard checks independent of the type of sensor and a more site-specific control model depending on the type of instrument (water level, flow or rainfall). The validation tool automatically diagnoses the quality of measurements (correct, uncertain and incorrect), if possible, by separately validating all measurements of one sensor. A detailed description of the validation process and the results of the data quality assessment are presented in appendix B.

2 Impact of sewer condition on urban flooding

2.1 Introduction

The hydraulic performance of a sewer system is affected by the operational and structural condition of its assets (Saegrov, 2006). Currently however, structural in-sewer defects are not explicitly incorporated in model-based assessments of pluvial flooding due to lack of knowledge and lack of data. As a result, the level of serviceability is likely to be overestimated. A common approach for assessing pluvial flooding is often based on hydraulic simulations using single storm events. However, the return period of rainfall events and resulting flooding differs due to the non-linear nature of the processes involved. Consequently, detailed flood frequency analysis requires long-term rainfall series.

This chapter addresses the impact of the internal operational condition of sewers on urban pluvial flooding in the two research catchments (see section 1.6). The studied in-sewer defects include root intrusion, surface damage, attached deposits, settled deposits and sedimentation. The analysis is based on Monte Carlo simulations with a full hydrodynamic model of the sewer system using measured rainfall series of 10 years and field observations of in-sewer defects. Monte Carlo simulations are applied to systematically study the variation of flooding impacts (frequencies, volumes, et cetera) due to in-sewer defects using a detailed InfoWorks© model of the sewer system. Realistic ranges for the inputs of the Monte Carlo simulations are based on the results of visual inspections.

2.2   Data collection

2.2.1   Field observations of in-sewer defects

Visual inspections were carried out in both systems to collect information on in-sewer defects. The inspection of the internal structural condition is carried out by CCTV (closed circuit television) from within the sewer. The determination of condition aspects is done according to a uniform classification system (NEN-EN 13508-2, 2003; NEN 3399, 2004). In this study, the following in-sewer defects were taken into account: root intrusion, surface damage, attached deposits and settled deposits.

In the 'Tuindorp' catchment, inspection was carried out in 28% (7.6 km) of the total sewer length. Approximately 34% of inspected conduits showed in-sewer defects. In the 'Loenen' catchment, 30% (3.8 km) of the sewer system was inspected showing defects in 82% of the inspected conduits. Figure 1.6 presents an overview of the inspected conduits (bold lines). Observed defects are translated into the parameters of the hydrodynamic models. The parameter values account for critical conduits with respect to the above-mentioned defects (see section 2.3).

2.2.2   Field observations of sediment depths

Despite recent developments in prediction methods, the ability of hydraulic models to predict sedimentation behaviour and the risk of sediment accumulation in a sewer section is still limited (e.g. Gérard and Chocat, 1999; Ashley et al., 2000; Ashley et al., 2004; Butler and Davies, 2004; Schellart, 2007). In this research therefore, observed sediment depths are used to account for the effects of sediment deposits in hydrodynamic model calculations.

In the city of Utrecht (including the 'Tuindorp' catchment), sediment depths are registered by cleaning engineers before jetting individual pipes while carrying out the annual cleaning program. Crabtree (1989) describes five categories of sediment deposits, based on observations of the provenance, nature, and location of the deposits within the sewer system. Sediment deposits in the Netherlands can typically be classified as type C: mobile, fine grained deposits found in slack flow zones. In this study, sediments are defined as type C deposits, which can be removed from a pipe by means of jetting. Attached deposits that have to be removed by other techniques and can only be detected by detailed visual inspection of sewer conduits, are included in the hydraulic roughness calculations.

16

Sediment depths are classified according to the percentage of obstructed conduit height. Observed sediment depths are not objective but depend on cleaning engineers' experience and opinion (Korving, 2004; Dirksen and Clemens, 2007). Before jetting an individual conduit the cleaning engineer makes an estimation of the sediment depth as can be seen from ground level after opening the manhole. After jetting the conduit, the removed amount of sediment for each conduit has been estimated as well.

In the 'Tuindorp' catchment, sediment depths were estimated and registered. In addition, in the complete sewer system of Utrecht sediment depths were estimated and registered. This data was also used in the analysis of the 'Tuindorp' catchment. The total data set includes observations on 28% of the sewer pipes in the sewer system of Utrecht: a total of 10,735 sewer pipes. The Wilcoxon rank sum test was used to compare the sets from 'Tuindorp' and Utrecht. This showed no significant differences between the two data sets. Therefore, it was concluded that both data sets could be used for the uncertainty analysis. Observed sediment depths are translated into model parameters. Uncertainty of observed depths is accounted for by choosing class ranges of 10%.

2.3 Model parameters

Monte Carlo simulations are applied to systematically study the impact of in-sewer defects on variation of flood frequencies, locations, volumes and threshold values. Simulations are performed with detailed InfoWorks© models of both sewer systems. These models have been validated to eliminate systematic errors in the model according to the method described by Van Mameren and Clemens (1997), Clemens (2001a) and Stichting RIONED (2004). This implies that the data in database holding structural and geometrical data, ground levels, pumping capacities etc. are verified in the field and that a comparison has been made between complaints and location in which the model predicts flooding.

In order to incorporate the in-sewer defects in the hydrodynamic models, they are translated into the following model parameters:
- Type 1: hydraulic roughness to account for root intrusion, surface damage, attached and settled deposits (hydraulic roughness for the total conduit length);
- Type 2: sediment depths to account for sedimentation (the sediment depth represents permanent, consolidated sediment deposits in the model, it does not allow for the erosion or deposition of sediment).

Both types of model parameters are characterised with a probability distribution. The type of probability distribution and the mean values and standard deviations of the parameters are mainly based on the field observations of in-sewer defects and sediment depths. Hydraulic roughness is described with a lognormal distribution, sediment depths with a beta distribution. The choice of the lognormal distribution for describing roughness is based on expert judgement. It is assumed that the distribution of roughness is skewed, i.e. it is left-truncated because values below zero are impossible and it has a tail to the right. Due to lack of field observations this assumption could not be checked. The parameters of the lognormal distribution have been estimated with the Maximum Likelihood Estimates method. The choice of the beta distribution for sediment depth is based on field observations from both the 'Tuindorp' catchment and the complete sewer system of Utrecht. Using both chi-square and Kolmogorov-Smirnov tests an appropriate distribution type has been selected. The parameters of the beta distribution have been estimated with the Maximum Likelihood Estimates method.

Hydraulic roughness

Only a limited number of defects are affecting the hydraulic roughness. In this research, the following defect codes are taken into account: surface damage (BAF), roots (BBA), attached deposits (BBB), settled deposits (BBC) and other obstacles (BBE). In the Monte Carlo sampling the results of the visual inspections are used to determine the probability of these defects. The visual inspections showed defects related to hydraulic roughness in 34% of the inspected conduits in the 'Tuindorp' catchment and in 82% of the inspected conduits in the 'Loenen' catchment (section 2.2.1). For every conduit in the computational models it was determined whether the conduit has a defect related to hydraulic roughness by drawing from a uniform distribution on the interval 0 to 1. Conduits with a drawn value smaller than the observed percentage of conduits with a defect (34% for the 'Tuindorp' catchment and 82% for the 'Loenen' catchment) are labelled as having a defect.

The Colebrook-White equation for hydraulic roughness is used in combination with the Nikuradse roughness (Nikuradse, 1933). In the Monte Carlo simulations, the roughness of pipes without defects equals 3.0 mm according to the Dutch standards. This value also accounts for local head losses due to manholes (Stichting RIONED, 2004). Using local head losses in hydraulic simulations is the consequence of assuming that the flow is one-dimensional. The disregarded velocity components produce extra friction losses. The local head losses due to manholes depend to a large extent on the geometry of the structure (Pedersen and Mark, 1990; Clemens, 2001a; Idelchik, 2007). Clemens (2001a) showed that the head loss coefficient, used for calculating the head losses in manholes, is not a constant value but is closely related to the water level in the manhole. In practice, there is a lack of exact knowledge on the value to be used in the hydraulic simulations.

18

Furthermore, it is not possible to change the head loss coefficient in the hydraulic simulations during every time step. Therefore, the roughness value of 3.0 mm in the hydraulic simulations accounts for local head losses as well. Hager (2010) also suggests that for sewers without specific information, the effective wall roughness corresponds to an operative roughness of the conduits.

In case of pipes that have a defect the roughness is characterised using a shifted lognormal distribution,

$$Logn(x \mid \mu,\sigma,c) = \frac{1}{(x-c)\sigma\sqrt{2\pi}} \exp\left(-\frac{(\ln(x-c)-\mu)^2}{2\sigma^2}\right), \quad x > 0 \qquad (2.1)$$

where x is the roughness, μ is the mean value, σ is the standard deviation and c is the location or shift parameter. Stanić (2017) measured roughness values up to 13 mm in case of studying the structural condition of sewer pipes, which is considerably above adopted values in the design of sewer systems. Camenen et al. (2006) described the roughness height as a function of the grain size, especially in case of the lower plane-bed regime. Furthermore, drain solids size distribution comparisons in Ashley et al. (2004) show particle sizes up to 8 mm in European drain solids. For flat deposits a commonly accepted value for the roughness is 3 * D_{90}. In addition, this means an effective roughness up to a maximum of 15-18 mm seems realistic. In case of the formation of patterns at the surface of the deposits, the effective roughness can increase even more (Kleijwegt, 1992). The parameters of the distribution given in equation (2.1) are derived from on inspection. The following values have been applied: a mean value of 6.0 mm, a minimum of 3.0 mm (i.e. shift parameter) and a standard deviation of 5.0 mm. For each pipe with a defect a value for hydraulic roughness is drawn from this distribution.

Sediment depths

The observed sediment depths are registered as relative sediment depths (ratio of observed depth and conduit height). These depths are translated to model parameters as follows. For each pipe shape (e.g. circular, egg) and dimension class, a distribution function is fitted on the observed sediment depths (10,735 observed depths).

To characterize the distribution of sediment depths a beta distribution with parameters a and b is applied which is defined on the interval between 0 and 1,

$$Be(x \mid a,b) = \frac{\Gamma(a+b)}{\Gamma(a)\Gamma(b)} x^{a-1}(1-x)^{b-1}$$

(2.2)

where Γ(a) is the gamma function which is defined as,

$$\Gamma(a) = \int_{t=0}^{\infty} t^{a-1} \exp(-t)dt, \quad a > 0$$

(2.3)

In the Monte Carlo simulations, the relative sediment depth of pipes is drawn from the corresponding beta distribution. The values of a and b of the beta distribution for each combination of pipe shape and dimension class are shown in Table 2.1.

Table 2.1: Parameters of beta distributions describing relative sediment depths for different pipe shapes and dimensions.

circular profile (mm)	a	b	egg-shaped profile (mm)	a	b
250	1.331	4.980	300/450	1.070	6.483
300	1.331	4.980	350/525	1.070	6.483
315	1.331	4.980	400/600	1.284	7.591
400	1.365	5.755	500/750	1.409	8.403
500	1.517	7.287	600/900	1.552	7.091
600	1.666	8.915	700/1,050	1.896	7.852
700	2.386	11.823	800/1,200	1.492	8.251
800	2.386	11.823	900/1,350	1.392	10.266
1,000	2.205	11.553	1,000/1,500	1.392	10.266
1,250	2.205	11.553	1,200/1,800	1.392	10.266

2.4   Monte Carlo simulations

In the Netherlands, the common approach to assess pluvial flooding is based on hydraulic simulations using predefined storm events with a specific return period based on rainfall statistics (Stichting RIONED, 2004; Van Mameren and Clemens, 1997). These predefined storm events are insufficient for detailed flood frequency analysis because the information on peak intensities is limited and the return period of storms and resulting flood events is different. Due to the random changes in the characteristics of the network in each run during the Monte Carlo procedure, it is impossible to predict which storm events will lead to flooding. This especially holds for the (partly) branched sewer system. Therefore, in the Monte Carlo simulations long-term rainfall series are used. This series was observed by the Royal Dutch Meteorological Institute in De Bilt during the period 1955-1964.

As Monte Carlo simulation is very time consuming, calculation time was reduced using a parallel computing approach. For that purpose, a cluster comprising 20 PCs was used. This technique has become more popular in the field of urban drainage for impact assessments and uncertainty analyses (e.g. Barreto et al., 2008; Burger et al., 2010). To reduce calculation time further, the measured rainfall series were filtered. This filter is based on in-sewer storage volume, pumping capacity and length of dry period between two storm events. This resulted in a collection of 322 independent storm events for the 'Tuindorp' catchment and 572 events for the 'Loenen' catchment. One single run in the Monte Carlo procedure was defined as the hydraulic simulation of the complete collection of independent storm events (either 322 or 572 events). As the main focus was to obtain estimates of mean and variance of flood frequencies and volumes, a limited number of simulations in the Monte Carlo procedure were allowed (Clemens, 2001a). In order to get reliable estimates of mean and variance, 750 runs have been performed. The results show that this number of runs is sufficient. The mean and variance of the flooding frequency became stable after 300 to 400 runs (Figures 2.1 and 2.2).

Figure 2.1: Average (top) and standard deviation (bottom) of relevant model output parameter flood frequency sediment for the 'Tuindorp' catchment during the Monte Carlo runs.
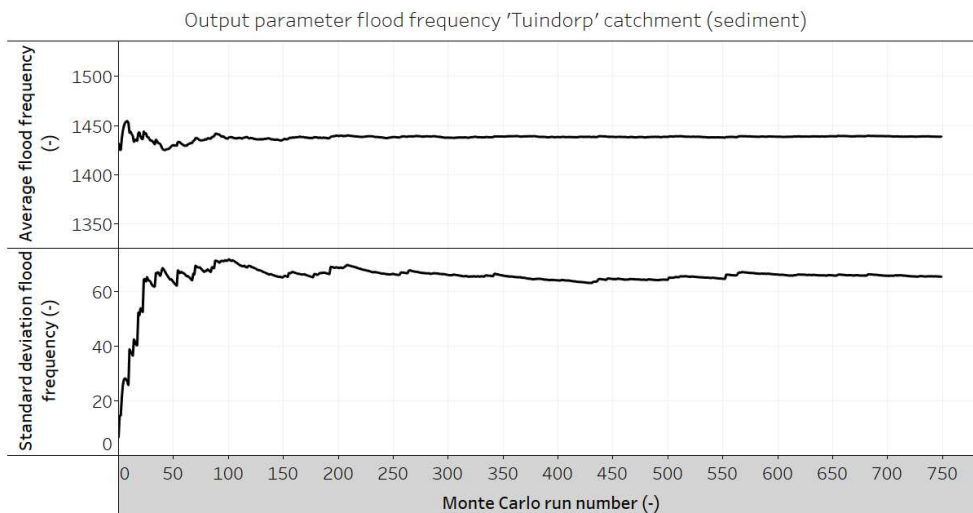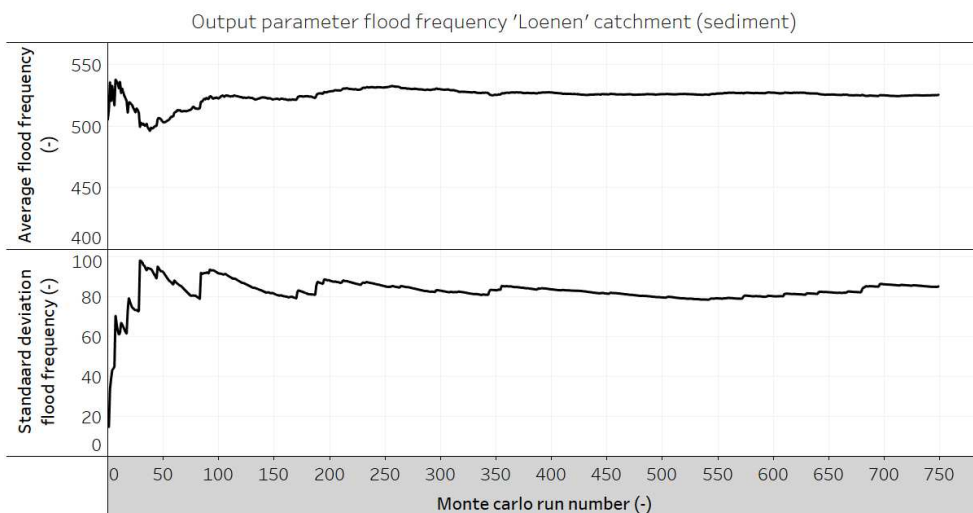

Figure 2.2: Average (top) and standard deviation (bottom) of relevant model output parameter flood frequency sediment for the 'Loenen' catchment during the Monte Carlo runs.

In the case of both catchments, for sediment depths as well as for hydraulic roughness, separate Monte Carlo simulations were applied (Figure 2.3). This led to four Monte Carlo procedures consisting of 750 runs each. Each run had a different set of parameter values for either sediment depths or roughness (i.e. the 'model condition'). In each run, the same set of selected storm events was applied.

In the Monte Carlo simulations regarding roughness, the roughness of each pipe has been determined as follows. For each pipe in the hydraulic model it was determined whether the pipe has defects or not. This task was performed by randomly drawing from a uniform distribution (Figure 2.3). If defects were assigned to the pipe, a value for hydraulic roughness was drawn from the shifted lognormal distribution. A pipe without defects received a hydraulic roughness equal to 3.0 mm.

In the Monte Carlo simulations regarding sediment depths, the sediment depth of each pipe in the hydraulic model depended on pipe shape and pipe dimension. A parameter value for sediment depth has been randomly drawn from the corresponding beta distribution function (Figure 2.3).

The parameter values for roughness and sediment depths were substituted in the InfoWorks© model using COM techniques and remained constant during each run. The depth of sediment in the invert of the pipe, reduced the capacity of the pipe by obstructing the flow. This sediment depth represents permanent, consolidated sediment deposits. InfoWorks© assumes that the sediment is constant. It does not allow for the erosion or deposition of sediment. Therefore, the transport of sediment through the system is not modelled (Wallingford Software, 2007).
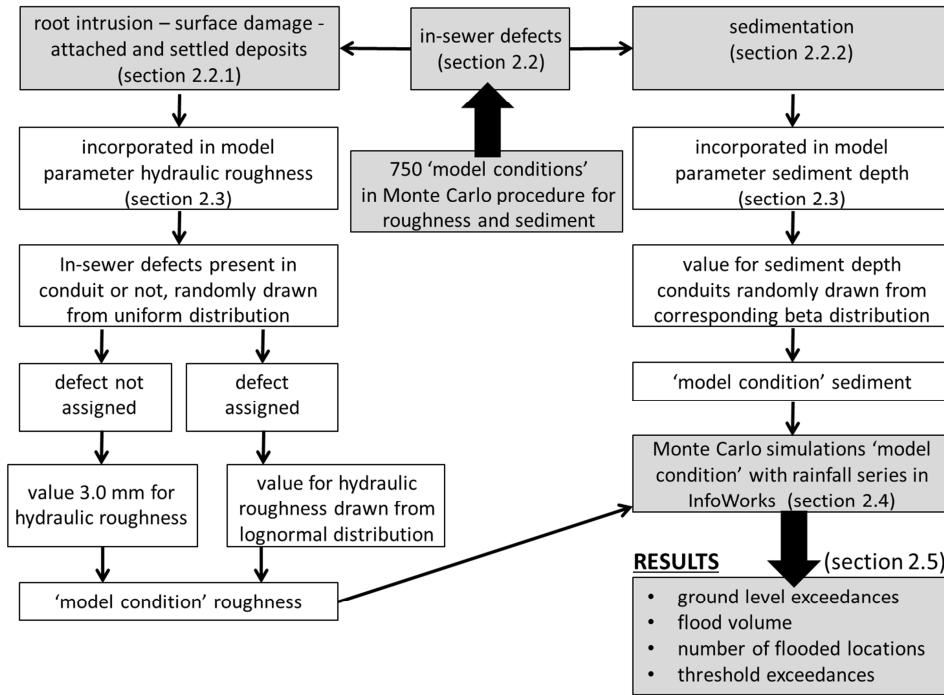
Figure 2.3:   Monte Carlo procedure for the 'Tuindorp' and 'Loenen' catchment.

2.5   Results and discussion

The variation of flooding impacts on network level due to structural in-sewer defects has been analysed. The outcomes of the Monte Carlo simulations were analysed to study statistical properties, not system changes. This analysis includes the variation in the number of times a water level exceeds ground level across all network manholes, total amount of flooded volumes at all manholes in the network, the total number of threshold exceedances 25 cm below ground level and the total number of flooded manholes. All during the 10 years rainfall series.

Manhole surcharges are defined as the total number of manholes where the calculated water level exceeds the level of the manhole cover during a rainfall event. This means that a manhole surcharge at two different manholes at the same time is counted for as two separate surcharges. The flood volume is defined as the calculated water volume on street level due to a flooding event at a specific manhole.

2. Impact of sewer condition on urban flooding

Water levels exceeding manhole cover levels are considered as flooding. The storage of floodwater is represented in the computational hydrodynamic model by adding a 'cone' on top of the manhole. The volume of water that exceeds manhole cover level is stored in this flood cone. The volume of water held by the cone will be discharged into the sewer system as the water level drops again. The shape of the flood cone is sketched in Figure 2.4. The floodable area ($A_{floodable}$) is the total area available for the storage of floodwater at a specific node. As a result, it is the sum of the contributing areas draining to this node. The shape of the flood cone (Figure 2.4) determines the relationship between flood volume and water level above manhole cover level. The part of the flood cone below 0.1 m represents the contributing areas of streets and adjacent pavements. The second part runs from 0.1 m to 0.5 m, with a linear increase in floodable area to 100%. Above 0.5 m, the floodable area remains 100% (Figure 2.4). This implies that, with flood depths < 0.1 m, the flooded area stays between the sidewalks, whereas for larger depths, the flooded area spreads across the entire contributing area of a node.
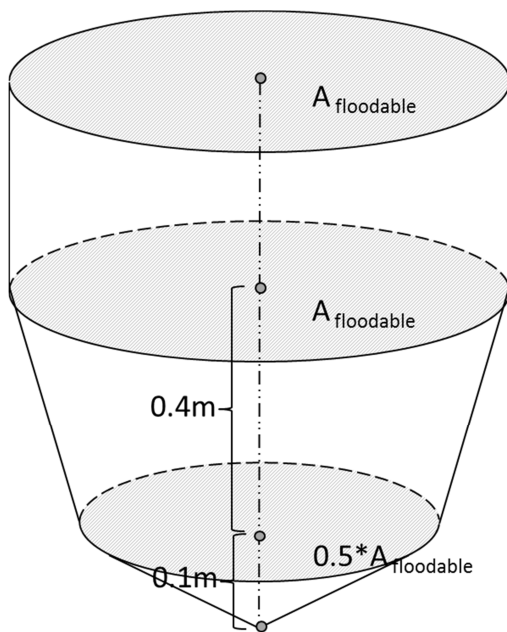
Figure 2.4: Flood cone on top of a manhole in the hydrodynamic model storing water above street level. The relationship between flood volume and water level above the street.

A threshold exceedance is defined as an event in which the calculated water level in the sewer system exceeds the threshold level 25 cm below the level of the manhole cover at a specific manhole. This means that an exceedance of this level at two different manholes at the same time is counted as two separate threshold exceedances as well. The number of flooded manholes refers to the sum of the manholes at which the calculated water level exceeds the level of the manhole cover at least one time during the 10 years rainfall series. In this case an exceedance of cover level during the rainfall series is counted as one flooded manhole location.

The overall picture for the 'Tuindorp' catchment is that the average number of manhole surcharges due to sedimentation is substantially larger than due to increased roughness (Figure 2.5). This finding also holds for calculated flood volumes and exceedances of the threshold level 25 cm below ground level. In addition, the variance due to sedimentation per simulation run is larger than the variance due to roughness.
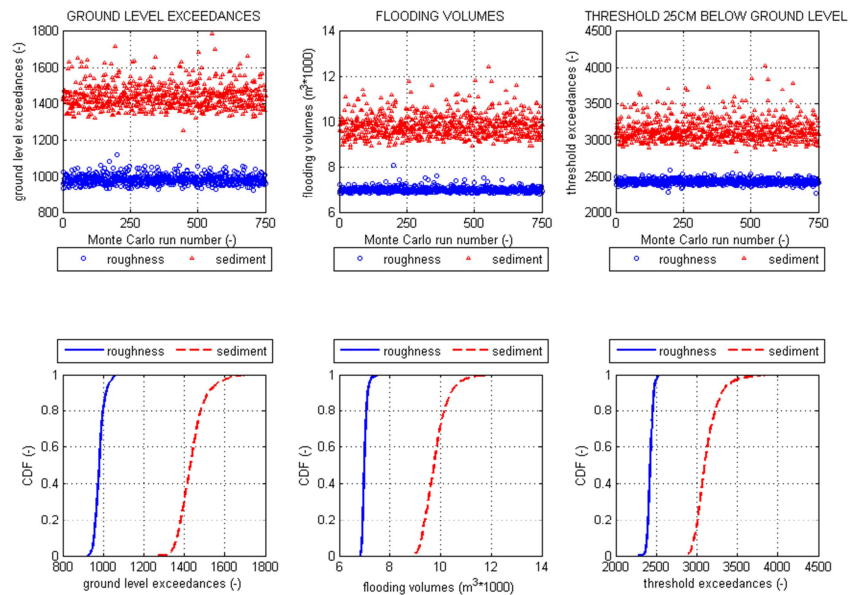
Figure 2.5:   Calculated variation of manhole surcharges, flood volumes and exceedances of threshold (25 cm below ground level) in the 'Tuindorp' catchment.

26

2. Impact of sewer condition on urban flooding

All calculated manhole surcharges in this catchment prove to be caused by 11 rainfall events in the 10 years series. This applies for the sewer model with in-sewer defects. Consequently, the average return period of flooding is approximately 1 year. Substantially higher values of manhole surcharges, flood volumes and threshold exceedances in Figure 2.5 are caused by sedimentation in important connections between sub-catchments.

Figure 2.6 shows the overall picture of the 'Loenen' catchment. The comparison of 'Tuindorp' and 'Loenen' shows the difference in system response between the flat-looped system and the mildly-sloping partly-branched system. In both catchments, the impact of sedimentation on all flooding characteristics is larger than the impact of roughness (Figure 2.7). The impact of both sedimentation and roughness in the 'Tuindorp' catchment, however, is larger than in 'Loenen'. This mainly results from the relative flatness of the first catchment. As a result, the number of potentially flooded locations is larger.
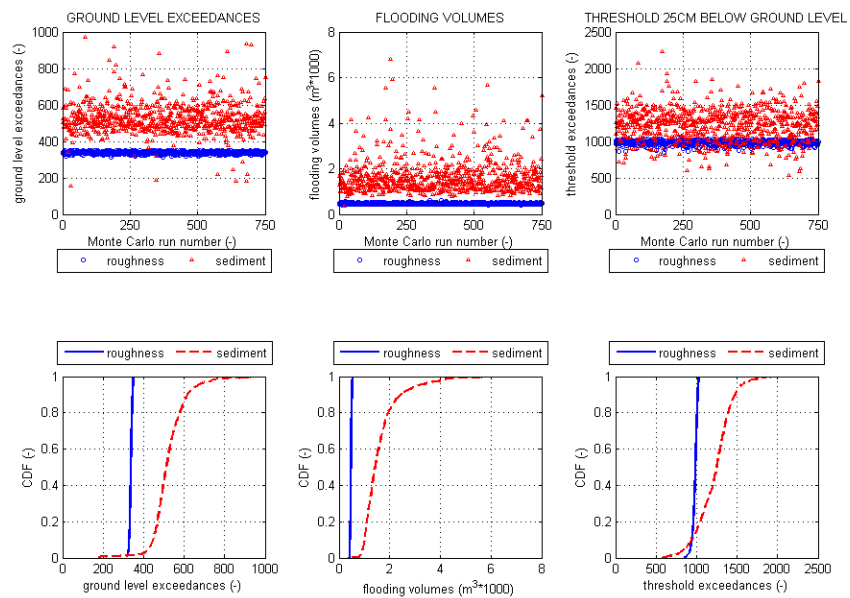
Figure 2.6: Calculated variation of ground level exceedances, flood volumes and exceedances of threshold (25 cm below ground level) in the 'Loenen' catchment.

27

For sedimentation, in particular, the variance of all flooding characteristics is substantially larger in 'Loenen' (Figure 2.7). Primarily, because of the partly-branched layout of the sewer system in comparison with the looped 'Tuindorp' system. Low street levels close to the CSO structure and the pumping station also affect calculated flooding impacts. Due to obstructions upstream, in-sewer storage is created leading to less flooding at these locations with lower ground levels.
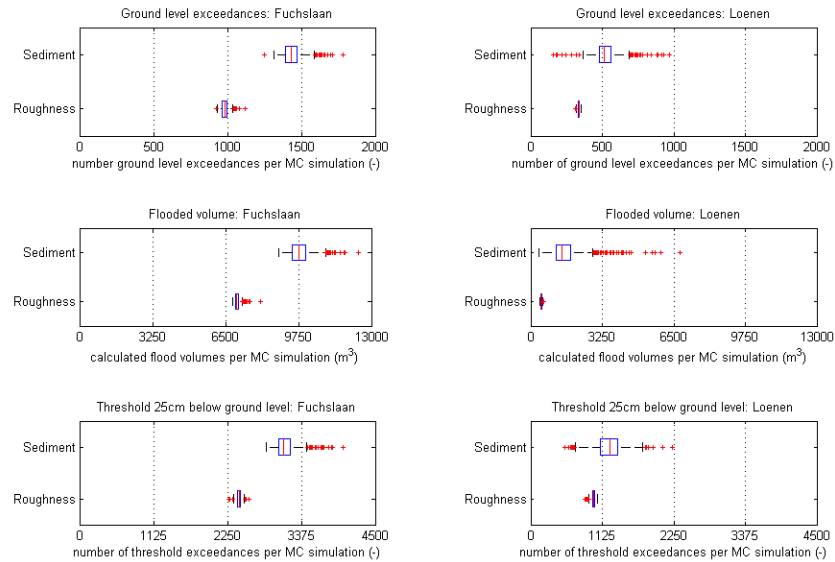
Figure 2.7:   Comparison of manhole surcharges, flood volumes and exceedances of threshold (25 cm below ground level) for both research catchments.

Table 2.2 shows the impact of roughness and sediment on calculated median values of flooding characteristics (manhole surcharges, number of flooded manholes and volumes) compared with the situation without in-sewer defects. It shows the impact of these model parameters on the median value of calculated results. Roughness in this table includes the following defects: surface damage, roots, attached deposits and settled deposits.

It is concluded that the increase in the total number of manhole surcharges is comparable in both research catchments. The increase of the number of flooded manholes and volumes however, is substantially larger in 'Loenen' than in 'Tuindorp'. The decrease in the number of manhole surcharges (-1%) in the 'Loenen' catchment in case of roughness is due to higher roughness values upstream in the Monte Carlo simulations. This results in less flooding at downstream locations close to the CSO structure and the pumping station. These downstream locations have relatively low ground levels associated with more frequent flooding in the situation without defects.

Table 2.2: Impact of roughness and sediment on median values of flooding characteristics (manhole surcharges, number of flooded manholes and volumes) compared with situation without in-sewer defects.

	'Tuindorp'		'Loenen'	
	roughness	sediment	roughness	sediment
manhole surcharges	4%	52%	-1%	50%
number of flooded manholes	2%	10%	12%	78%
flood volumes	4%	45%	32%	302%

2.6 Conclusions and further research

The objective of this chapter is to describe the impact of sewer condition on urban flooding. This impact has been quantified using Monte Carlo simulations on full hydrodynamic models. The statistics of in-sewer defects (root intrusion, surface damage, attached deposits, settled deposits and sedimentation) have been derived from visual inspections in two research catchments. These defects have been translated to specific model parameters (hydraulic roughness and sediment depth).

The analysis of simulation results shows that in-sewer defects significantly affect calculated return periods, flood volumes and threshold exceedances. A comparison with calculated flooding without in-sewer defects shows that the protection level with respect to urban pluvial flooding drastically deteriorates. The results also show that flooding is much more affected by sedimentation than by roughness.

Furthermore, in the 'Tuindorp' catchment a monitoring network (see appendix A) is installed to observe the hydraulic behaviour of the sewer system, including all the observed defects. The monitoring results are compared with model simulations to study the impact of in-sewer defects on hydrodynamic system behaviour. This next step is described in chapter 3 and appendix C.

3 Calibration of hydrodynamic models to drive sewer maintenance

3.1 Introduction

The operational condition of the assets of a sewer system (sewers, pumps, gully pots, combined sewer overflows (CSOs)) affects hydraulic performance of the sewer system (see e.g. chapter 2; Saegrov, 2006). However, sewer performance, including pluvial flooding and emissions, is usually assessed by hydrodynamic models, assuming absence of in-sewer defects. Consequently, the actual hydraulic performance maybe overestimated. A common approach to assess hydraulic performance of a sewer system is based on hydrodynamic simulations. The advantage of hydraulic simulations is that they can be done at relatively low cost and require limited time to obtain detailed knowledge of hydraulic system behaviour. The main drawbacks, however, are the uncertainties in the results due to data errors, the fact that several process parameters have to be estimated (Clemens, 2001a; Van Mameren and Clemens, 1997) and the absence of in-sewer defects in the model. Chapter 2 showed that in-sewer defects, such as root intrusion, surface damage, attached deposits and settled deposits, may substantially affect pluvial flooding with respect to calculated return periods and flood volumes. In addition, Stegeman (2012) demonstrates that calibration results can be improved by incorporating observed defects as local hydraulic resistance at specific locations in the model calibration.

This chapter describes the application of model calibration, to obtain a 'hydraulic fingerprint' as a means to improve the prediction of maintenance requirements. Model calibration is used to show that, given a chosen calibration parameter set which predominantly contains runoff parameters, a change in residuals after calibration is an indication for local changes in system behaviour (i.e. root intrusions and sediment deposits). To this end, the combined 'Tuindorp' system in Utrecht (the Netherlands) was first monitored to obtain the hydraulic performance with known defects in the system. After this first monitoring period, the sewer system was cleaned and monitored continuously to obtain a calibrated model that functions as a reference 'hydraulic fingerprint'. The calibration results of both periods have been used to determine the applicability of the 'fingerprint' method based on model calibration.

3.2 Materials and methods

3.2.1 System description

The 'Tuindorp' catchment area (Utrecht, the Netherlands) is a sewer system constructed during the 1970s as a looped gravity flow system (see section 1.6). The catchment is relatively flat and the system type is predominantly combined. The catchment area comprises a range of contributing areas in terms of types of roofs and types of pavement. The collected sewage in this area is transported to the pumping station in the southern part of the catchment area. The sewer system comprises five CSO structures. The layout of the 'Tuindorp' catchment is presented in Figure 1.6 and the main characteristics are shown in Table 1.1. More information about the 'Tuindorp' system is described in section 1.6.

3.2.2 Monitoring network

A monitoring network (30 sensors) has been installed to obtain data on the hydraulic performance of the sewer system and to understand the impact of in-sewer defects on hydrodynamic system behaviour. Flows (F1), water levels (Lev1, Lev2, … , Lev27) and rainfall (R1 and R2) are monitored at several locations in the catchment area (Figure 3.1 and appendix A). Monitoring network design is based on a combination of hydraulic simulations, reported incidents and observed in-sewer defects. For example, several water level sensors are installed in the manholes just upstream and downstream of an observed defect. Two tipping-bucket rain gauges (R1 and R2) have been used to measure rainfall in 'Tuindorp'. At all sensors data are registered each 5 min.
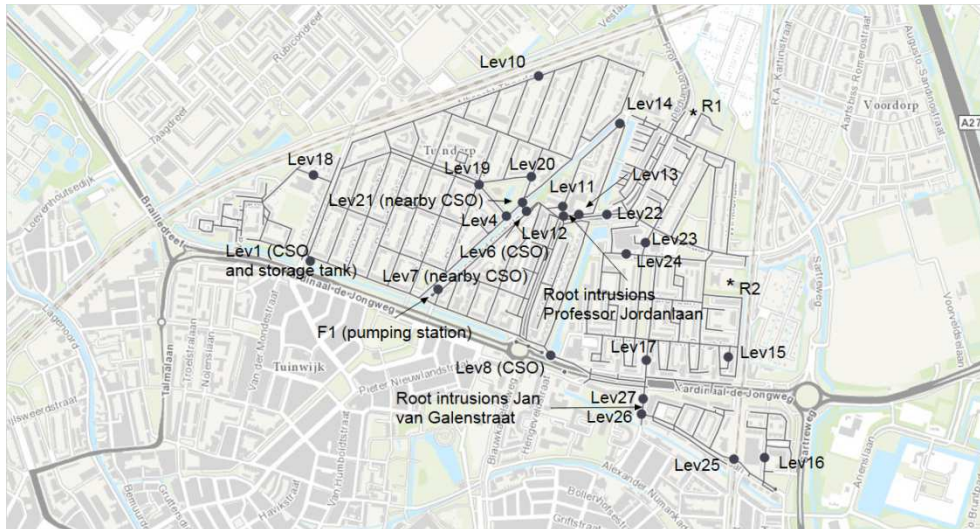
Figure 3.1: Monitoring network 'Tuindorp' catchment. Flows (F1), water levels (Lev1, Lev2, … , Lev27) and rainfall (R1 and R2) are monitored at several locations in the catchment area. Monitoring network design is based on a combination of hydraulic simulations, reported incidents and observed in-sewer defects. For example, several water level sensors (Lev12 and Lev13 Professor Jordanlaan, Lev23 and Lev24 Troosterlaan, Lev26 and Lev27 Jan van Galenstraat) are installed in the manholes just upstream and downstream of an observed defect. Two tipping-bucket rain gauges (R1 and R2) have been used to measure rainfall in 'Tuindorp'.

Figure 3.2 shows a chronology of relevant events during the 6-year research period. The 'Tuindorp' system was monitored during the period January 2010–September 2015 to obtain the hydraulic characteristics with known defects in the system. In order to collect information on in-sewer defects, visual inspections (CCTV, closed-circuit television) were carried out in 2008 in part of the 'Tuindorp' system. The inspections were carried out using a uniform classification system (NEN 3399, 2004; NEN-EN 13508-2, 2003). The classification system is a standardised list of images of condition issues, recognisable in sewers. For each condition issue, there is a main code in the classification system. The description of a condition issue is indicated by a class number from 1 to 5. Class 1 means that the condition issue was not present (observed) or to a very limited extent only. Class 5 means that the condition issue was observed to its maximum extent (as defined in NEN 3399, 2004). At the end of 2008, in total 28% (7.6 km) of the system has been inspected. Approximately 34% of inspected conduits showed in-sewer defects. In the first months of 2012, the whole sewer system has been cleaned and visual inspections were carried out again in the same sewers as in 2008. Afterwards the observed defects were removed, except for the observed root intrusion (class 5) between locations Lev12–Lev13 (Professor Jordanlaan) and Lev 23–Lev24 (Troosterlaan). The latter were removed in April 2015.

The observed root intrusion (class 5) between the locations Lev26–Lev27 (Jan van Galenstraat) has been removed in July 2013. From April to October 2015, the system has been monitored to obtain information suitable for calibrating the model of the clean system. This calibrated model can function as a reference for the 'hydraulic fingerprint'.
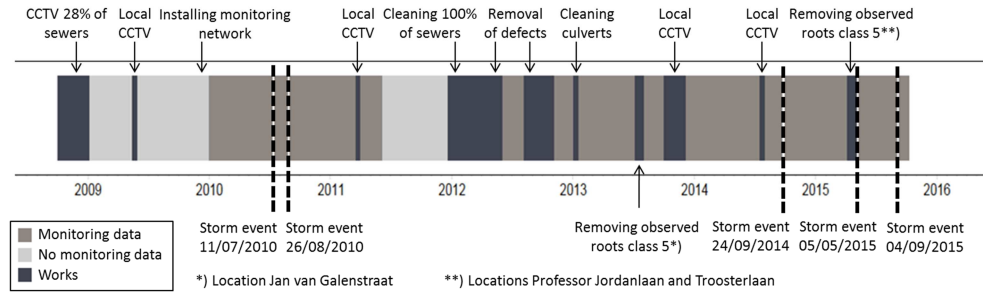
Figure 3.2: Storm events and works 'Tuindorp' sewer system for 1 October 2008 – 6 October 2015.

3.2.3   Measurement data

Calibrating models requires high-quality monitoring data (Bertrand-Krajewski, 2007; Dotto et al., 2010; Henrichs et al., 2008) and data validation prior to the model calibration is necessary given the harsh monitoring conditions in sewers (see e.g. Mourad and Bertrand-Krajewski, 2002; Rosen et al., 2003; Schilperoort et al., 2008). Systematic errors in monitoring data will unnoticeably be incorporated in the parameter values obtained in the calibration process, whereas random errors are of less relevance (Dotto et al., 2010).

The data obtained were validated using automated techniques as described in Van Bijnen and Korving (2008) and section 1.7, focusing on correlation between sensors and deviations in system behaviour. Depending on the type of instrument (water level, flow or rainfall), a combination of algorithms was used to determine whether a measurement is correct. The tests account for outliers, signal variance, double measurements, out of range measurements, missing values, spatial correlations and linear and step trends. The quality of measurements is expressed as 'correct', 'uncertain' and 'incorrect'. Incorrect data are left out. After validation, the data are suitable for model calibration. The results of the data quality assessment are presented in appendix B.

3.2.4 Model calibration

This chapter uses model calibration as a means to define a 'hydraulic fingerprint' of a sewer system. Model calibration is used to show that, given a chosen calibration parameter set which predominantly contains runoff parameters, a change in residuals after calibration is an indication for local changes in system behaviour (i.e. root intrusions and sediment deposits). The applied calibration process and necessary data are presented in Figure 3.3 and described in more detail in the Sections 3.2.4.1 - 3.2.4.7. In addition, the calibration process is conducted on the 'Tuindorp' sewer system in Section 3.3. The definitions according to Hemker (1996) have been applied.

Figure 3.3: Calibration process (after Hemker, 1996).

3.2.4.1 Model concept

The model concept (see step 1 in Figure 3.3) is defined by choices made for the three general components of an urban drainage model:
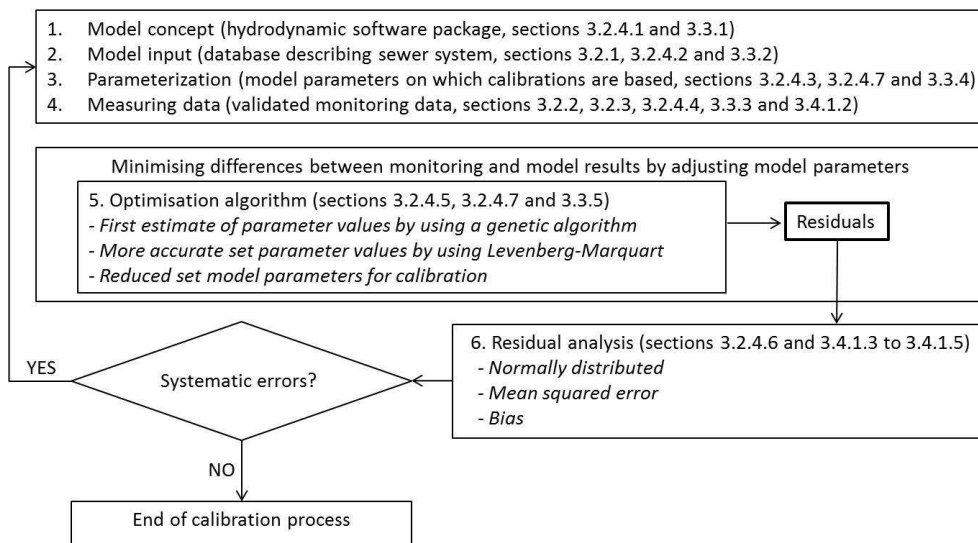
- The geometry and structure of the network and contributing areas;
- A model describing the hydraulic processes, combined with in-sewer processes;
- A model describing the rainfall-runoff process.

3.2.4.2   Model input

The model input (see step 2 in Figure 3.3) describes the sewer system as a network consisting of links (representing sewers) and nodes (representing manholes, CSO structures, outlets, etc.). In addition, the details of the components are defined, i.e. the diameter and upstream and downstream invert level of each sewer pipe or the width and level of a weir. The accuracy of the database is crucial with respect to the achievable accuracy of the calculation results. Errors in the database are an important source of bias when calibrating a model. In order to achieve a good calibration, the quality of the basic information must meet high standards.

3.2.4.3   Parameterisation

The parameterisation (see step 3 in Figure 3.3) determines the model parameters to be assessed. This typically comprises run-off parameters, catchment area properties, hydraulic parameters, geometry parameters and the structure of the drainage system. In order to be able to fully benefit of the calibration procedure, the only parameters that should be incorporated in the parameter optimisation process are 'process-related' parameters. Fixed parameters, such as system geometry and catchment area size, are to be addressed accordingly and derived from physical survey (Price and Osborne, 1986).

3.2.4.4   Measurement data

The measuring data (see step 4 in Figure 3.3) determine the amount of information available to quantify the model parameters. The information content is determined by type of monitoring, the measuring locations, the length of the measuring period, the measuring interval in relation to the measuring accuracy (Clemens, 2001a, 2001b and 2001c).

3.2.4.5   Optimisation algorithm

By systematically comparing model results with measured system response, an optimisation algorithm (see step 5 in Figure 3.3) may be used to define parameter values, calculate residuals and apply statistical analyses, like evaluating the performance using the Nash–Sutcliffe criterion (Nash and Sutcliffe, 1970). Calibration in this research is defined by minimising the differences between monitored results and model result by adjusting model parameter values.

3.2.4.6   Residual analysis

The residual analysis (see step 6 in Figure 3.3) studies the differences between modelled and measured values (water levels) after an optimal set of parameter values is obtained given the model and given the measured data. These residuals originate from measuring errors, database errors and processes not taken into account in the model concept chosen. The analysis shows the bias in calibration results, which is a measure for the quality of these results (i.e. presence of systematic errors). Consequently, it may reveal the need for adjustments of model concept, related model input and subsequent parameterisation.

Since Maximum Likelihood Estimation (MLE) is used, prior assumptions are that residuals show a Gaussian probability density function and monitoring data are statistically independent (i.e. no correlation between individual data points obtained from the experiments). This requires randomly distributed residuals (in space and time) implying that auto-correlation of residuals at one gauging point is negligible. Furthermore, there is no cross-correlation between residuals at different gauging locations. Consequently, the residuals are analysed with respect to the following:
- Posterior checking of Gaussian distribution;
- Remaining mean squared error (MSE);
- Bias.

3.2.4.7   Parameter set for calibration

As mentioned before, to be able to fully benefit of the calibration procedure, the only parameters that should be incorporated in the parameter optimisation process are process-related parameters. In this study, two types of process-related parameters are distinguished:
- physical characteristics:
  - hydraulic roughness of the conduits;
  - overflow coefficient for the weirs in the CSO structures;
- inflow parameters:
  - dry weather flow, consisting of wastewater and infiltration/inflow;
  - types of contributing areas.

3.3 Model calibration of case 'Tuindorp'

This section describes the model calibration as outlined in the previous section 3.2. The calibration procedure (Figure 3.3) starts with the choice of modelling concept (software package InfoWorks©) followed by preparing the model input consisting of the database describing the sewer system. This database must meet high standards because it affects the results of the calibration. Third, an applicable parameter set (process related parameters) on which the calibration will be based have to be chosen. In addition, differences between monitoring and model results are minimised by adjusting model parameters applying a genetic algorithm and the Levenberg–Marquart algorithm. To check prior assumptions and the quality of the calibration, the residuals have to be checked for bias, Gaussian distribution and correlation. Depending on the results the calibration has finished or has to be optimised. In case of sufficient calibration, the final results can be analysed.

3.3.1 Model concept

The model concept applied is a 1D hydrodynamic model using the full De Saint Venant equations combined with a hydraulic rainfall runoff model, simulated in InfoWorks© (version 13.0.6; Innovyze, 2012). The model is calibrated continuously in order to guarantee that it describes system behaviour as good as possible. If changes in residual characteristics occur, this is an indication of changes in system behaviour in time and most probably obstructions in the sewer system (i.e. blockages in pipes). Therefore, a 1D hydrodynamic model is needed. The rainfall runoff model is the NWRW 4.3 model, which is the standard rainfall runoff model applied in the Netherlands (Stichting RIONED, 2004; Van Luijtelaar and Rebergen, 1997; Van Mameren and Clemens, 1997). It describes evaporation, infiltration, storage on street surfaces and overland flow (Figure 3.4). In the model, each type of contributing areas is characterised by a routing coefficient (F), an initial storage loss (B) and an infiltration capacity (I). Initial losses (wetting of dry surfaces and storage in local surface depressions) are introduced as an average constant value depending on the type of contributing surface. The routing coefficient is based on the Desbordes runoff routing model (Desbordes, 1978; Fuchs, 1998). The infiltration capacity as a function of time is described with the Horton infiltration model (Horton, 1940). Evaporation is taken into account as a monthly averaged value based on potential evaporation (Penman, 1948; Stichting RIONED, 2004) in order to empty the surface storage in between storm events (Figure 3.4).

38
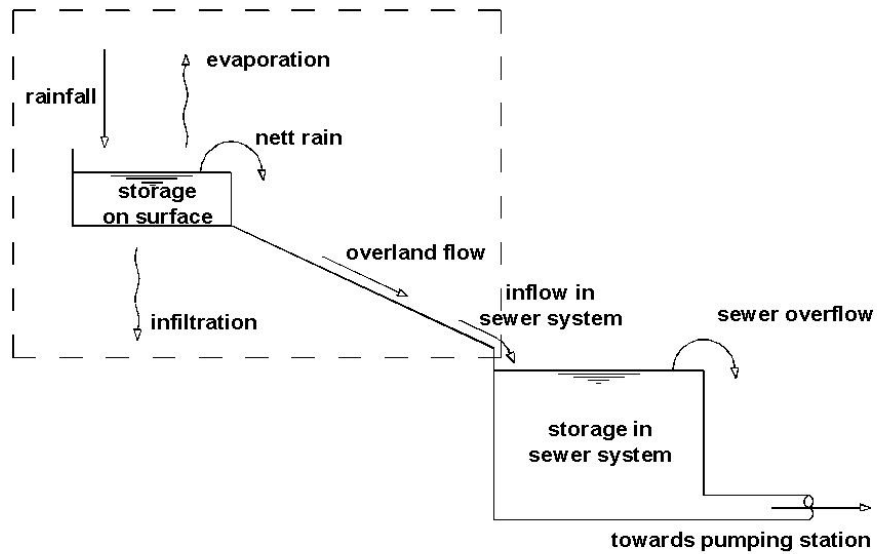
Figure 3.4: Rainfall runoff model (Stichting RIONED, 2004).

3.3.2 Model input

In order to minimise the uncertainties in the calibration results due to data errors in the model, the model input (i.e. network of nodes and links) has been validated to eliminate systematic errors in the model following the method described in Van Mameren and Clemens (1997) and Clemens (2001a). This required verification of structural and geometrical data (ground levels, unconnected nodes, illogical invert levels, crest width and level and so on) in the field.

The pumping station of the catchment transports the collected wastewater to a downstream catchment area. This discharge is incorporated in the model as a head discharge table. The discharge varies depending on the water level in the pump chamber. Variations in discharge are related to a changing static head. The table is based on information obtained from the measurement data at the pumping station (flow and water level) during the period June 2014 till May 2015. The head discharge relation is graphically represented in Figure 3.5.
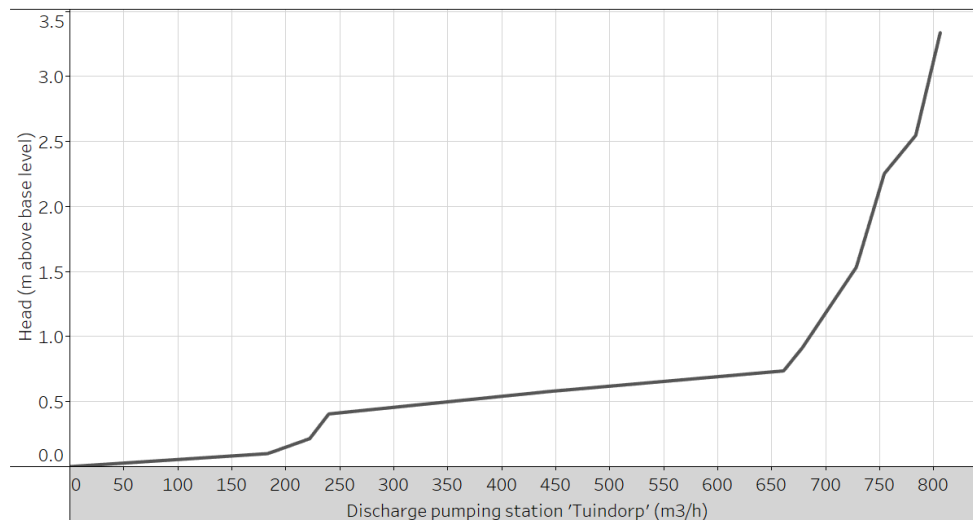
Figure 3.5: Outgoing discharge 'Tuindorp' pumping station based on flow and water level measurements at the pumping station for June 2014 – May 2015.

3.3.3   Measurement data

Two recorded storm events (11/07/2010 and 26/08/2010) have been used to demonstrate the impacts of observed in-sewer defects on the calibration results (Figure 3.6). The first storm event represents a short but heavy storm, the second event a storm with low rainfall intensities and a relatively long duration. Both storm events caused an overflow at all CSOs. These events have been chosen because of the high data quality and availability.

Two recorded storm events (05/05/2015 and 04/09/2015) have been used to calibrate the clean system (Figure 3.6). This is after removing the known defects in 2012 and the observed roots in July 2013 and April 2015 (Figure 3.2). Both storm events comprise low rainfall intensities and the latter one has a relative long duration. During event 05/05/2015 the total rainfall volume is 17 mm, for event 04/09/2015 this is 44 mm. During the first event no overflows occurred, the second caused overflows at all CSOs.

For obtaining a reduced parameter set applicable for all calibrations, the recorded storm event on 24/09/2014 has been used (Figure 3.6). This event has been chosen to obtain a representative reduced parameter set for calibrating both, a model affected by observed in-sewer defects and a model without the observed defects.
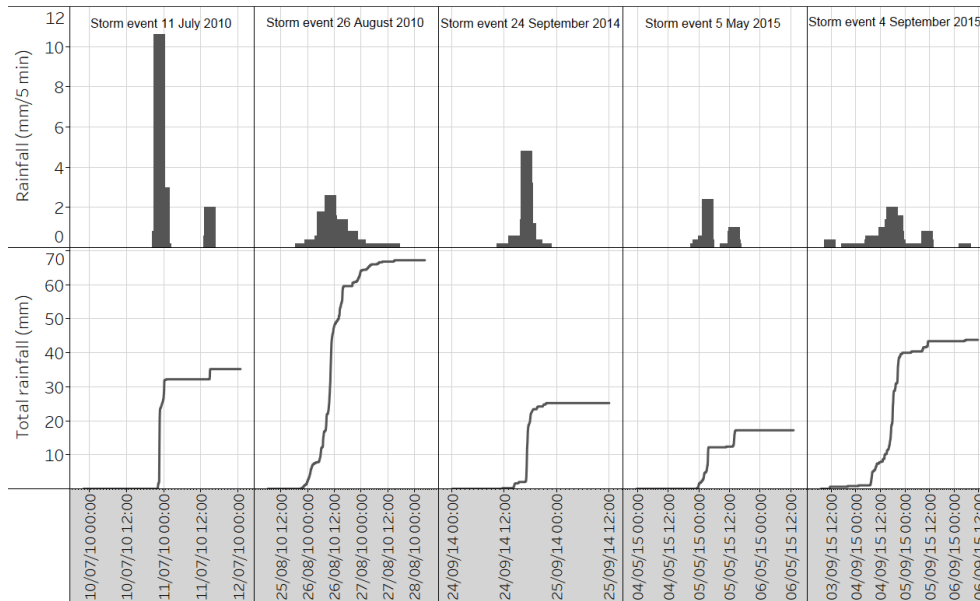
Figure 3.6:   Observed storm events for model calibration (11/07/2010, 26/08/2010, 05/05/2015) and obtaining the reduced parameter set (24/09/2014).

3.3.4   Parameter set for calibration

Theoretically, each manhole, conduit, surface type and weir can be assigned its own model parameter(s). However, this would lead to over 1,400 parameters to be calibrated for the 'Tuindorp' catchment. Since the number of model parameters should be an order of magnitude smaller than the amount of measurement data, the number of model parameters used for calibration should be reduced.

Rainfall runoff has been modelled as follows. Initially, five types of contributing areas are included as listed in Table 3.1. Typically, only four types are used in Dutch practice namely flat impervious (type 2), flat semi-pervious areas (type 5), flat roofs (type 8) and inclining roofs (type 7). However, in this catchment it is known that some larger flat semi-pervious areas, such as school play grounds or parking lots, have been provided with a very small number of gully pots, thus limiting the hydraulic inflow. In addition, the total amount of runoff water draining from large flat roofs during storm events is strongly affected by the local hydrological circumstances (Figure 3.7), resulting in very high initial losses. The influence of these high initial losses has also been measured by Jacobs et al. (2015) who demonstrated that during the days after a storm event, measured evaporation is higher than the reference evaporation due to evaporation of storm water

captured on flat roofs during storm events. These types of area have been modelled using a fifth type of contributing area indicated as catchment type 6.

Table 3.1: Parameter set for calibration of the hydrodynamic model.

full parameter set		reduced parameter set	
parameter	Description	parameter	Description
B2 (mm)	initial losses on flat, impervious areas	B2 (mm)	initial losses on flat, impervious areas and inclining roofs
B5 (mm)	initial losses on flat, semi-pervious areas	B5 (mm)	initial losses on flat, semi-pervious areas and flat roofs
B6 (mm)	initial losses on large flat, semi-pervious areas	B6 (mm)	initial losses on large flat, semi-pervious areas and large flat roofs
B7 (mm)	initial losses on inclining roofs	F2 (s)	routing coefficient for flat, impervious areas and inclining roofs
B8 (mm)	initial losses on flat roofs	F5 (s)	routing coefficient for flat, semi-pervious areas and flat roofs
F2 (s)	routing coefficient for flat, impervious areas	F6 (s)	routing coefficient for large flat, semi-pervious areas and large flat roofs
F5 (s)	routing coefficient for flat, semi-pervious areas	I5 (mm/h)	maximum infiltration capacity flat, semi-pervious areas and flat roofs
F6 (s)	routing coefficient for large flat, semi-pervious areas	I6 (mm/h)	maximum infiltration capacity large flat, semi-pervious areas and large flat roofs
F7 (s)	routing coefficient for inclining roofs	K (mm)	hydraulic roughness for all conduits
F8 (s)	routing coefficient for flat roofs	CC (m$^{0.5}$/s)	overflow coefficient for all CSOs
I5 (mm/h)	maximum infiltration capacity semi-pervious areas		
I6 (mm/h)	maximum infiltration capacity large, semi-pervious areas		
KZ (mm)	hydraulic top roughness for all conduits		
K2 (mm)	hydraulic bottom roughness for all conduits		
CC (m$^{0.5}$/s)	overflow coefficient for all CSOs		

Figure 3.7:   Local hydrological circumstances on roofs affecting total amount of runoff water (vegetation and storage).

First, the number of parameters has been reduced by incorporating the dry weather flow in the calibration process as a daily pattern. This daily pattern is based on information obtained from the measurement data at the pumping station (flow and water level). It is known that the dry weather flow in the 'Tuindorp' catchment also holds an amount of groundwater due to infiltration at leaking joints. Therefore, the dry weather flow is determined from measurement data during periods without precipitation and/or increased groundwater levels after a storm event. Days with (partly) missing data and data affected by maintenance activities in sewers and of sensors are also ignored in the analysis. Due to a lack of data (flowmeter and groundwater sensors were out of order for a long period) during the years 2011, 2013 and 2014, the analysis has been based on the data at the pumping station during 2010 and 2012. Figures 3.8 and 3.9 present the daily average dry weather flow and daily pattern. The average dry weather flow is approximately 1,444 m^3/d. With 10,656 inhabitants, this adds up to a wastewater production of 136 l/inh/d. This confirms the presumption of groundwater entering the system, since the average drinking water consumption is 125 l/inh/d.

To incorporate dry weather flow in the model, the dry weather flow production per manhole was determined. For that purpose, inhabitants are assigned to the manholes in the model according to the population and the observed hourly discharge is translated into a dry weather flow pattern as a function of the total dry weather flow production per inhabitant per day (Figure 3.9). Second, the parameter set has been reduced by clustering. This means that each conduit receives the same top and bottom hydraulic roughness and each CSO with the same overflow coefficient. Third, correlation analysis has been performed to identify parameters less relevant for the calibration process and reduce the parameter set accordingly.
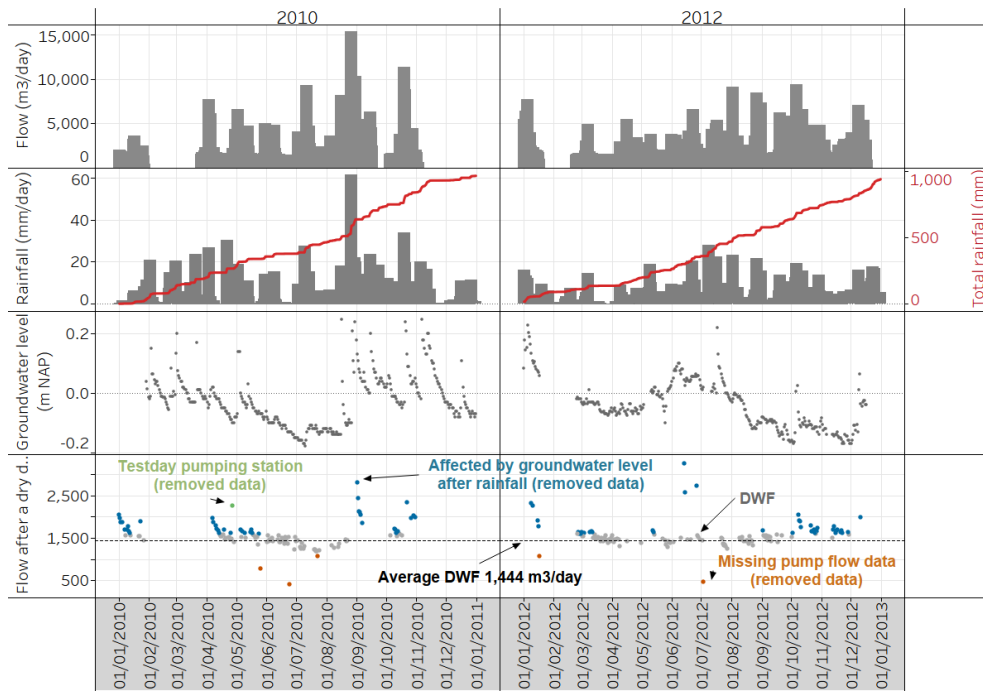
Figure 3.8: Average daily dry weather flow obtained from measurement data at the pumping station in the 'Tuindorp' catchment. The dry weather flow is determined from measurement data during periods in which no precipitation occurred and increased groundwater level (after a storm event) no longer affects the dry weather flow because of infiltration. Furthermore, days with (partly) missing data and data affected by maintenance or construction activities are also ignored in the analysis.
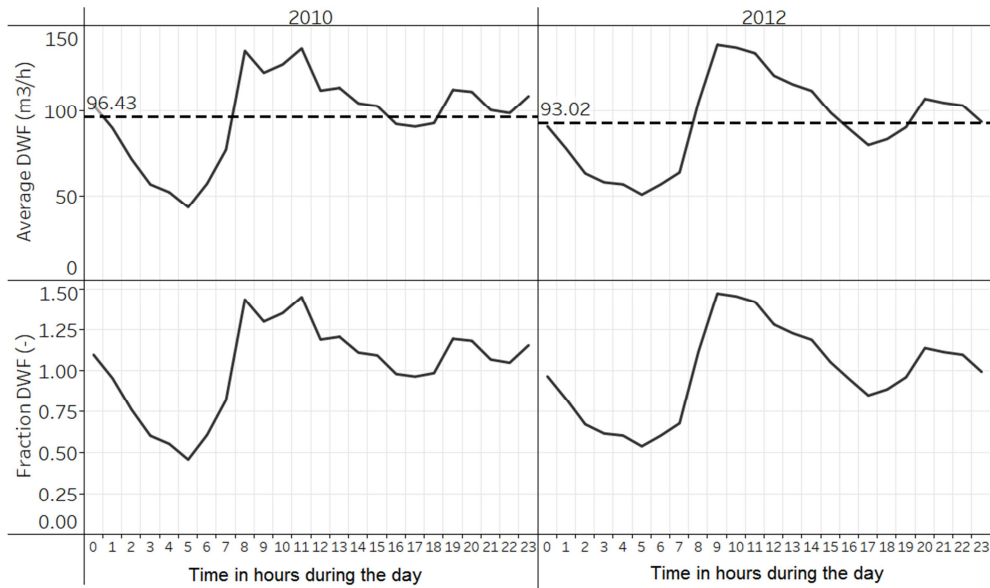
Figure 3.9: Daily pattern dry weather flow on the 'Tuindorp' catchment for 2010 and 2012.

3.3.5 Identifiability of parameters

The correctness of parameters after calibration can be judged in terms of uniqueness and identifiability (Carrera and Neuman, 1986b). Uniqueness of the parameters is achieved by applying a genetic algorithm (see subsection 3.3.7). Identifiability means that one set of parameters leads to just one possible result. Information to judge identifiability of parameters is available in a Jacobian matrix (Carrera and Neuman, 1986b). The Jacobian uses the difference between measured and simulated water levels to describe the sensitivity of the object function for each parameter.

If the Jacobian is (nearly) rank deficit, the dimensionality of the optimisation problem is chosen too large given the available information. Singular value decomposition (SVD) provides an efficient way to judge whether a matrix is (nearly) rank deficit (Jacobson, 1985). Mutual interdependency of parameters can also be analysed using SVD. When a singular vector has elements corresponding to more than 1 parameter this implies that only a linear combination of these parameters can be identified by calibration. Finally, when the SVD of the Jacobian reveals one or more singular values (almost) equal to zero, the corresponding parameter(s) are not identifiable.

45

When there is no physical explanation of parameter interdependency, interdependency of calibrated model parameters may result from errors in the model concept (missing processes that significantly affect monitoring result, but not accounted for in the model), or an incorrect choice of parameters to be calibrated. When, however, physical explanation can be formulated for parameters being interdependent, these parameters can be clustered in the model. Correlation between the model parameters after calibration is described with the covariance matrix. This matrix can be easily derived from the Jacobian (see e.g. Clemens, 2001a). The diagonal terms of the covariance matrix give an indication of the quality of the parameter estimates. The off-diagonal terms give an indication of the correlation between the parameters.

The results of the SVD of the Jacobian at the minimum value of the goal function and the eigenvectors of the parameter covariance matrix provide valuable information on the identifiability of the model parameters. The Jacobian uses the difference between measured and simulated water levels for the sensitivity of the object function for each parameter. Consequently, the SVD provides information on the identifiability of each parameter given the model applied and given the measurements. The parameter set has been reduced accordingly. This means that model parameters with the largest singular values are selected for calibration, parameters with a singular value of (almost) zero are excluded and parameters with a too large mutual correlation are combined into a joint parameter (see also Clemens, 2001a).

3.3.6   Reduction of parameter set

As it is impossible to find a parameter set that fits for every storm event, choices have to be made with respect to which parameters should be incorporated in the calibration process. In Table 3.1 the full parameter set is presented. The reduction of parameters is explained by means of the calibration of the storm event on 24 September 2014 (Figure 3.6).

As can be seen in the correlation matrix of the full parameter set in Figure 3.10, the parameters B2, B7 and B8 are strongly correlated. This also counts for the parameters F5-B6, F2-F6, I5 with B5-B6 and F5 and the roughness parameters KZ-K2. This implies that those parameters are less identifiable. A positive correlation means that in order to keep the residuals small, an increase of one parameter value will be compensated by an increased value of the other parameter. The opposite is true for a negative correlation. The other correlations in the matrix in Figure 3.10 are small enough.

46

	B2	B5	B6	B7	B8	F2	F5	F6	F7	F8	I5	I6	KZ	K2	CC
B2	1.00														
B5	-0.11	1.00													
B6	0.08	-0.30	1.00												
B7	0.67	-0.12	0.08	1.00											
B8	-0.88	0.17	-0.14	-0.74	1.00										
F2	0.01	-0.01	0.01	0.00	-0.01	1.00									
F5	0.10	-0.22	0.80	0.05	-0.04	0.01	1.00								
F6	0.01	-0.01	0.00	0.00	-0.01	0.85	0.01	1.00							
F7	0.05	-0.39	0.39	0.09	-0.30	0.01	0.00	0.00	1.00						
F8	-0.15	0.03	0.07	-0.08	-0.01	-0.03	0.07	-0.03	-0.12	1.00					
I5	-0.02	-0.54	-0.49	-0.01	-0.06	0.00	-0.54	0.00	-0.03	-0.10	1.00				
I6	0.00	0.01	-0.01	0.00	0.00	0.00	0.00	0.00	-0.02	0.00	0.00	1.00			
KZ	0.02	0.08	0.41	0.04	0.11	-0.01	0.19	-0.02	-0.22	-0.04	-0.22	0.00	1.00		
K2	-0.06	0.06	-0.26	-0.03	-0.14	0.00	-0.11	0.01	-0.03	0.01	0.27	0.01	-0.63	1.00	
CC	0.00	0.01	-0.02	0.00	0.00	0.00	0.00	0.00	-0.02	0.00	0.01	0.00	0.00	0.01	1.00

Figure 3.10: Correlation matrix full parameter set storm event 24/09/2014. B is initial storage, F is the routing coefficient, I is infiltration, K is roughness and CC is the overflow coefficient. Significant values in bold. For more explanation of the presented parameters see table 3.1.

Because of the high correlation between several parameters after calibration, the set has been reduced to 10 parameters. This has been done by clustering the runoff parameters initial storage and routing coefficient for the area types flat impervious and inclining roofs (B2, F2), flat semi-pervious and flat roofs (B5, F5) and large flat semi-pervious and large flat roofs (B6, F6). Furthermore, the hydraulic top and bottom roughness for all conduits are clustered (K).

Figure 3.11 illustrates that there remains a negative correlation in the reduced set between the parameters routing coefficient for flat, impervious areas and inclining roofs (F2) and the routing coefficient for flat, semi-pervious areas and flat roofs (F5). In addition, there is also a (negative) correlation of importance present between the maximum infiltration capacity on flat, semi-pervious areas and flat roofs (I5) and the initial losses on this area type (B5). This implies that in case of increasing one of the parameters, the other corresponding parameter must be decreased in order to maintain the fit between measurements and model results.

	B2	B5	B6	F2	F5	F6	I5	I6	K	CC
B2	1.00									
B5	0.00	1.00								
B6	0.00	-0.01	1.00							
F2	0.00	0.18	-0.01	1.00						
F5	0.00	-0.28	0.01	-0.85	1.00					
F6	-0.02	0.06	0.00	-0.25	0.27	1.00				
I5	0.00	-0.95	0.00	-0.06	0.10	-0.11	1.00			
I6	0.00	0.00	0.00	0.00	0.00	-0.01	0.00	1.00		
K	0.00	0.02	0.00	0.04	-0.05	-0.01	0.00	0.00	1.00	
CC	0.00	0.00	0.00	0.01	-0.01	-0.02	0.00	0.00	0.00	1.00

Figure 3.11: Correlation matrix reduced parameter set storm event 24/09/2014. B is initial storage, F is the routing coefficient, I is infiltration, K is roughness and CC is the overflow coefficient. Significant values in bold. For an explanation of the presented parameters see table 3.1.

However, as the correlation between parameter values for different types of contributing area is limited to the routing coefficient only, this remaining over parametrisation has been accepted to be able to also calibrate storm events with a different characteristic. The parameter CC in Table 3.1 represents the overflow coefficient which is used for the weir flow equations in InfoWorks©. The parameter has the same value in the calibrations for all five CSO structures.

3.3.7 Optimisation algorithm

The optimisation is based on MLE, see e.g. Carrera and Neuman (1986a). The likelihood of the model parameters is maximised given the objective function and the data. The advantage of formulating it statistically is that this enables the estimation of both the parameters controlling system behaviour and their uncertainties (e.g. variance). Parameter values are estimated based on the water level measurements obtained at each measurement location. In order to minimise the differences between measured and modelled water levels, the optimisation algorithm has to be able to explore the full range of the objective function and also converge properly.

As the objective function in model calibration typically shows multiple optima (Clemens, 2001a), classical gradient-based optimisation techniques have a limited applicability. To overcome this problem, a genetic algorithm (Holland, 1975; Rauch and Harremoës, 1999a, 1999b) has been applied for obtaining a first estimate for the parameter values and an impression of the shape of the goal function in terms of the presence of local minima and the curvature of the goal function around the solutions found.

This first estimate is followed by the Levenberg–Marquart algorithm (Marquardt, 1963) for fine-tuning the parameter estimates. For the calibration, the Parameter ESTimation package has been applied (Doherty, 2005). The Levenberg–Marquart method not only provides information on the best fit, but also reveals whether or not the parameters are independent from each other and information on the accuracy of the parameter estimates.

3.4   Results and discussion

3.4.1   Results

3.4.1.1   System condition in time

The 'Tuindorp' system was monitored during the period January 2010 - September 2015 to obtain the hydraulic characteristics with known defects in the system. In the first months of 2012, the whole sewer system has been cleaned. Afterwards observed defects were removed, except the observed root intrusions (class 5) between the locations Lev12 - Lev13 (Professor Jordanlaan), Lev 23 - Lev24 (Troosterlaan) and the locations Lev26 - Lev27 (Jan van Galenstraat). Those root intrusions were removed afterwards in 2013 and 2015 (see Figure 3.2). From April to September 2015, the system has been monitored to obtain information suitable for calibrating the model of the clean system. As the last cleaning operation was in 2012 and the regular average cleaning frequency of sewers in the Netherlands is between 7 and 10 years, the system under observation has been considered to be 'clean'.

3.4.1.2 Selected storm events for calibration

In the period April 2015 and September 2015, after removing the known defects (Figure 3.2) the following two recorded storm events have been selected as representative for calibrating the clean system: 05/05/2015 and 04/09/2015 (Figure 3.6). The calibration results of the clean system are compared with the calibration results of the two storm events 11/07/2010 and 26/08/2010. In the calibration results of the latter, two storm event impacts of observed in-sewer defects were present (Figure 3.2).

3.4.1.3 Residual analysis event 04/09/2015

An analysis of the residuals provides information on the quality of the calibration results. As an example, in case of three measurement locations (Lev7, Lev10 and Lev19) the measured and calibrated water levels and the residuals for storm event 04/09/2015 are shown in the Figures 3.12 - 3.14 (see also Figure 3.1 for the monitoring locations in 'Tuindorp'). Lev7 (Figure 3.12) is situated downstream in the sewer system, nearby the pumping station and a CSO. Lev10 (Figure 3.13) is located more upstream in the sewer system. Finally, Lev19 (Figure 3.14) is situated in the centre of the sewer system. At all three monitoring locations (for storm event 04/09/2015), the residuals have an order of magnitude of ±0.10 m. The order of magnitude of the residuals at the other monitoring locations is in accordance with the order of magnitude found for the three monitoring locations Lev7, Lev10 and Lev19.
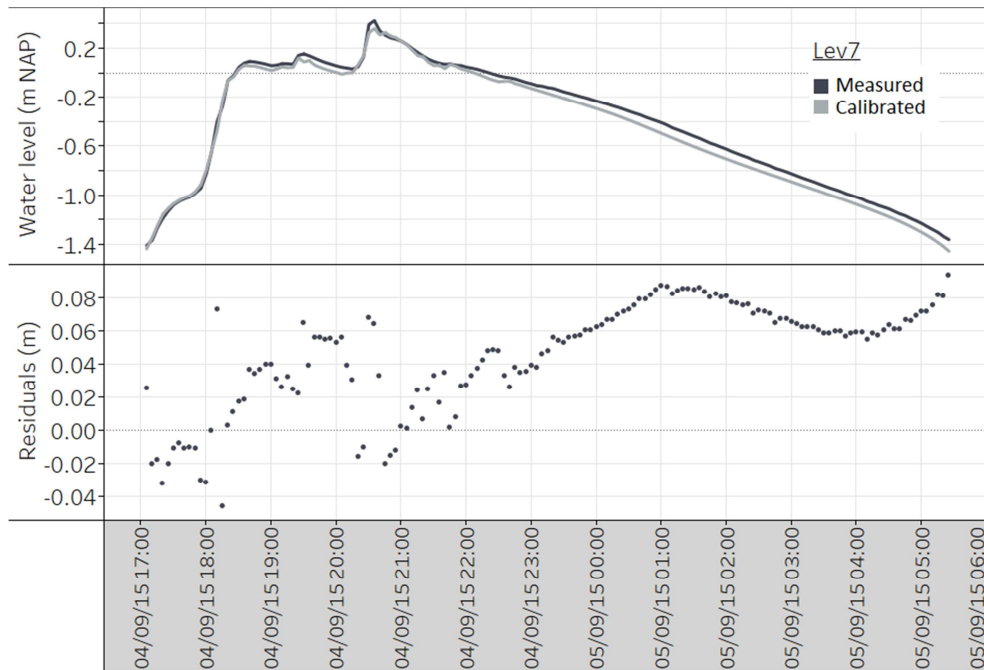
Figure 3.12: Measured and calibrated water levels Lev7 storm event 04/09/2015 (top). Lev7 is situated downstream in the 'Tuindorp' sewer system, nearby the pumping station and a CSO (see also Figure 3.1 for the location). NAP is reference level for the measured and calibrated water levels. Negative measured and calibrated values represent water levels below this reference. The residuals are the differences between measured and calibrated water levels in m (bottom).
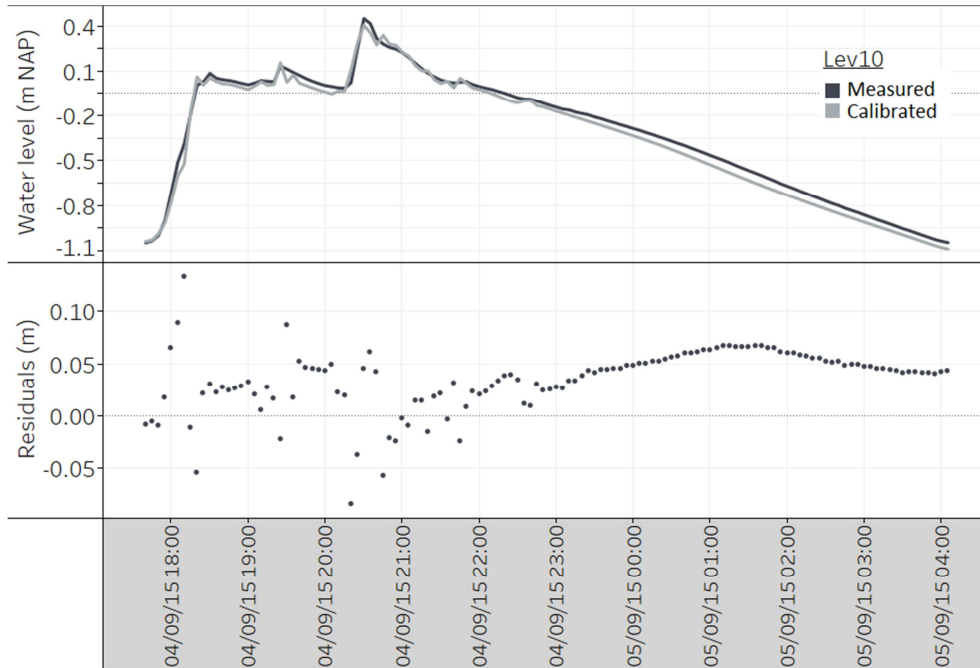
Figure 3.13: Measured and calibrated water levels Lev10 storm event 04/09/2015 (top). This monitoring location is located more upstream in the 'Tuindorp' sewer system (see also Figure 3.1 for the monitoring location). NAP is reference level. Negative measured and calibrated values represent water levels below this reference. The residuals are the differences between measured and calibrated water levels in m (bottom).

Figure 3.14: Measured and calibrated water levels Lev19 storm event 04/09/2015 (top). This monitoring location is situated in the centre of the 'Tuindorp' sewer system (see also Figure 3.1 for the monitoring location). NAP is reference level. Negative measured and calibrated values represent water levels below this reference. The residuals are the differences between measured and calibrated water levels in m (bottom).
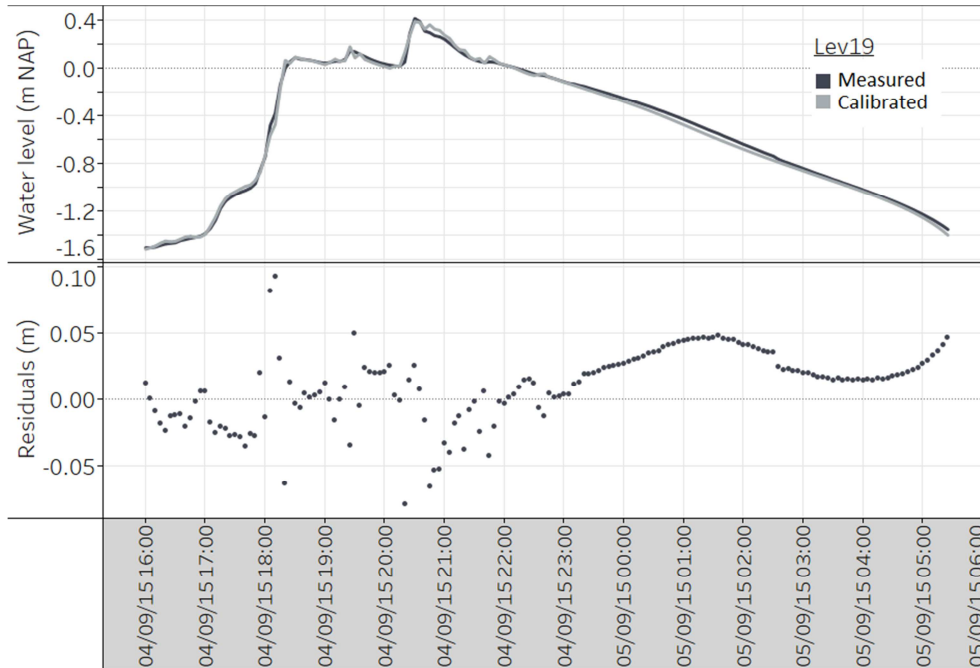
In Figure 3.15, the normal probability plots of the four different storm events are shown. The storm events 05/05/2015 and 04/09/2015 are representing the results of calibrating the clean system and the storm events 11/07/2010 and 26/08/2010 are representing the results of the calibration of the system including defects for all monitoring locations. Comparison of the figures shows that the calibration of the system including defects produces residuals with substantially more systematic errors compared to the calibration of the clean system. The residuals are displayed with the symbol '+' and the normal distribution is displayed with the symbol '– –'.

The residuals are also checked for normality using the Lilliefors test (Conover, 1999). This test returns a statistic for the null hypothesis that the residuals after calibration are normally distributed, against the alternative that they are not. Based on the Lilliefors test, the null hypothesis (at the 5% significance level) is rejected for all four storm events. The residuals of all events appear to have heavier tails than is expected for Gaussian distributions.
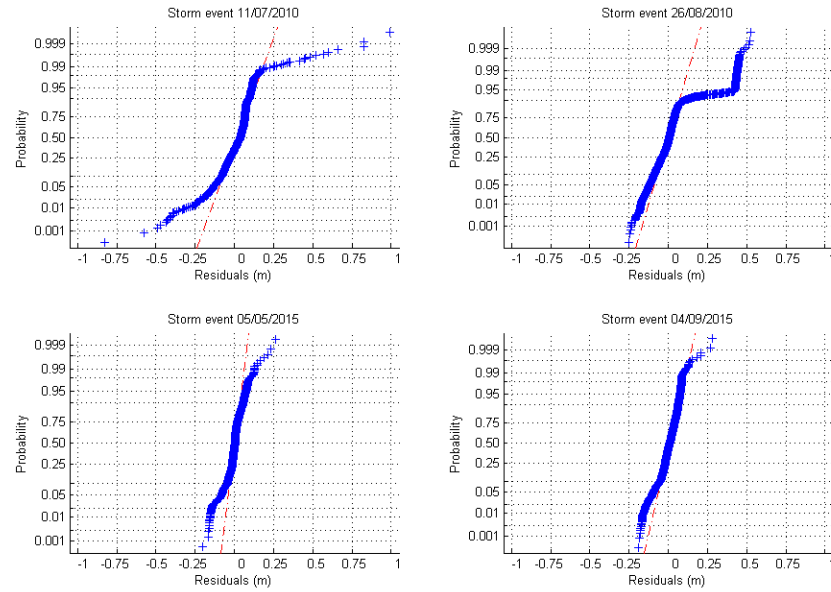
Figure 3.15: Normal probability plots of residuals after calibration of the clean system (storm events 05/05/2015 and 04/09/2015) (bottom) and the system including defects (storm events 11/07/2010 and 26/08/2010) (top). Residuals of all measuring locations.

3.4.1.4   Systematic errors and possible causes

It is concluded that in all cases systematic errors are present, although they are smaller for the clean system. Because the monitoring data and data errors in the model have been validated to eliminate systematic errors as much as possible, the remaining systematic errors are likely due to the presence of in-sewer defects and/or model structure.

When comparing the calibration results from the clean system (storm events 2015) with the calibration results including the observed defects (storm events 2010), it is clear that a larger deviation from Gaussian is present in case of the storm events in 2010. Cleaning of the system and the removal of the observed defects in 2012 can be an explanation for these changes.

3.4.1.5   Bias analysis event 04/09/2015

In Figure 3.16, the distribution over time for the remaining bias and MSE for location Lev19 is shown. Both the bias and the MSE increase during the overflow stage and during the emptying stage and are at their maximum when the system is being emptied. The latter is possibly caused by varying pumping capacities due to changes in pressure head at

the suction side of the pump. In addition, after cleaning the system in 2012 it is possible that sedimentation during the period after 2012 affects the bias. In general, the results with respect to the remaining bias and MSE are comparable with the values found for the applied systems in Clemens (2001a). The analyses of both parameters for the other locations are comparable with location Lev19.
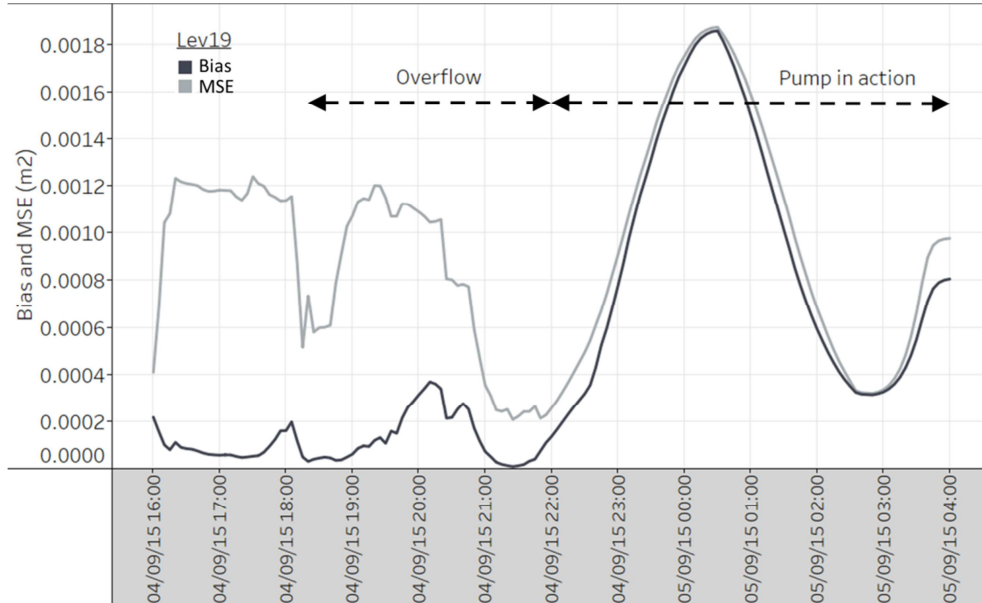
Figure 3.16: Bias and MSE for location Lev19 during storm event 04/09/2015. In this case the system is considered to be clean.

3.4.1.6   Correlation analysis of residuals

In the perfect case residuals show no spatial (or temporal) correlation. Hence, spatial correlation between residuals is an indication for some change in the system. This, however, is only achievable when the model describes the processes perfectly, the geometry of the system is perfectly known and there are no systematic measuring errors. It is clear that this is not achievable in practice. A larger correlation between the residuals of a number of monitoring locations in one storm compared to another is an indication of some type of change in the system (provided of course that the same model concept, geometry and quality of monitoring data are applied).

The presence of spatial correlation between residuals is illustrated with an example. Assume the sewer system under consideration consists of two parts connected with a pipe. The water level is monitored in each part. After calibrating the model for storm 1, the correlation between the residuals for both parts is small (e.g. 0.1) and a value for K is found to be 2 mm. Now suppose a blockage occurs in the connecting pipe and the model calibrated for storm 2. After calibration a much larger correlation (e.g. 0.9) and K value (e.g. 10 mm) are found. The increased K value indicates that there is an increase in resistance. The increased correlation indicates that this increased resistance is caused by an obstruction between both parts of the system.

It should be noted that the increased value for K will be mainly caused by the calibration algorithm trying to increase the head difference assuming that this is caused by an increased wall roughness, while in reality it is a blockage (i.e. a change in the geometry of the system). This will, however, result in a systematic error between model and monitoring result because during the emptying phase after the storm event, the discharges and flow velocities are very low and it is no longer feasible to keep the head difference in the model in line with the monitoring data by further increasing the value for K.

Hence spatial correlation between residuals is an indication for some change in the system. Certainly, this is strongly dependent on the characteristics of the storm event: higher rain intensities will result in increased discharges which in turn translate into an increased head difference. The characteristics of the emptying stage of the system, on the other hand, only depend on the pumping capacity and the geometry of the system.

The results of the correlation analysis of residuals may be disturbed by the occurrence of flooding. This turns out when comparing the storm events of 11/07/2010 and 26/08/2010. The first represents a short but heavy storm, the second a storm with low rainfall intensities and relatively long duration. Only the event of 11/07/2010 caused flooding in the model simulation. As the water-level measurements did not reach ground level, it is clear that the model simulated higher water levels in comparison with reality. Because overland flow is not modelled the simulation results will be inaccurate due to the flooded period. This may affect the correlation between the residuals considerably. Therefore, the model results with flooding should not be used for checking the correlation between residuals at different locations.

3.4.1.7 Correlation analysis per event

The two locations with root intrusion, Professor Jordanlaan (Lev12-Lev13) and Jan van Galenstraat (Lev26-Lev27), have been studied with respect to correlation between the measured water levels down and upstream of the roots and the correlation between the final residuals after calibration. Regarding the location of Professor Jordanlaan, the downstream measurement locations are Lev6, Lev12 and Lev22 and the upstream measurement locations are Lev13 and Lev14 (see Figure 3.1). The downstream measurement locations of Jan van Galenstraat areLev27, Lev15 and Lev17, upstream it concerns Lev26, Lev25 and Lev16 (see Figure 3.1).

In Table 3.2 the correlation between the measured water levels at different locations is shown for storm event 11/07/2010. The measured water levels downstream the roots for Professor Jordanlaan (Lev6, Lev12 and Lev22) are highly correlated with the measured water levels upstream the roots (Lev13 and Lev14). In the case of Jan van Galenstraat, similar observations can be made. In general, the results are comparable with the values found in case of the two other storm events 26/08/2010 and 04/09/2015 at both locations.

Table 3.2: Correlation between measured water levels up- and downstream the observed root intrusion Professor Jordanlaan and Jan van Galenstraat for storm event 11/07/2010. Monitoring locations located in the upstream part are in bold. See Figure 3.1 for the monitoring locations.

	Professor Jordanlaan				
	Lev6	Lev12	**Lev13**	**Lev14**	Lev22
Lev6	-	0.85	0.78	0.81	0.80
Lev12	0.85	-	0.94	0.96	1.00
Lev13	0.78	0.94	-	0.99	0.93
Lev14	0.81	0.96	0.99	-	0.96
Lev22	0.80	1.00	0.93	0.96	-

	Jan van Galenstraat					
	Lev15	**Lev16**	Lev17	**Lev25**	**Lev26**	Lev27
Lev15	-	0.992	0.940	0.992	0.941	0.865
Lev16	0.992	-	0.957	0.999	0.971	0.902
Lev17	0.940	0.957	-	0.966	0.989	0.982
Lev25	0.992	0.999	0.966	-	0.974	0.913
Lev26	0.941	0.971	0.989	0.974	-	0.977
Lev27	0.865	0.902	0.982	0.913	0.977	-

Tables 3.3 and 3.4 present the correlation between the residuals of three locations downstream of the root intrusion at location Jan van Galenstraat and three locations upstream. The downstream (DS) cluster comprises the sensors Lev17, Lev15 and Lev27, the upstream (US) cluster the sensors Lev26, Lev25 and Lev16 (see Figure 3.1). The tables are showing that the within cluster correlations are relatively high (> 0.8). On average, 0.98 and 0.96 for the 11/07/2010 event and 0.89 and 0.93 for the 26/08/2010 event. The between cluster correlations, on the other hand, are much lower (on average 0.62 and 0.17, respectively).

Table 3.3:   Correlation between residuals after calibration up- and downstream observed root intrusion Jan van Galenstraat for storm event 11/07/2010. See Figure 3.1 for the monitoring locations.

	Jan van Galenstraat, downstream of root intrusion		
	Lev15	Lev17	Lev27
Lev15	-	0.98	0.98
Lev17	0.98	-	0.99
Lev27	0.98	0.99	-
	Jan van Galenstraat, upstream of root intrusion		
	Lev16	Lev25	Lev26
Lev16	-	1.00	0.93
Lev25	1.00	-	0.94
Lev26	0.93	0.94	-

Table 3.4:   Correlation between residuals after calibration up- and downstream observed root intrusion Jan van Galenstraat for storm event 26/08/2010. See Figure 3.1 for the monitoring locations.

	Jan van Galenstraat, downstream of root intrusion		
	Lev15	Lev17	Lev27
Lev15	-	0.87	0.81
Lev17	0.87	-	0.99
Lev27	0.81	0.99	-
	Jan van Galenstraat, upstream of root intrusion		
	Lev16	Lev25	Lev26
Lev16	-	0.99	0.92
Lev25	0.99	-	0.88
Lev26	0.92	0.88	-

Tables 3.5 and 3.6 display the correlation between the residuals of three locations downstream of the root intrusion at location Professor Jordanlaan and two locations upstream. The downstream cluster comprises the sensors Lev6, Lev12 and Lev22, the upstream cluster the sensors Lev13 and Lev14 (see Figure 3.1). The tables are showing that the within cluster correlations are relatively high (>0.73). On average, 0.87 (DS) and

0.98 (US) for the 11/07/2010 event and 0.85 (DS) and 0.87 (US) for the 26/08/2010 event. The between-cluster correlations, on the other hand, are much lower (on average 0.17 and 0.48 respectively). Unfortunately, for the 04/09/2015 event not all sensors provided good data. As a result, a comparison for this event was not possible.

Table 3.5: Correlation between residuals after calibration up- and downstream observed root intrusion Professor Jordanlaan for storm event 11/07/2010. See Figure 3.1 for the monitoring locations.

	Professor Jordanlaan, downstream of root intrusion		
	Lev6	Lev12	Lev22
Lev6	-	0.81	0.83
Lev12	0.81	-	0.97
Lev22	0.83	0.97	-
	Professor Jordanlaan,upstream of root intrusion		
	Lev13	Lev14	
Lev13	-	0.98	
Lev14	0.98	-	

Table 3.6: Correlation between residuals after calibration up- and downstream observed root intrusion Professor Jordanlaan for storm event 26/08/2010. See Figure 3.1 for the monitoring locations.

	Professor Jordanlaan, downstream of root intrusion		
	Lev6	Lev12	Lev22
Lev6	-	0.83	0.74
Lev12	0.83	-	0.97
Lev22	0.74	0.97	-
	Professor Jordanlaan,upstream of root intrusion		
	Lev13	Lev14	
Lev13	-	0.87	
Lev14	0.87	-	

The high within-cluster correlation can be explained because the calibration process accounts for the in-sewer defect root intrusion. This does not depend on the sensor which is chosen within each cluster. Hence, it is not necessary to have monitoring equipment exactly upstream and downstream of an obstruction, as is the case for this catchment, in order to observe changing system behaviour due to in-sewer defects using model calibration.

Correlation analysis demonstrates that the impact of the roots cannot be proven just by studying the existence of correlation between the measured water levels. For both situations, the system including defects and the clean system, correlations between measured water levels up and downstream the root intrusion can be high. However, correlation analysis of residuals after calibration reveals differences and allows identification of in-sewer defects. For reliable results the correlation analysis should be combined with the previous results.

3.4.1.8   Comparison of system condition

The boxes, whiskers and data points located beyond the whiskers in Figure 3.17 present the distributions of the different sets of mean values of residuals for all locations during the four storm events. From this figure, it can be seen how these distributions change. Each box encodes 50% (the middle two quartiles of the data's distribution) of mean values of residuals for the storm event. The edge between the dark and light grey colour represents the median of the residuals per event. The two lines (whiskers), one extending upwards from the top of the box and the other one extending downwards from the bottom of the box, encode additional information about the shape of the distribution. The length of the whiskers is 1.5 times the width of the adjoining box. The remaining mean values of residuals are located beyond the whiskers.

The storm events of 05/05/2015 and 04/09/2015 (clean system) have a lower mean median value of the residuals than the other two storm events (system with defects). The residuals originate from measuring errors, database errors and processes not taken into account in the modelling (i.e. sediment deposits and in-sewer defects). As the monitoring data and database of the sewer model have been validated, the only remaining systematic differences between the events are the known in-sewer defects. Antecedent conditions (e.g. available infiltration capacity) affect the residuals only to a limited extent.

In addition, the mean values of residuals per measuring location show a greater range in the two 2010 events (with defects) in comparison with the 2015 events (without defects). The measurement locations with the lowest mean differences are part of the May 2015 event. The highest mean residuals in the July and August 2010 events are increased substantially to 0.17 and 0.38 m at location Lev13. Furthermore, Lev14 in both 2010 events also reveals a high value. Looking at the 2015 events, it can be seen that Lev22 (event 05/05/2015) and Lev6 (event 04/09/2015) have the highest mean residuals in the 2015 events.
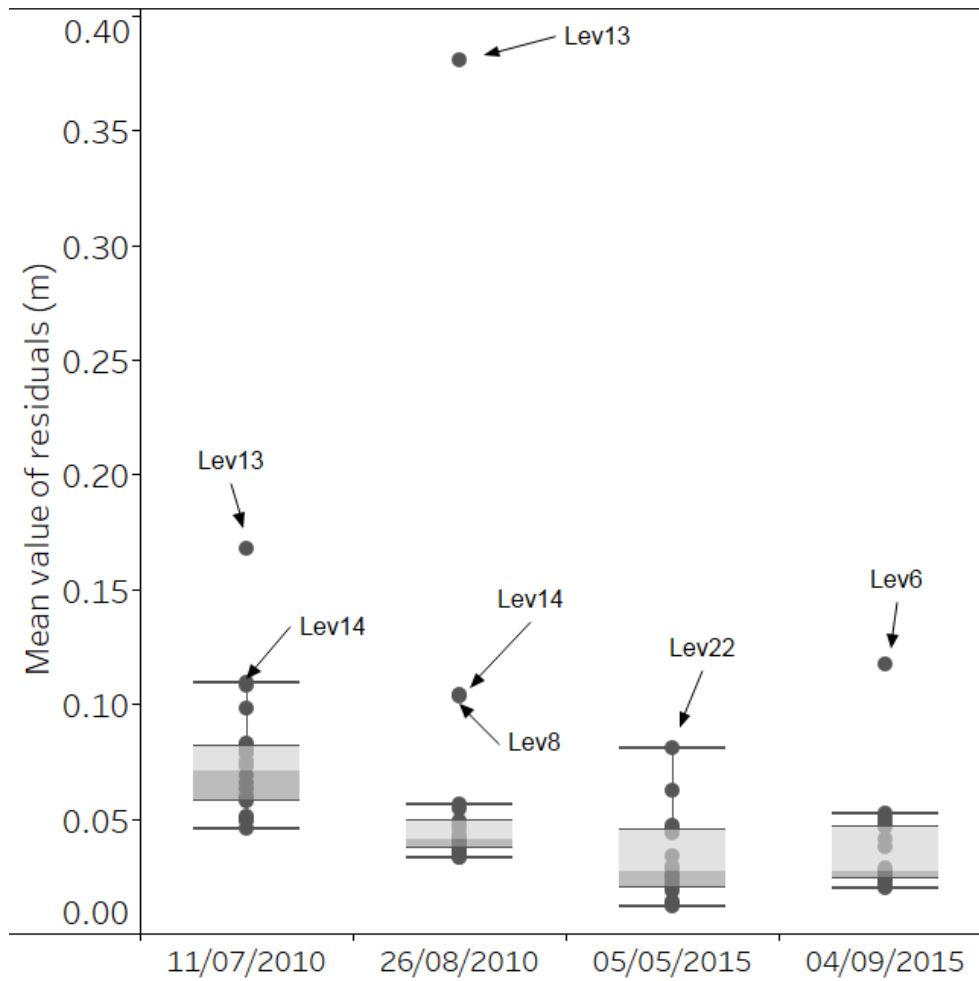
Figure 3.17: Mean value of residuals per event after calibration of the clean system (events 05/05/2015 and 04/09/2015) and the system including in-sewer defects (events 11/07/2010 and 26/08/2010).

In general, the results show that the presence of defects substantially influences the calibration results. Less accurate (or more biased) calibration results are an indication that system behaviour is changing. This is revealed by the fact that most of the mean residuals per location, in the results of the two storm events with defects are higher than those for the storm events in the clean system.

3.4.1.9 Comparison of results per event

In Figure 3.18, the bars are representing the individual mean values of the residuals for the different measurement locations. In addition, the applied events are positioned next to each other on the horizontal axes for each measurement location. This allows comparison of residuals per monitoring location and event.
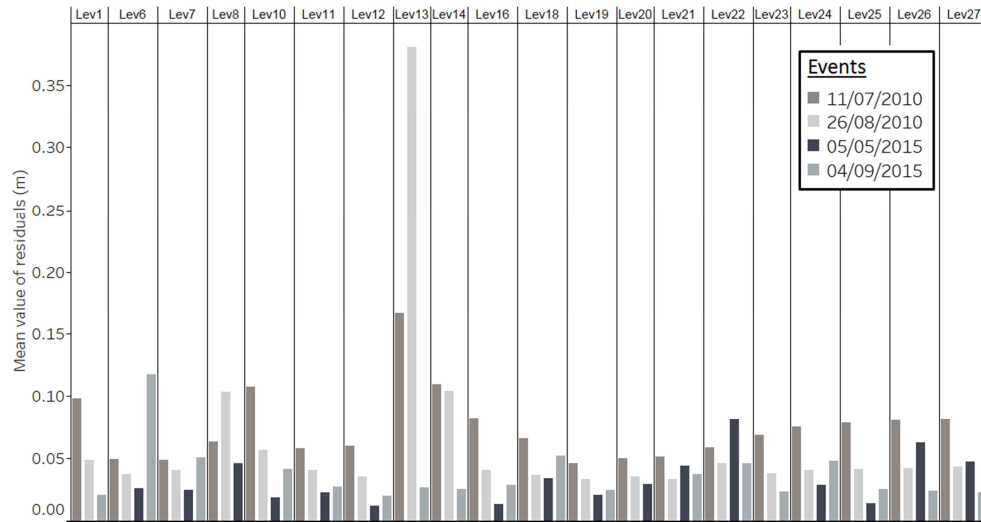

Figure 3.18: Mean value of residuals per sensor after calibration of the clean system (events 05/05/2015 and 04/09/2015) and the system including in-sewer defects (events 11/07/2010 and 26/08/2010).

The highest mean residuals in the July and August 2010 events appear at Lev13 and Lev14 (0.15 and 0.38 m, respectively). This is caused by root intrusion between the locations Lev12 and Lev13 (see Figure 3.1). This root intrusion is presented in Figure 3.19. In this figure for storm event 26/08/2010, the calibrated and measured water levels have been compared for the upstream measurement location Lev13. NAP is reference level. Consequently, negative values represent measured and modelled (calibrated) water levels below this reference level. It shows that there is an initial backwater effect upstream of the root intrusion, resulting from dirt that sticks to the roots and obstructs the small remaining opening below the roots.

Figure 3.19: Measured and modelled (calibrated) water levels upstream (Lev13) root intrusion Professor Jordanlaan for event 26/08/2010. NAP is reference level. Negative measured and calibrated values represent water levels below this reference.

3.4.2   Discussion

In the Netherlands, sewer systems are designed and assessed based on the Urban Drainage Guideline (Stichting RIONED, 2004). This guideline provides default values for runoff and process parameters. Although the guideline allows to adapt the model parameters after model calibration, the default values are typically used for assessing the performance of sewer systems. The default values are considered to be on the safe side, i.e. underestimating runoff losses as well as hydraulic friction.

Calibration of the 'Tuindorp' catchment has shown that initial losses on the large, flat, semi-impervious areas with a low gully pot density as well as large roof areas are often nearly equal to the total rainfall depth. These values are much higher than the default values. Thus, showing that for this specific catchment using the default model parameter values results in a design, which is safer than assumed. Consequently, engineers using this default parameter values in practice for designing systems should be aware of the fact that this could lead to over or underestimated system design.

The calibration has also shown that in-sewer defects, such as root intrusion, result in very high (local) hydraulic losses, exceeding the default hydraulic roughness values by far. This means that using the default values for hydraulic roughness will overestimate sewer system performance. The objective of this chapter was to demonstrate the principle of 'hydraulic fingerprinting' based on model calibration to identify in-sewer defects affecting hydraulic performance. This is demonstrated with the 'Tuindorp' combined sewer system. An extended monitoring network and a validated model database have been used for this purpose.

The application of the proposed methodology shows very promising results when applied to the 'Tuindorp' sewer system. Given the background of the methodology, i.e. detecting changes in system behaviour based on changes in characteristics of residuals, it is expected that it will also work for other systems. This is supported by results of earlier work on the calibration of hydrodynamic models by Langeveld (2004), Korving (2004) and Clemens (2001a). These studies showed that the applied calibration procedure in this chapter is applicable for other sewer systems. In addition, Langeveld (2004) and Korving (2004) also demonstrated that the accuracy of the database of the structural sewer properties is crucial with respect to the calibration results. In Langeveld (2004), an incorrect level of the weir level of a CSO construction was noticed based on calibration results showing a systematic error. Korving (2004) obtained similar findings for a sewer model built using a database with structural errors, compared to a model in which these errors were removed. The research described in this chapter shows that model calibration can be used not only to detect errors in the structural properties of a sewer model, but also to detect changes in system behaviour due to changes of system properties over time because of, for example, root intrusion. The application of the proposed methodology in other sewer systems requires the steps mentioned earlier in this chapter (see also Figure 3.3):

(1) model validation;
(2) calibration parameter selection;
(3) selection of storm event for calibration;
(4) monitoring data validation;
(5) reduced parameter set for calibration;
(6) model calibration;
(7) residual analysis.

3.5   Conclusions

In-sewer defects are known to affect sewer system performance. These defects are normally detected using CCTV inspections. As the inspection frequency is typically once per decade or less, the sewer asset manager has to rely on sparse data on in-sewer defects. Hydraulic monitoring provides long-term, high-frequency data on the hydraulics. This chapter examined the added value of model calibration to obtain information on in-sewer defects from hydraulic monitoring data either without or in-between periodic inspections.

It is shown that each model calibration results in a set of model parameter values, their uncertainties and residuals. Model parameters change between the different events. However, their values also incorporate the antecedent condition of the catchment of the event calibrated and are therefore less suitable to identify in-sewer defects. The residuals on the other hand, and more specifically the combination of their absolute values, statistical properties and cross-correlations between residuals at different locations, are very strong indicators of the occurrence of in-sewer defects.

Model calibration is used to show that, given a chosen calibration parameter set which predominantly contains runoff parameters, a change in residuals after calibration is an indication for local changes in system behaviour (i.e. root intrusions and sediment deposits). The calibration process is conducted on the Dutch sewer system 'Tuindorp' (see section 1.6). It is concluded that model calibration is able to demonstrate changes in the hydraulic properties of the sewer system and can be used to optimise sewer asset management and especially operation and maintenance actions. This can be done by means of 'hydraulic fingerprinting', where the fingerprint is defined by the model parameters and the residuals after calibration.

4 Identifying critical elements in sewer networks using Graph-theory

4.1 Introduction

As generally acknowledged, infrastructure is becoming more and more important to keep cities functioning. In order to maintain the desired level of serviceability the infrastructure has to be properly maintained and rehabilitated (Gauffre et al., 2007; Wirahadikusumah et al., 2001). Two important parts of the infrastructure for human wellbeing are water supply networks and sewer systems. These systems are essential for public health and preventing epidemics. As the infrastructure is ageing there is wide felt need for strategy development for maintenance and rehabilitation.

Sewer systems and water supply networks are underground infrastructure; therefore, it is not straightforward to determine the actual condition of the assets. The maintenance and rehabilitation of sewer systems is often solely based on the results of visual inspections (Van Riel et al., 2016). Studies have been carried out to develop methods for optimizing the locations and frequencies of visual inspections. A generally used optimization concept is the combination of the likelihood of failure (LoF) with the consequence of failure (CoF) (see e.g., Anbari et al., 2017; Arthur et al., 2008; Arthur and Crow, 2007; Baah et al., 2015; Lukas and Merrill, 2006; Mancuso et al., 2016; McDonald and Zhao, 2001; Pienaar, 2013). The likelihood of failure is often related to the soil type, the load on the system and the material type where the consequence of failure is often related to the conduit characteristics (e.g. conduit size, conduit depth) and the location of the conduit in the urban area. The criteria and weights of the criteria used in decision support methods for the prioritization of rehabilitation projects influences the outcomes of the decisions (Tscheikner-Gratl et al., 2016).

Sewer systems and water supply systems are networks consisting of many elements. The performance of the network depends on the functioning of the individual elements. The importance of an element for the network depends on the characteristics of the element and its position in the network. If the degree of criticality of the elements in a network is known, the maintenance and rehabilitation can be adjusted accordingly to the degree of criticality instead on maintaining all elements to the same quality level. The criticality can also be combined with the consequences of failure. Failure of (sewer) systems has impact on the service level (drainage of water) and on the surrounding (health risks, floods, blocked roads, damage to other infrastructure). The degree of criticality can therefore be used as a basis for risk-based asset management. It can be used to analyse the robustness of a network and to evaluate measures to increase the robustness as well.

Only a limited number of methodologies on how to determine the importance of the individual elements in relation to the complete network is described in literature. Arthur et al. (2008) and Arthur and Crow (2007) describe a methodology to identify critical assets. This methodology is based on surcharged capacity, combined with surcharging water level, and is applicable to gravity systems. A second method, called the Achilles approach, is used in the planning tool for the identification of weak points during operation and emergency for the urban water infrastructure (Mair et al., 2012; Möderl et al., 2009; Möderl and Rauch, 2011; Sitzenfrei et al., 2011). In this approach, the capacity of each conduit in a hydrodynamic model is reduced to (almost) zero and the hydraulic consequences are determined. For large (> 5.000 conduits) (looped) systems both methods require a large calculation effort.

Chapter 3 describes the concept of 'hydraulic fingerprinting' based on model calibration to identify in-sewer defects affecting hydraulic performance of a sewer system. The 'fingerprint' is defined by the model parameters and the residuals. In addition, model calibration enables detection of changes in hydraulic properties of the sewer system. This method can be a powerful tool for directing sewer asset management actions.

The model calibration is based on an extended monitoring network. In addition, this means that monitoring design is important with respect to the calibration results. Therefore, it is necessary to identify critical sewer conduits in a sewer network. Those conduits are important assets in the hydraulic performance of the sewer system and the monitoring locations can be chosen based on those critical conduits.

This chapter proposes an approach towards identifying the criticality of individual conduits in water related networks such as sewer systems. The proposed Graph-theory method (GTM) is independent of the selected storm events and requires limited calculation effort. This chapter focuses on sewer networks but the described approach has a wider applicability (e.g. drinking water networks). First, the theory of the method and an existing method to compare with is presented, secondly, the existing method is tested for various storm events, thirdly, some examples of both methods are presented based on urban drainage networks and the results and performance are compared with the traditional method. Finally, the results are discussed and the conclusions are formulated.

4.2   Materials and methods

4.2.1   Studied sewer systems

For the sewer systems 'Tuindorp' and 'Loenen' the degree of criticality of the conduits are determined. Both systems are described in section 1.6. Table 1.1 shows the characteristics of the systems and Figure 1.6 shows the layout of the systems. The conduit diameters of both systems are depicted in the Figures 4.1 and 4.2. Table 4.1 includes additional information about the networks that is used in this chapter. For the 'Loenen' catchment, two situations are studied in this chapter: 'Loenen-2' including both CSO structures and 'Loenen-1' where a weir that only becomes active during storm events with high rainfall intensities is closed (see 'CSO high crest level' in Figure 4.2).

Table 4.1:   Network characteristics 'Tuindorp' and 'Loenen' catchments.

Characteristics	'Tuindorp' catchment	'Loenen' catchment
number of conduits	778	352
number of nodes	684	337
number of conduits that, when deleted, lead to unconnected nodes*)	188	176

*) If these conduits are deleted, the network is divided into 2 sub-networks and one of these sub-networks is no longer connected to a CSO.
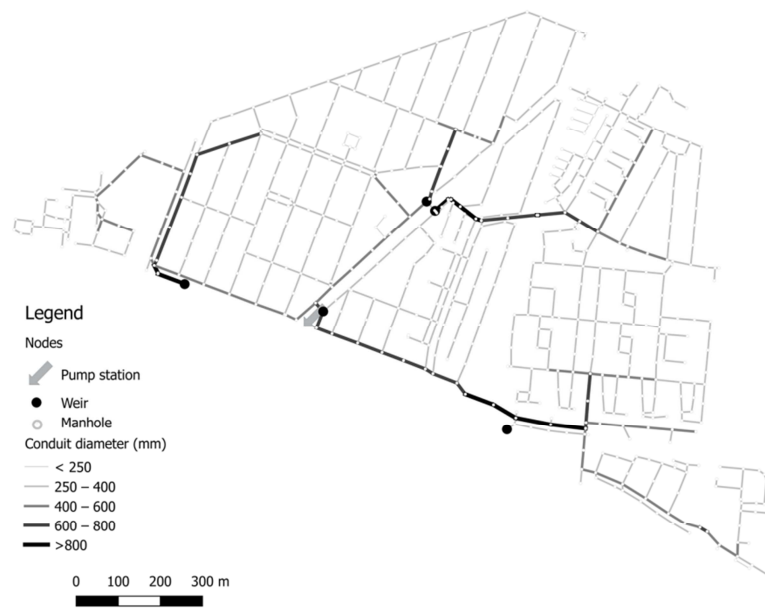
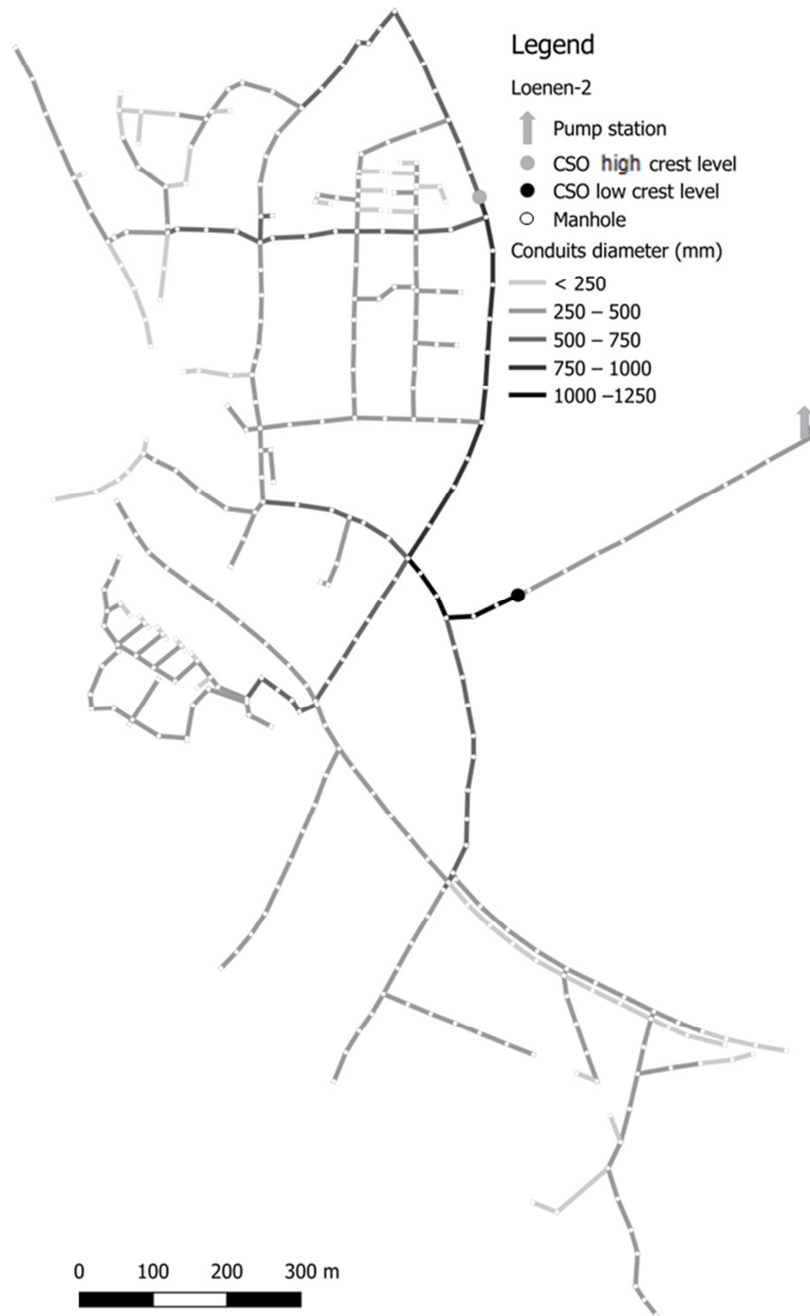**Figure 4.1:** Conduit diameters in the 'Tuindorp' sewer system.

Figure 4.2: Conduit diameters in the 'Loenen' sewer system.

71

In order to identify the most critical conduits in relation to the hydraulic performance of a total sewer network, simulations with the hydrodynamic models have been made with different types of storm events. The latter has been done to obtain an impression of the sensitivity of different rainfall loads to the results of the simulations (locations of critical conduits). Firstly, 10 design storm events from the Dutch national guidelines for hydrodynamic modelling of urban drainage systems (Stichting RIONED, 2016) are used. These storm events cover a range of return periods (0.25, 0.50, 1, 2, 5 and 10 years), pattern shapes (peak intensity at the beginning or at the end of the event) and durations (45, 60 and 75 minutes). The storm events vary between 10.5 mm in 75 minutes (maximum intensity 40 l/s.ha. (14 mm/h) to 35.7 mm in 45 minutes (maximum intensity 210 l/s.ha (75.6 mm/h)). Secondly, the most commonly used stationary design storm events in the Netherlands 40, 60 and 90 l/s.ha (14, 21.6 and 32.4 mm/h) are used for 'Loenen-1' and 'Tuindorp'. For 'Loenen-2' (including both CSO structures), 10 storm events are used with a stationary rainfall intensity varying from 10 - 100 l/s.ha (3.6-36 mm/h) and a during of 24 hours. Thirdly, for the 'Tuindorp' catchment, 13 independent storm events are selected from the rainfall series observed by the Royal Dutch Meteorological Institute in De Bilt (period 1955-1964) as well. In chapter 2, Monte Carlo simulations were applied to systematically study the impact of in-sewer defects on hydraulic performance of the 'Tuindorp' catchment. Based on the outcomes of the Monte Carlo simulations, a collection of 41 relevant independent storm events has been selected from the long-term rainfall series, to systematically study the impact of individual conduits on hydraulic performance in the 'Tuindorp' catchment. The selection criteria used are: i) the water level reached a level higher than the threshold level 25 cm below ground level or ii) at least 2 CSOs started working. In addition, a selection of conduits has been applied to determine the impacts on hydraulic performance. The conduit locations have been chosen based on the system layout and expert judgement. This resulted in a total number of 198 conduits. In the hydraulic simulations regarding pluvial flooding, the diameter of the selected conduits has been reduced individually to 10% of the original conduit diameter.

A total amount of 8118 simulations were performed (198 conduits and 41 events) with a fully detailed InfoWorks© (version 13.0.6; Innovyze, 2012) model to determine the criticality of each of the 198 conduits on the hydraulic performance of the 'Tuindorp' sewer system. The results of the simulations showed that the calculated number of flooded locations, flood volumes and threshold exceedances in the 'Tuindorp' were caused by 13 of the 41 rainfall events. The total calculation time was 273 hours, which is a very time consuming method for this looped system. To achieve acceptable simulation times, only the 13 storm events that caused flooding are used in this chapter to determine the criticality of conduits.

4.2.2   The Achilles approach

A general applicable method to determine the criticality of an element in a sewer system is shown in Figure 4.3. This method is part of the Achilles approach (Mair et al., 2012; Möderl et al., 2009). The Achilles approach can be used to determine vulnerable sites of water infrastructure. For the identification of vulnerabilities, the outcomes of a hydrodynamic model are used (Hydrodynamic Model Method, HMM). First, a simulation is done with the original model in which all conduits function well. After the diameter of the conduits are one by one reduced to zero to simulate a blockage. For every blocked conduit a simulation is carried out so the number of simulations is equal to the number of conduits plus one. The results are compared based on the increase of the calculated ponded volumes. The reduced conduit diameter that causes the largest increase in ponded volume is the most critical conduit.
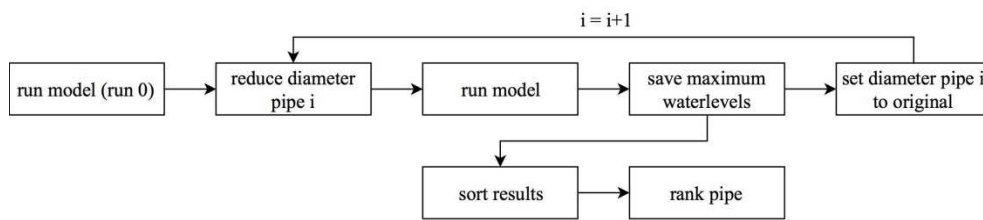

Figure 4.3:   Process to determine the degree of criticality with the hydrodynamic model method (HMM).

In literature about the Achilles approach, two methods to sort the results are applied. The first method is a performance indicator based on the maximum ponded volume and the total rainfall runoff (Möderl et al., 2009),

$$
PI = 1 - \frac{\sum_{i=1}^{N} \max(V_{P,i})}{\sum_{j=1}^{C} V_{R,j}}
\tag{4.1}
$$

where V_P is the ponded volume of each node and V_R is the total rainfall runoff volume for each runoff catchment. The main assumption in Möderl et al. (2009) is that the performance indicators are independent of the rainfall events.

Method 2 shows a performance indicator that indicates the probability of damage caused by flooding (Mair et al., 2012),

$$F = \frac{\sum_{i=0}^{\#J} \min(x, \max(0, F_i)) / x}{\#J} \qquad (4.2)$$

where x is the threshold flooding volume in m^3 in the simulation period and $\#J$ is the total number of junctions.

The HMM will be used as benchmark for the outcomes of the method based on the GTM. The method described by Arthur and Crow (2007) is not applicable for fully surcharged systems and this is often the case in flat areas like the Netherlands and therefore not used.

The outcomes of the traditional HMM (Figure 4.3) are used as reference for the degree of criticality based on the GTM. In the GTM, it is possible that a node no longer is connected to a part of the network with a sewer overflow after a conduit is deleted (section 4.2.3 and 4.2.4). This can cause problems in the simulations of the HMM, and therefore the conduits are not deleted but the diameter is reduced to 10 mm (the minimum allowed diameter in the software package).

When a part of the network is not connected to a CSO because of a blocked conduit, floods will occur at every storm event. The severity of the blockage depends on the area that is disconnected from the CSO. The blocked conduits that lead to 'unconnected nodes' are ranked based on the runoff surface connected to these nodes. After that the other conduits are ranked based on the results of the HMM.

In each run of the HMM, the diameter of one conduit is reduced to 10 mm. When the increase in water levels is divided into categories to rank the links the outcome of the ranking depends on the used categories. Therefore, the links are ranked based on the increase in flood volume and the increase of water level in the sewer system. After each run, the increase in flood volume and the increase of water level, relative to the original model, are determined for each manhole. The results of all manholes are summed and the links are sorted: first based on the total increase in ponded volume and then on the total increase of water level. The conduit with the largest total increase in the flood volume is ranked as most critical after the conduits that causes 'unconnected nodes'. If the increase

in flood volume is the same for two conduits, the conduits are sorted based on the increase in water level.

There are two differences between the HMM as described in the Achilles approach and used in this research. The first difference is the use of a minimum diameter of 10 mm instead of a fully closed conduit. The effect of this adjustment is described in the section of the results. The second is the method to rank the conduits. Instead of ranking the conduits between 0-1 based on the ponded volume and the rainfall runoff (see equation 4.1), the conduits are ranked based on the surface that is disconnected, the increase in ponded volume and the increase in water level. For the blocked conduits that cause flooding, this adjustment will not influence the ranking and this adjustment makes it possible to rank all conduits including the blocked conduits that do not cause flooding.

To validate the assumption of the Achilles approach that the performance indicators are independent of the rainfall events (Möderl et al., 2009), the HMM is used to determine the degree of criticality for various storm events (see paragraph 4.3.2).

4.2.3 Introduction to the Graph-theory

The Graph-theory is a mathematical theory and is widely used in, for example, route problems and optimization of flow problems. A graph consists of nodes and links. Graphs are used to represent relations in for example physical, information and social systems. Leonhard Euler laid the foundation of the Graph-theory in 1736 with the Königsberg bridge problem (Harju, 2011).A graph can be u sed to simplify a network and its connectivity in nodes and links (Rodrigue et al., 2017). Networks such as water supply networks, sewer systems, electricity networks are typical examples of graphs consisting of links (conduits, cables) and nodes (connections or manholes). In hydrological models, graphs are used to represent the structure of the network. There is little literature known about the use of the Graph-theory to analyse criticality of conduits in sewer networks (e.g., Laakso et al. (2017) used the cut-edge analysis to reveal sewers that serve a high number of connections).

A graph G=(V, E) is a set V of nodes and a set E of links formed by pairs of nodes (König, 1936). A path in a graph between a source node and a target node is a route between the source node and the target node without a node occurring more than once. Each link can have a weight, costs or penalty. The term most often used is costs and is adopted here as well.

The costs in, for example, a road network can be defined as the distance between two places, the speed limit, the toll, fuel consumption or the risk of getting stuck in a traffic jam. The costs are a metric for determining shortest or cheapest paths. For piped water systems the necessary amount of energy to transport the water (head loss) is utilized as costs. This is explained in more detail in section 4.2.4. For the graph in Figure 4.4 a path v1–v6 is v1, v2, v3, v4, v5, v6 (costs = 5) and the shortest path v1–v6 is v1, v3, v4, v6 (costs = 3).There are different kinds of graphs. The upper left graph in Figure 4.4 is a graph in which v1, v2 = v2, v1. This graph can be used when the costs of opposite flow directions in a conduit are the same, in this example the costs are 1.

A directed graph or digraph is formed by nodes connected by directed links. In a digraph the link $v_1,v_2 \neq v_2,v_1$ while in a graph $v_1,v_2 = v_2,v_1$ (Figure 4.4, digraph). A digraph can be used when the costs of opposite flows are different. In this example the costs of the edges in positive direction are 1 and in the negative direction are 2. When all nodes in a directed graph are connected in two directions, it is called a strongly connected graph. The removal of a conduit can result in one or more strongly connected digraph(s). The lower left graph in Figure 4.4 shows the situation in which the connection v5, v6 and v6, v5 is removed and the result is a strongly connected digraph. The lower right graph in Figure 4.4 shows the situation in which the connection v3, v4 and v4, v3 is removed and the result is two strongly connected sub-digraphs.
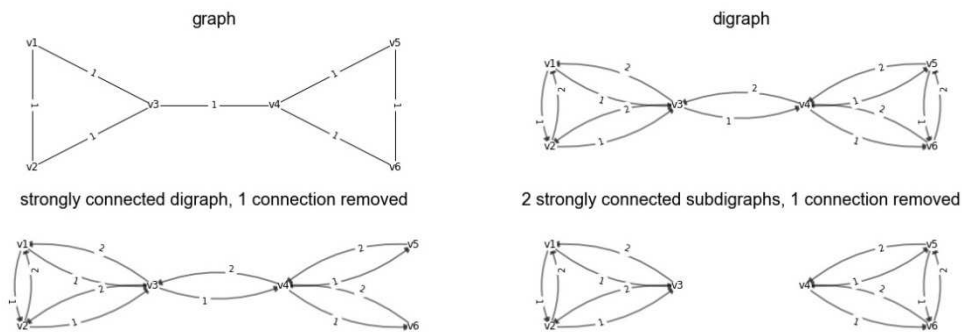

Figure 4.4: Brief overview of some basic principles of the Graph-theory. The numbers along the edges show the costs of the edges. The upper left figure represents a graph in which v1, v2 = v2, v1. The upper right figure represents a digraph in which v1, v2 6= v2, v1. The lower left graph shows a strongly connected digraph after one connection is removed and the lower right figure shows two strongly connected sub-digraphs after a connection is removed.

4.2.4   Graph-theory applied on sewer systems

The Graph-theory is applied as a concept to determine the degree of criticality of a conduit during storm conditions. The sewer system is represented as a digraph. Each manhole is represented as a node and each conduit as a link. Between each pair of nodes two links are used, each with its own costs. This allows making a distinction between a positive and negative flow direction (Figure 4.4, digraph). This is necessary because a blockage of a link can result in a reversed flow.

During storm events most of the water flows out of the sewer systems via a CSO. For each node (source), a path is determined to one of the overflows (targets) in the sewer system. Each path has its own length or 'costs'. For each node, the cheapest path to the CSO structure is determined based on the Dijkstra algorithm (Dijkstra, 1959).

For each node the costs of the shortest path to the combined overflow structure (C_{vi-vn}) is multiplied with the runoff area connected to the source node (A_i),

$$C_{graph} = \sum_{i=1}^{n} C_{vi-vn} * A_i$$

(4.3)

where the total costs of a graph are determined for the complete graph by summing the costs of all nodes to a CSO structure. To determine the criticality during dry weather conditions the target is a pumping station instead of a CSO structure.

In case of more than one overflow structure in a sewer network, each node has multiple targets. In such a case the costs of all nodes to all targets are calculated. For every node the lowest cost of the path from the node to an overflow is used to determine the total costs of the graph. To reduce the calculation time the calculations are not carried out from the source to the target node but from the target(s) to all nodes. Therefore, the positive and negative conduit costs are turned around to obtain the right total costs.

After calculating the total costs of the complete graph, a connection between a pair of nodes is deleted to simulate a conduit blockage (see lower images in Figure 4.4). This implies that the edges v_x, v_y and v_y, v_x are deleted. When all nodes are connected the new graph remains a strongly connected digraph (Figure 4.4, lower left). Otherwise the result is two strongly connected sub-digraphs (Figure 4.4, lower right). Two situations are possible. First, all (sub)digraph(s) contain at least one target node. Second, only one of the sub-digraphs contains at least one target node. If the first situation, the total costs of the (sub)digraph(s) are determined. If the second situation, the runoff surface is summed of the nodes that are not connected to a target (see section 4.2.2).

The process as shown in Figure 4.5 is applied. The result is a list of deleted connections with the total costs of each digraph or the runoff surface that is not connected anymore to a target. The deleted connections are sorted, firstly by the amount of runoff surface that is not connected to a target, secondly by the total costs of the digraph from large to small amount of runoff surface and from high to low costs. The deleted connections are ranked from 1 (most critical connection) to the total number of edges (less critical).
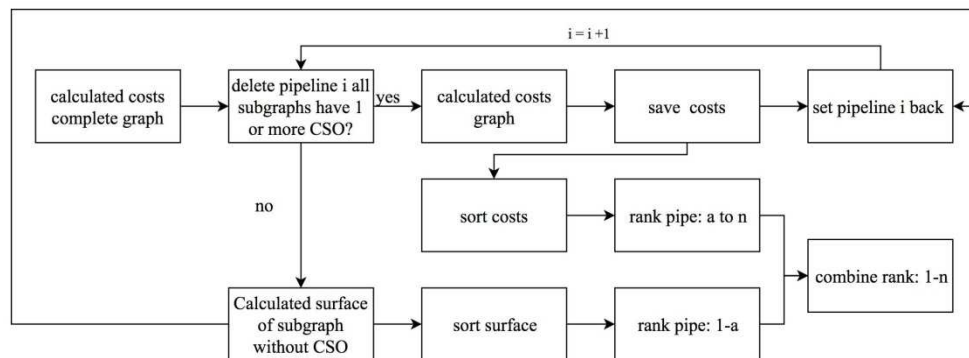

Figure 4.5: Process to determine degree of criticality with Graph-theory.

The links' costs are derived from the head loss in a link. The head loss is the amount of energy needed to transport water from point A to point B. The head loss comprises two parts. The first part is the static head and is the amount of energy needed to lift water. The amount of energy is equal to height differences between A and B. The second part is the dynamic head. Energy is needed to let water flow from A to B. The amount of energy that is lost due to the resistance of water to flow between A and B is expressed as the dynamic head loss. The dynamic head loss depends on the characteristics of the liquid and the conduit dimension and hydraulic characteristics.

In a gravity sewer system, the head loss comprises a dynamic part and two static parts (see Figure 4.6). The first static component is the height difference between the water level in the manhole upstream of the conduit and the upstream invert level of a conduit. If the water level in the manhole upstream of the conduit is higher than the upstream invert conduit level this value is zero. For the water level in a sewer system the crest level of the CSO with the lowest crest level of the system can be used. The second static component is the height difference between the upstream and downstream invert level of the conduit. If the water level is higher than the invert level this value is zero. If the downstream invert level is lower than the upstream invert level the value is also zero.

The dynamic head loss in a conduit is described as,

$$\Delta H = \frac{L(q/A)^2}{C^2 R}$$
(4.4)

where L is the length between point A and point B, q is the discharge and C is the Chézy coefficient which is defined as,

$$C = 18\log(\frac{12R}{k})$$
(4.5)

where R is the hydraulic radius and k is the wall roughness.

In a gravity flow sewer system, the head loss consists of a dynamic part and two static parts (see Figure 4.6). The first static component is the height difference between the water level in the manhole upstream of the conduit and the upstream invert level of a conduit. If the water level in the manhole upstream of the conduit is higher than the upstream invert conduit level this value is zero. For the water level in a sewer system the crest level of the CSO with the lowest crest level of the system can be used.
The second static component is the height difference between the upstream and downstream invert level of the pipe. If the water level is higher than the invert level this value is zero. If the downstream invert level is lower than the upstream invert level the value is also zero.
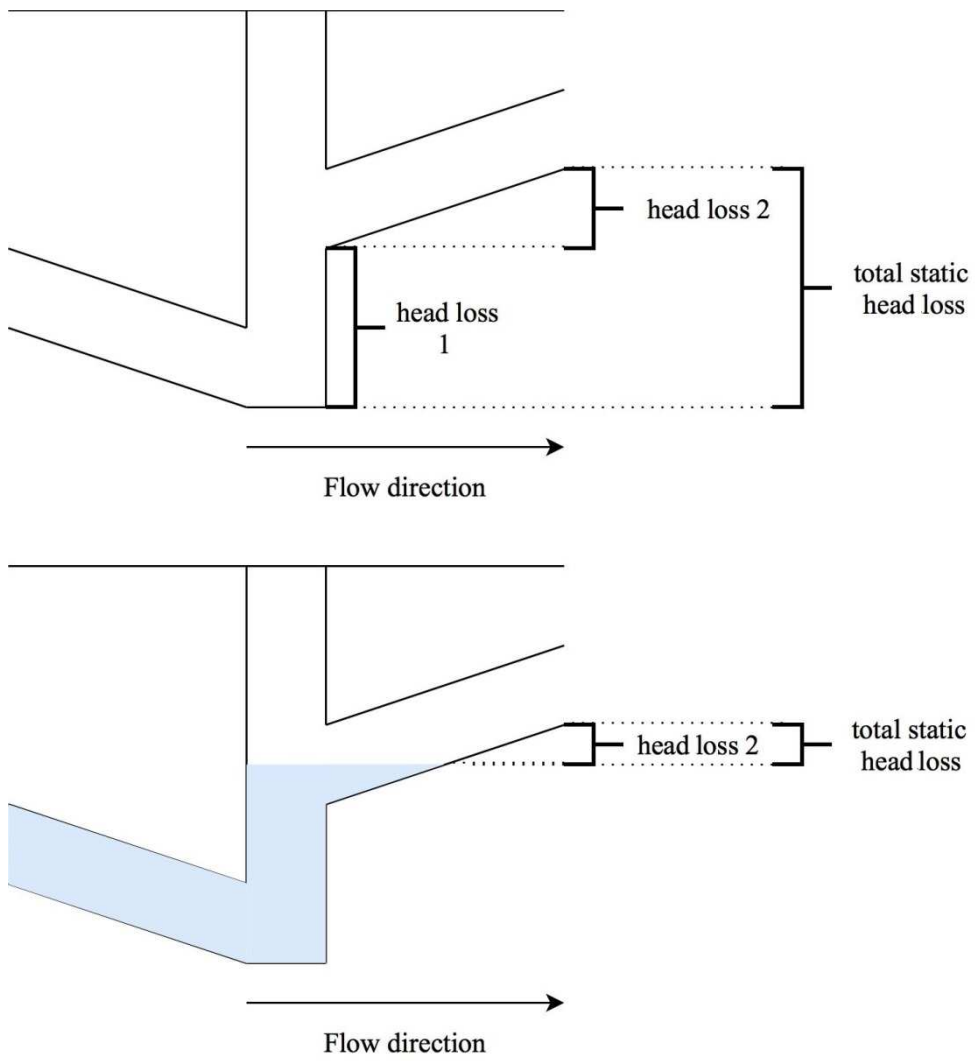
Figure 4.6: Static costs of conduits for an empty system (top) and a system with a certain water level (bottom).

4.2.5 Comparison of criticality between hydrodynamic model method and Graph-theory method

The Kendall rank correlation coefficient (Kendall, 1945), commonly referred to as Kendall's tau-b coefficient (τ_b) is used to determine the relationship between the outcomes of the HMM and the GTM,

$$\tau_b = \frac{(P-Q)}{\left(\sqrt{(P+Q+X_0)*(P+Q+Y_0)}\right)} \tag{4.6}$$

where τ_b is a nonparametric measure of association based on the number of concordances (P) and discordances (Q) in paired observations. X_0 is the number of pairs tied only on the X variable and Y_0 is the number of pairs tied only on the Y variable. τ_b is used to compare the relationship of datasets and not of individual conduits. Minus one (-1) implies a 100% negative association and one (1) is a 100% positive association.

4.2.6 Software and hardware

For the hydrodynamic modelling method, the software package SOBEK 2.14.001 (Deltares, Delft, the Netherlands) is used. The hydrodynamic simulation engine of SOBEK is based upon the complete Saint-Venant Equations.

For the Graph-theory method, the following software is used: Python 2.7.11 64-bit version (Python Software Foundation, Beaverton, OR, USA). Including the modules collections, CSV (Comma Separated Values) and operator and the packages: matplotlib.pylab 1.5.1 (Hunter, 2007) (Matplotlib Development Team), numpy 1.12.1 (Van der Walt et al., 2011) (NumPy developers), networkx 1.11 (Hagberg et al., 2008) (NetworkX Developers, Pasadena, CA, USA), pandas 0.18.0 (McKinney, 2010) (Pandas Core Team) and scipy 0.19.0 (Jones et al., 2018) (SciPy developers) and the Development Environment Spyder 2.3.8 (Anaconda, Inc., Austin, TX USA).

The calculations are made on a laptop with an Intel® Core™ i5-3380M CPU @ 2.90 GHz processor and 8.00 Mb RAM and a Windows 7 operating system (Microsoft, Washington, DC, USA).

4.3 Results and discussion

4.3.1 Effect of small opening instead of fully blocked pipe

In contrast to the Achilles approach, the conduits are not completely blocked but the internal conduit diameter is reduced to 10 mm. The minimum internal conduit diameter in the used models is 151 mm. The assumption is that the effect of a 10 mm conduit instead of a fully closed conduit is negligible because of the relatively large difference in surface between a conduit with a diameter of 10 and 151 mm. Figure 4.7 shows the results of the comparison of the degree of criticality based on the HMM for the 'Tuindorp' catchment. In one situation the conduit is completely blocked, in the other situation the diameter is reduced to 10 mm. The figure shows that the results are not exactly the same but are similar to each other and the τ_b value is 0.98. The degree of criticality is ranked from most important (1) to less important (778).
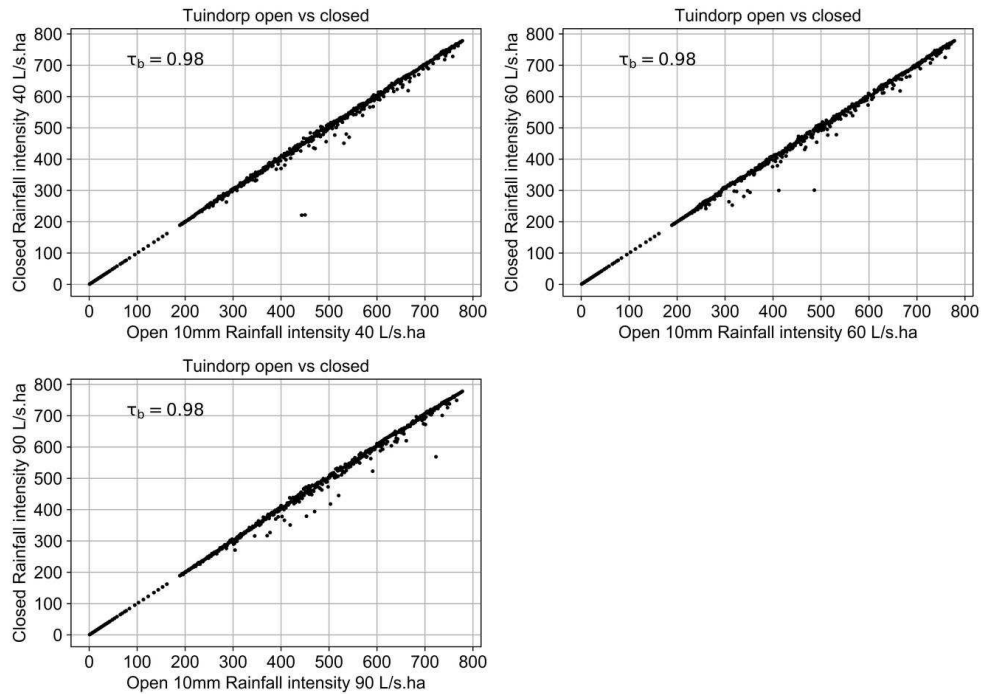

Figure 4.7: Comparison between the degree of criticality based on the HMM where conduits are completely blocked (closed) and where the conduit diameter is reduced to 10 mm (open).

82

4.3.2 The degree of criticality based on hydrodynamic model method

With the HMM, the criticality of the conduits is determined for different storm events. For the three types of storm events (stationary, dynamic and series) the degree of criticality of the conduits is per two events plotted against each other and τ_b is determined. If the degree of criticality is independent of the storm event the τ_b value is 1. In Table 4.2 - Table 4.5 and Figure 4.8 some of the results are shown. The tables and figure show that the type of storm event does affect the degree of criticality of the conduits. If the differences in maximum rainfall intensity and/or shape between the storm events are limited, τ_b approaches 1 and the degree of criticality of the individual elements is almost the same. If the differences between the storm events become larger, τ_b drops below 0.6 (see Table 4.5) and the degree of criticality of the individual elements changes. This can be both an increase and a decrease of the degree of criticality. Figure 4.8 shows an overview of the degree of criticality of the conduits based on the HMM of the sewer system 'Tuindorp', for the dynamic storm events 580818, 600623, 560823 and 620725 of the long-time rainfall series.

Table 4.2: 'Loenen-1', τ_b value of the comparison of the degree of criticality based on the HMM of various stationary storm events.

Rainfall intensity	40 l/s.ha (14.4 mm/h)	60 l/s.ha (21.6 mm/h)	90 l/s.ha (32.4 mm/h)
40 l/s.ha (14.4 mm/h)	1.00	0.89	0.77
60 l/s.ha (21.6 mm/h)		1.00	0.85
90 l/s.ha (32.4 mm/h)			1.00

Table 4.3: 'Loenen-2', τ_b value of the comparison of the degree of criticality based on the HMM of various stationary storm events.

Rainfall intensity	40 l/s.ha (14.4 mm/h)	60 l/s.ha (21.6 mm/h)	90 l/s.ha (32.4 mm/h)
40 l/s.ha (14.4 mm/h)	1.00	0.92	0.88
60 l/s.ha (21.6 mm/h)		1.00	0.92
90 l/s.ha (32.4 mm/h)			1.00

Table 4.4: 'Tuindorp', τ_b value of the comparison of the degree of criticality based on the HMM of various stationary storm events.

Rainfall intensity	40 l/s.ha (14.4 mm/h)	60 l/s.ha (21.6 mm/h)	90 l/s.ha (32.4 mm/h)
40 l/s.ha (14.4 mm/h)	1.00	0.97	0.90
60 l/s.ha (21.6 mm/h)		1.00	0.90
90 l/s.ha (32.4 mm/h)			1.00

Table 4.5: 'Tuindorp', τ_b value of the comparison of the degree of criticality based on the HMM of various storm events from the rainfall series.

Storm event	550717	560823	570920	580818	600623	601007	601201	610605	620725	621001	630802	630817	640817
550717	1.00	0.62	0.66	0.67	0.68	0.66	0.67	0.66	0.58	0.69	0.67	0.60	0.66
560823		1.00	0.64	0.67	0.66	0.60	0.62	0.65	0.57	0.65	0.68	0.58	0.61
570920			1.00	0.74	0.72	0.66	0.68	0.72	0.61	0.73	0.73	0.61	0.68
580818				1.00	0.91	0.74	0.79	0.84	0.68	0.89	0.87	0.65	0.75
600623					1.00	0.74	0.79	0.84	0.67	0.86	0.89	0.64	0.75
601007						1.00	0.81	0.74	0.67	0.75	0.73	0.64	0.79
601201							1.00	0.83	0.70	0.80	0.79	0.64	0.84
610605								1.00	0.65	0.80	0.88	0.61	0.77
620725									1.00	0.70	0.65	0.64	0.65
621001										1.00	0.83	0.63	0.76
630802											1.00	0.63	0.75
630817												1.00	0.63
640817													1.00

The removal of a conduit of the 'Loenen' network results in 176 cases in one or more nodes that are no longer connected to a combined sewer overflow. For 'Tuindorp' this is the case for 188 conduits. These conduits are ranked based on the runoff surface that can no longer drain to a CSO. The degree of criticality of these conduits is therefore storm independent.

As the dynamics of the hydraulic load is an important factor in the distribution of water flows in networks, it is not feasible to determine a single value for the criticality of an element in a network when applying the HMM method. The results also show that the degree of criticality varies both for conduits with a lower and higher degree of criticality. This is observed for stationary storm events as well as for dynamic design storm events and observed storm events. The effect is present in both sewer systems.
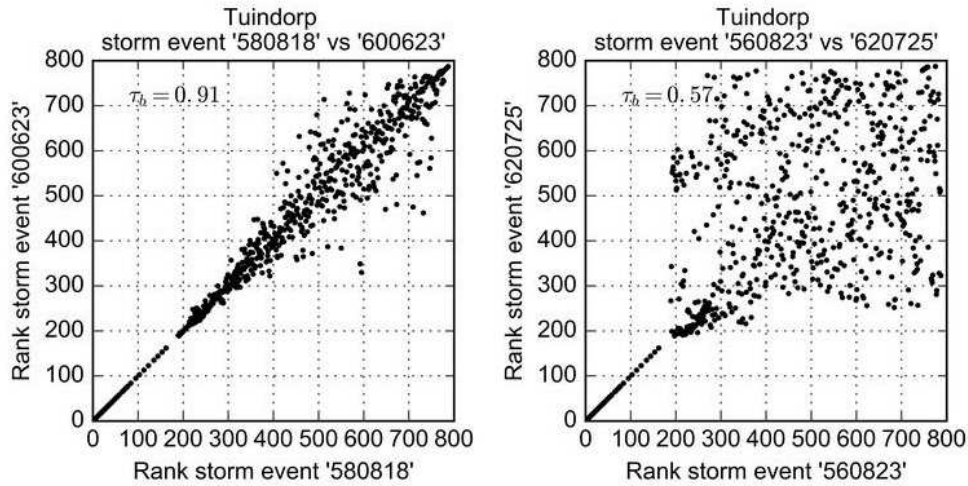
Figure 4.8: Overview of the degree of criticality of the conduits based on the HMM of the sewer system 'Tuindorp', for the dynamic storm events 580818, 600623, 560823 and 620725 of the long-time rainfall series.

4.3.3 Comparison degree of criticality based on hydrodynamic model and on the Graph-theory

The degree of criticality based on the GTM is compared with the outcomes of the HMM in terms of the Kendall's τ_b. For the GTM, the costs of the conduits are decisive for the outcomes. As described in section 4.2.4 the costs of the conduits depend on the parameters discharge, water level and crest difference. The impact of the value of the parameters is described in more detail in section 4.3.5.

Figure 4.9 shows the results of the comparison with the dynamic and stationary storm events with the highest and lowest τ_b for 'Loenen-1'. τ_b varies between 0.97 - 0.90. That implies that for all combinations of parameters and storm events there is a strong relation in the outcomes of the HMM and the GTM. The 'Loenen-2' network is more complex than the 'Loenen-1' network because of the additional CSO. For 'Loenen-2', τ_b varies between 0.80–0.96: that is 0.01-0.1 less than the τ_b of 'Loenen-1'. A τ_b of 0.80-0.96 implies that also for 'Loenen-2' there is a strong relation in the outcomes of the HMM and the GTM. Figure 4.10 shows the results of the comparison with the dynamic and stationary storm events with the highest and lowest τ_b.

Figure 4.11 and Figure 4.12 are showing the results for the 'Tuindorp' case. The 'Tuindorp' network is more complex than the 'Loenen' network because the number of conduits and CSO structures is more than twice as large. The Kendalls' τ_b between the results of the HMM and the GTM are less than for the 'Loenen' cases. The Kendalls' τ_b varies between 0.46-0.78. Although the Kendalls' τ_b is reduced, it is still possible to identify the 250-300 (30-40%) most important conduits with the GTM.
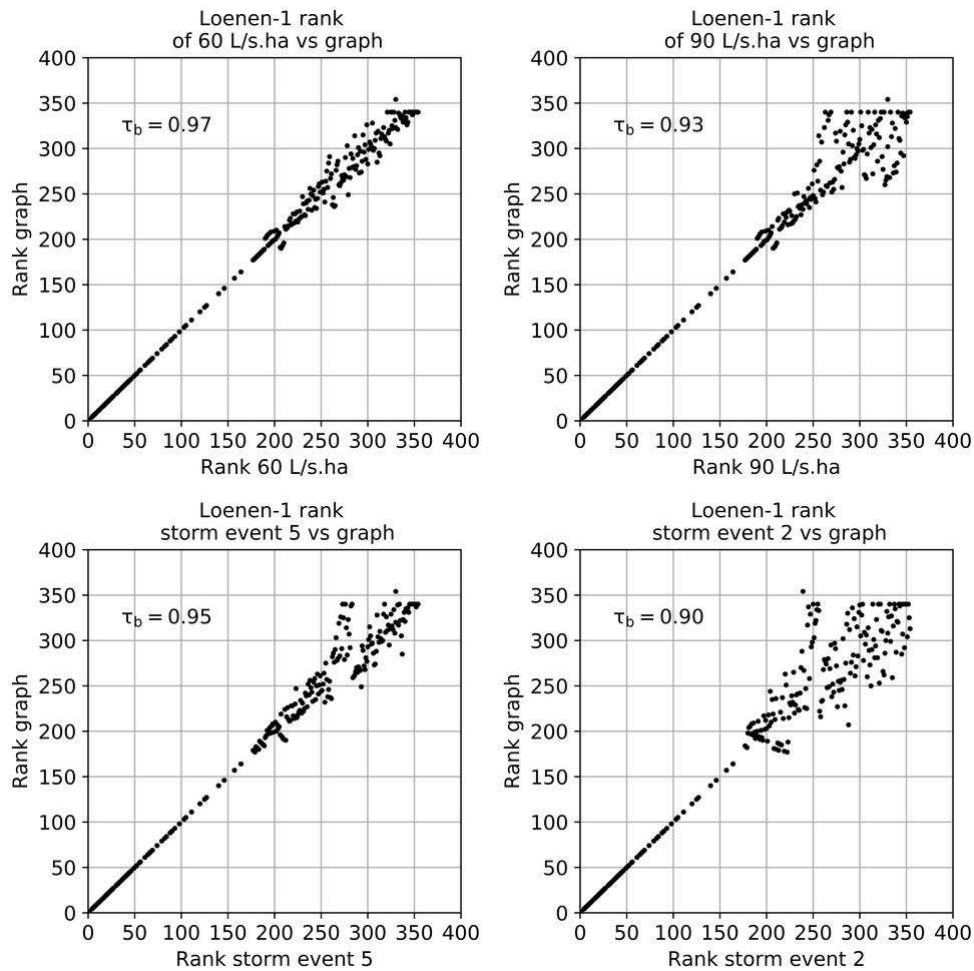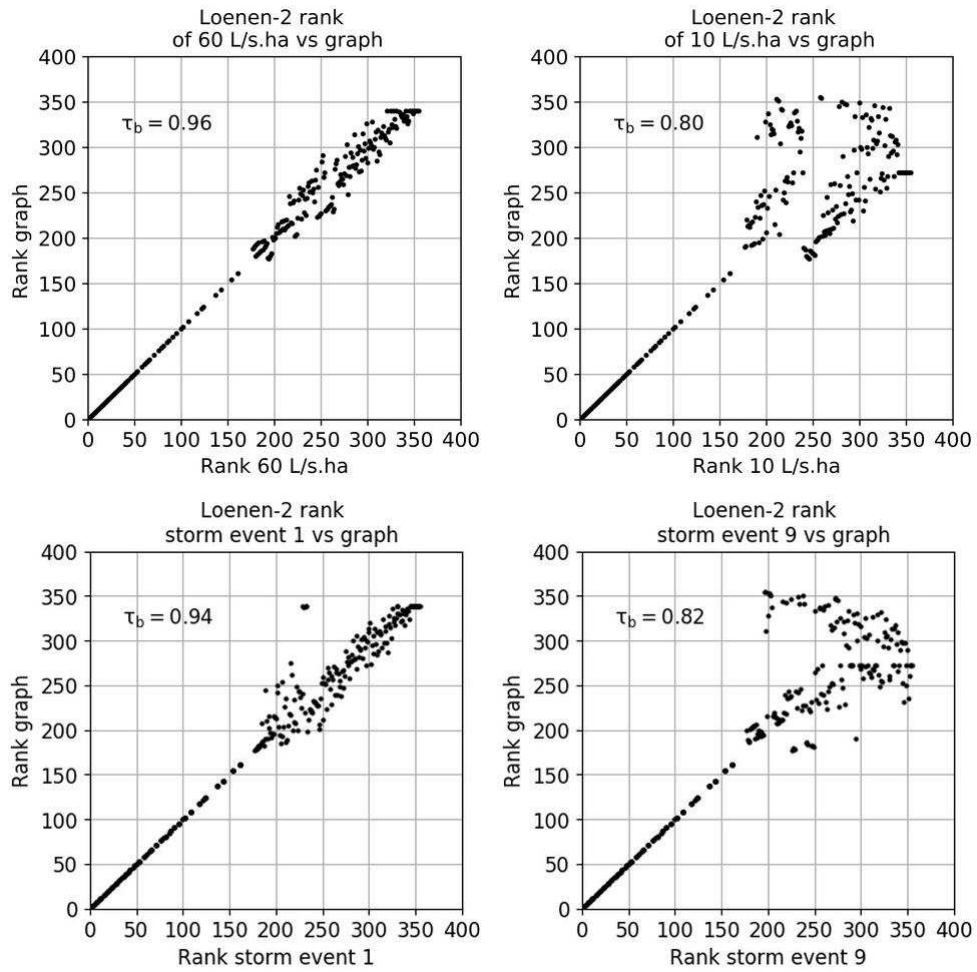

Figure 4.9: Comparison of the degree of criticality of the conduits based on the GTM and the HMM. The figures show the results for 'Loenen-1'. The graphs at the left side show the ranking with the highest τ_b of both the stationary storm events (upper graph) and the dynamic storm events (lower graph). The graphs at the right side show the ranking with the lowest τ_b of both the stationary storm events (upper graph) and the dynamic storm events (lower graph).

Figure 4.10: Comparison of the degree of criticality of the conduits based on the GTM and the HMM. The figures show the results for 'Loenen-2'. The graphs at the left side show the ranking with the highest τ_b of both the stationary storm events (upper graph) and the dynamic storm events (lower graph). The graphs at the right side show the ranking with the lowest τ_b of both the stationary storm events (upper graph) and the dynamic storm events (lower graph).
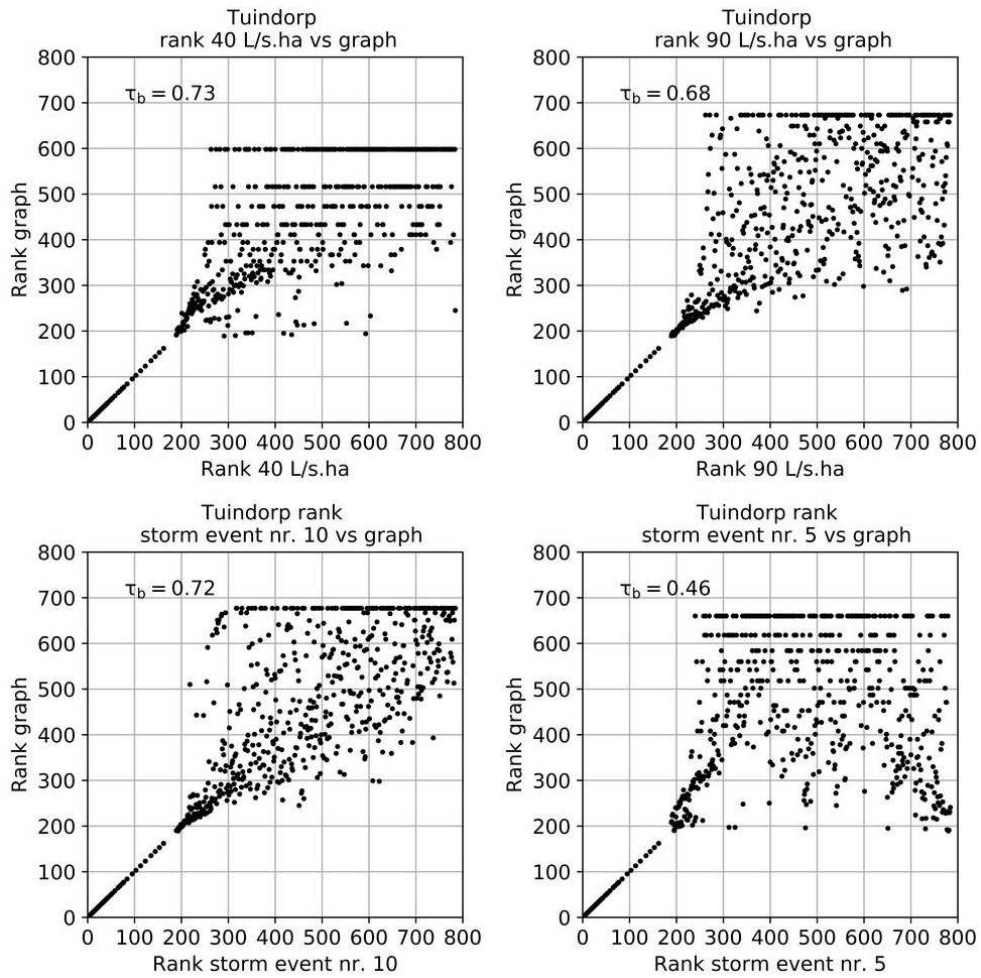
Figure 4.11: Comparison of the rank of importance of the pipes based on the GTM and HMM. The figures show the results for 'Tuindorp'. The graphs at the left side show the ranking based on the graph and hydraulic model outcomes with the highest τ_b of the stationary storm events (upper graph) and the dynamic storm events (lower graph). The graphs at the right side show the ranking based on the graph and hydraulic model outcomes with the lowest τ_b of both the stationary storm events (upper graph) and the dynamic storm events (lower graph).
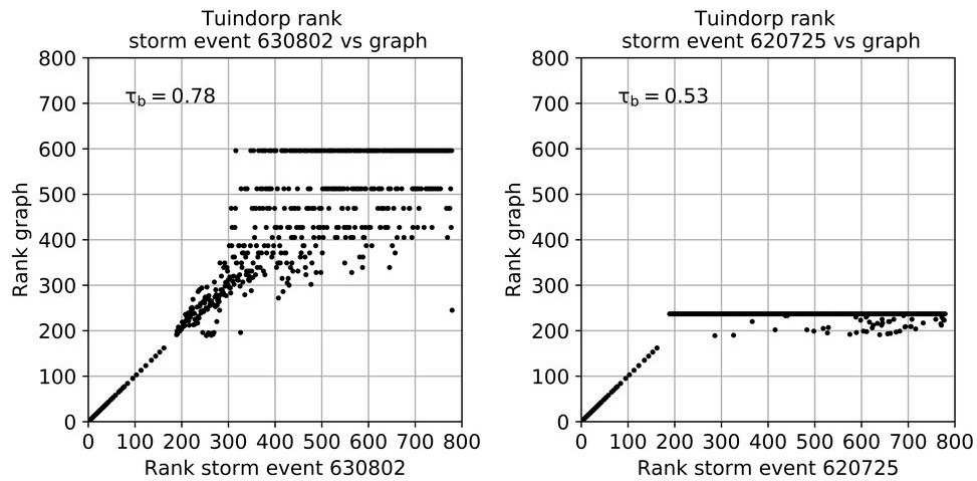
Figure 4.12: Comparison of the rank of importance of the conduits based on the GTM and HMM. The figures show the results for 'Tuindorp'. The graph at the left side shows the ranking based on the graph and hydraulic model outcomes with the highest τ_b of event 630802 of the rainfall series. The graph at the right side shows the ranking based on the graph and hydraulic model outcomes with the lowest τ_b of event 620725 of the rainfall series.

4.3.4   Discussion

An analysis is made of the causes of the differences between the HMM and the GTM as presented before. As explained in section 4.2.2, a major difference between the methods discussed is the fact that the HMM is not storm independent.

An important cause of the differences in results between the HMM and the GTM is that a fixed discharge is used for all conduits in the GTM. The GTM does not take into account that in case of a blockage the discharge in the other conduits increases. An increase in discharge causes a higher head loss in the HMM. This is clearly observed in case of parallel links. In the HMM, blockage of one of the parallel links results in an increase of the water levels, along with an increased degree of criticality. In the same situation, the GTM shows almost no increase in costs when one of the parallel conduits is blocked. This is because the costs of both parallel conduits are almost the same and are not adjusted for the hydraulic processes taking place.

The same effect is visible when two CSOs are connected by a conduit with a relatively large hydraulic capacity. When a conduit close to the CSO is blocked, the water either has to flow to the other CSO or flooding occurs. In the HMM, this causes an increase of the water levels at many manholes because the discharge in the conduits to the not blocked CSO increases. So the conduit is ranked as important. The additional costs in the GTM are limited when the hydraulic capacity of the conduit between the two CSOs is large so the conduit is not ranked as important.

A second cause of the difference in outcomes is the fact that the HMM makes distinctions between flooding and increases in water level. The GTM only calculates the increase in costs in case of a blocked conduit. An increase in costs is weighted equally everywhere. In the HMM, the same increase in water level is marked as more important when the increase results in flooding. The intensity and the shape of the storm event influence this aspect.

For the 'Tuindorp' catchment the dynamic storm events 5 and 6 have a lower correlation than the other storm events (Figure 4.13 - 4.15). Storm events 5 and 6 have a return period of 1 year. Storm event 5 is an event with the peak intensity at the beginning of the storm event and storm event 6 has a peak intensity at the end. These are storm events with maximum water levels for the fully operational sewer system between 0.1-0.25 cm below ground level in the most critical parts of the network while in the less critical parts of the network the maximum water level remains deeper below ground level. A diameter reduction of a conduit in a less critical part of the network that causes a larger increase in water level than a diameter reduction in a critical part is ranked as less important if the diameter reduction in the lower part causes a flooding. The network of 'Tuindorp' clearly shows the influence of the characteristics of the storm event on the ranking based on the hydraulic models. In case of storm events with high rainfall intensity at the start of the event, conduits in the surrounding of the pumping station are ranked as more important because the water degree of the sewer system influences the ponded nodes. When the peak intensity is at the end of the event the system is already completely filled and the discharge via the pumping station is no longer relevant.

A third cause of difference is the variation in ground level in combination with the network layout. In the 'Loenen' catchment a conduit is situated on a slope. There are two paths to a CSO and the length of the two paths is different. This results in a relative large difference in costs. If the shortest route is blocked the additional costs for the GTM are relatively high and the degree of criticality is relatively high. For the HMM the longer path results in an increase of water levels at only one node and the degree of criticality is relatively low.
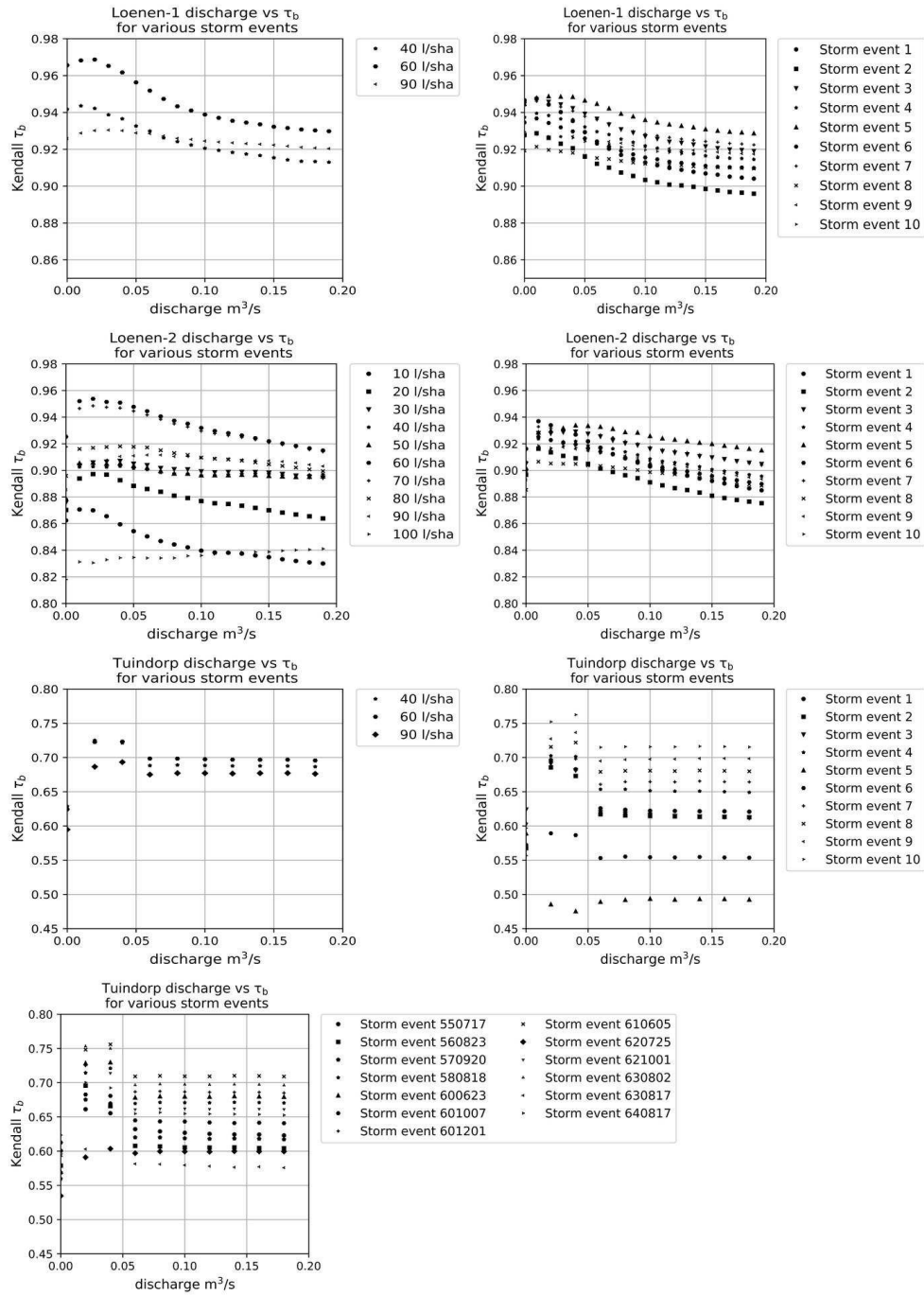
Figure 4.13: The results of the sensitivity analysis of the GTM. The x-axis shows the discharge and the y-axis Kendall's τ_b. Please note that the scale of the y-axis varies.
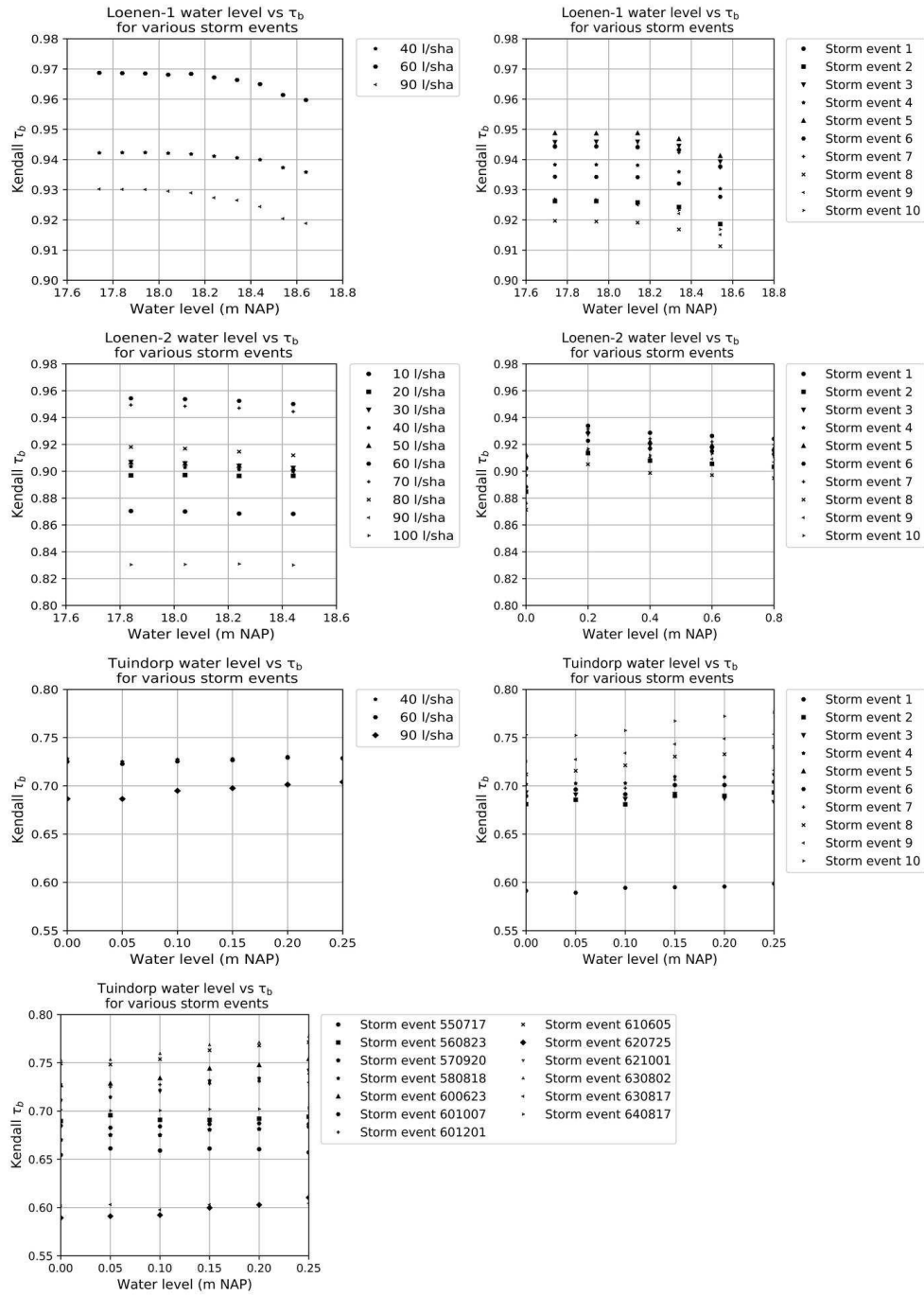
Figure 4.14: The results of the sensitivity analysis of the GTM. The x-axis shows the water level and the y-axis Kendall's τ_b. Please note that the scale of the y-axis varies.
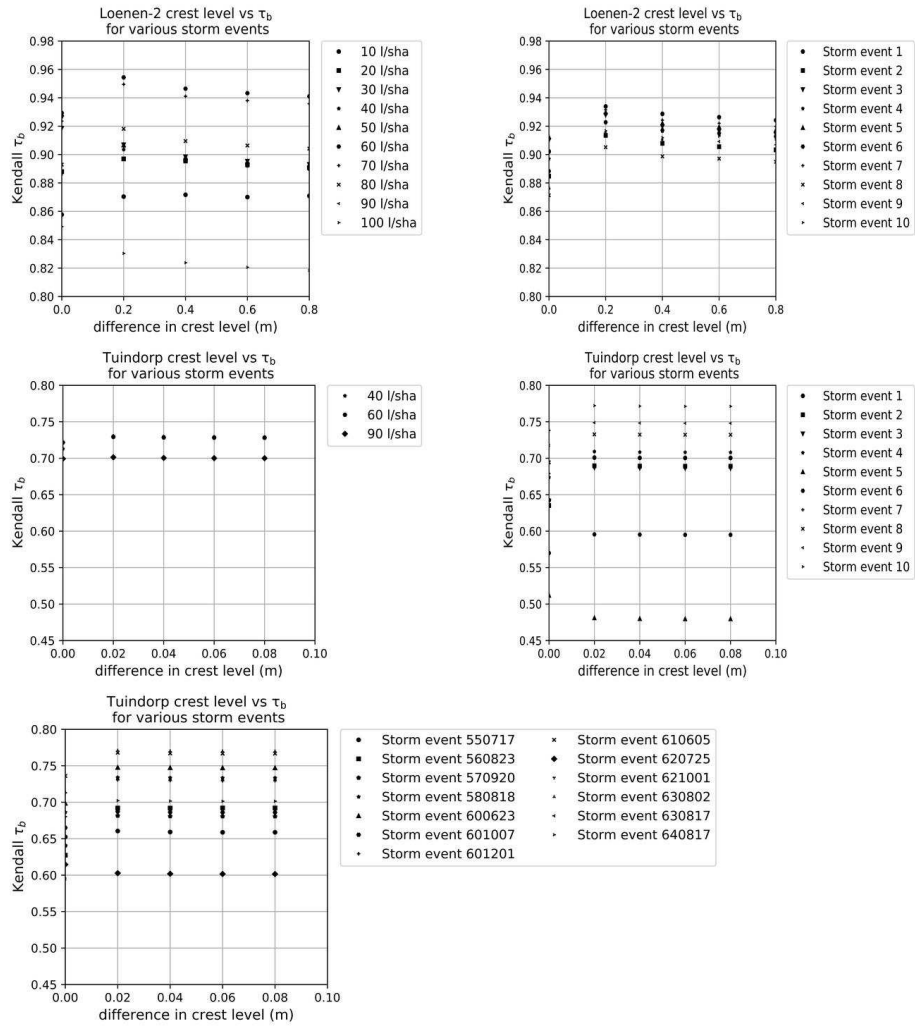
Figure 4.15: The results of the sensitivity analysis of the GTM. The x-axis shows the difference in crest levels and the y-axis Kendall's τ_b. Please note that the scale of the y-axis varies.

4.3.5 Sensitivity of parameters in the Graph Methodology

The costs of the conduits depend on two variables: discharge and water level. The difference in crest levels of combined overflow structures is a third variable for networks with more than one CSO. The discharge influences the dynamic part of the costs of the conduits. If a discharge of 0 m^3/s is used, the dynamic part of the costs of the conduits is zero. With an increasing discharge, the relative importance of the dynamic part of the costs of the conduits increases. The ratio of the dynamic part of the costs between the conduits remains the same because for all conduits the same discharge is used.

The water level influences the static parts of the conduit costs. The conduits with both invert levels below the water level have no static costs. If the water level varies between the lowest and highest invert level the static cost component decreases if the water level increases and vice versa. The difference in crest levels of combined overflow structures determine the additional costs of the use of an overflow with a higher crest level as target node. To determine the influence of these variables on the degree of criticality these variables have been varied (Figures 4.13 – 4.15). The discharge has been varied between 0 - 0.2 m^3/s, the water level between 0 - 1 m above the lowest crest level, the costs for the differences in crest level between 0 - 0.5 for the 'Tuindorp' case and between 0 - 1 for the 'Loenen' case. For each value the degree of criticality is determined. The outcomes of the graph method are compared with the outcomes of the hydraulic model. For the comparison of the degree of criticality the Kendall's τ_b has been used.

4.3.5.1 Discharge

Figure 4.13 shows the results of the sensitivity analysis of the discharge on the results of the GTM. The graphs show that a discharge of 0.02 m^3/s results in a maximum for τ_b. The variation in τ_b is limited to approximately 0.05 m^3/s. τ_b is small if the discharge is 0 m^3/s, and after a peak around 0.02 m^3/s τ_b decreases with increasing discharge. As mentioned before, the discharge influences the dynamic costs. With a discharge of 0 m^3/s the dynamic costs are ignored and with a higher discharge the dynamic costs become relative high in relation to the static costs. It is important that the dynamic costs have the same order of magnitude as the static costs. Because 'Loenen' is situated in a mildly sloped area, the static costs are more important than the dynamic costs. Due to the variation of the ground level, the height differences determine (in combination with the structure of the network) to an important extent the criticality of the conduits. The costs to overcome differences in altitude (static costs) are higher than the additional dynamic costs caused by smaller conduit diameters (dynamic costs).

94

4.3.5.2   Water level sewer system

For 'Loenen-1' and 'Loenen-2' the effect of the water level is limited (see Figure 4.14) because 'Loenen' is situated in a mildly sloped area and a higher water level affects only a limited number of conduits. For 'Tuindorp', the effect of the water level is also limited because only less than 10% of the invert levels of the conduits are situated above the lowest weir. A water level equal to the lowest CSO or equal to the design level of the flow over the CSO (in the Netherlands 0.3 m) is a valid assumption.

4.3.5.3   Difference in crest levels sewer system

For the sewer systems with more than one CSO and with different crest levels, a small (<0.1) additional cost for the CSOs with a higher crest level have a positive effect on τ_b but the effect is limited (<0.05) (see Figure 4.15). The degree of criticality can change strongly if another crest height is used. Conduits with a high degree of criticality can get a low degree of criticality when another difference in crest height is used and vice versa. This means that it is important to select the additional costs for overflows with different crest heights carefully in flat areas. The additional costs for higher crest levels must be in the same order of magnitude as the dynamic costs. So, if a low discharge is used the additional costs also must be low and if a higher discharge is used the additional costs can be higher.

4.3.6   Performance

Table 4.6 shows the performance of the hydraulic model and the GTM. All calculations are made on the same computer. The table shows that the GTM based on the Graph-theory is a few hundred to a few thousand times faster than the HMM method based on the hydraulic models if one storm event is used in the HMM.

Table 4.6:   Comparison of the performance of hydraulic model and the Graph-theory. The time of the hydraulic model is based on 1 storm event.

Network	number of elements	computer time hydraulic model	computer time graph methodology	computational gain factor
'Loenen-1'*)	337	2 h 45 min	2 s	4950
'Loenen-1'**)	337	2 h 24 min	2 s	4320
'Loenen-2'*)	337	2 h 45 min	4 s	2475
'Loenen-2'**)	337	2 h 24 min	4 s	2160
'Tuindorp'*)	778	6 h 24 min	38 s	606
'Tuindorp'**)	778	4 h 12 min	38 s	398

*) Stationary storm event.
**) Dynamic storm event.

4.3.7 Criticality of the pipes

Figure 4.16 and 4.17 show the results of the criticality of the conduits for 'Loenen' and 'Tuindorp' based on the GTM. The figures show that, as expected, the conduits that cause a part of the network to be disconnected when these conduits are blocked are classified as important. Other important conduits are the conduits in the direction of the combined overflow structures. For 'Loenen' there is a clear difference between the situations with 1 and 2 CSOs ('Loenen-1' and 'Loenen-2'). This is also visible in the results of the hydraulic model. For 'Tuindorp', the links between the CSOs are linked as moderate important by the GTM. These conduits are ranked as more important based on the HMM.
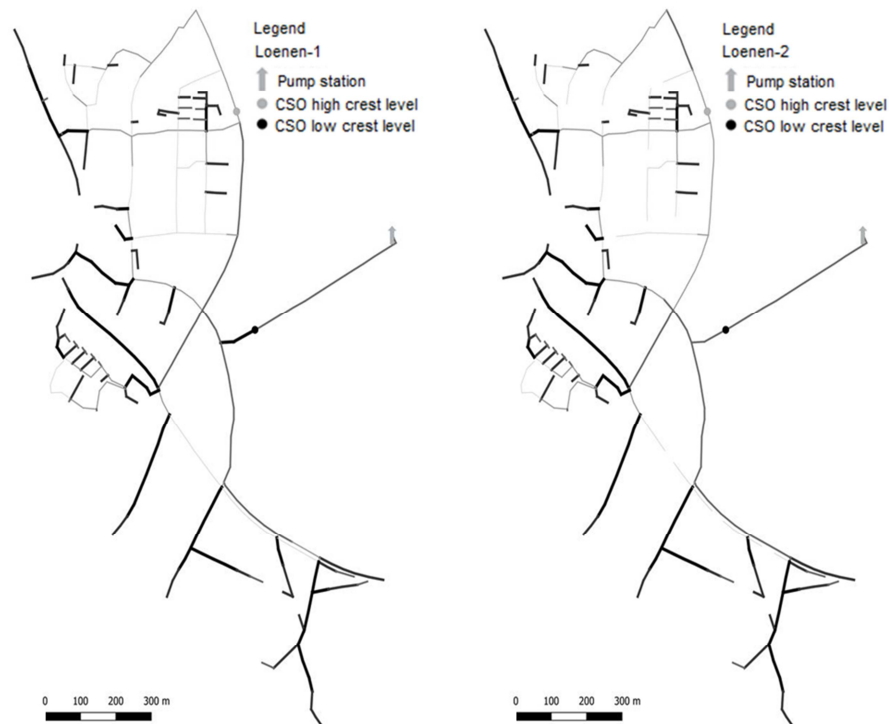

Figure 4.16: Degree of criticality for 'Loenen-1' (left) and 'Loenen-2' (right). The darker the lines the more critical the conduits. A part of the conduits has the same degree of criticality, but the conduits south of the high overflow structure have a different degree of criticality. In 'Loenen-2', these conduits are less important because in the case these conduits are blocked the water can flow to the high overflow structure which is not possible in the 'Loenen-1' system.

96

Figure 4.17: Degree of criticality of 'Tuindorp'. The darker the lines the more critical the conduits.

Figure 4.18 and 4.19 show the results of the comparison between the results of the HMM and the GTM. The darker the line the smaller the difference in criticality rank between the two methods.
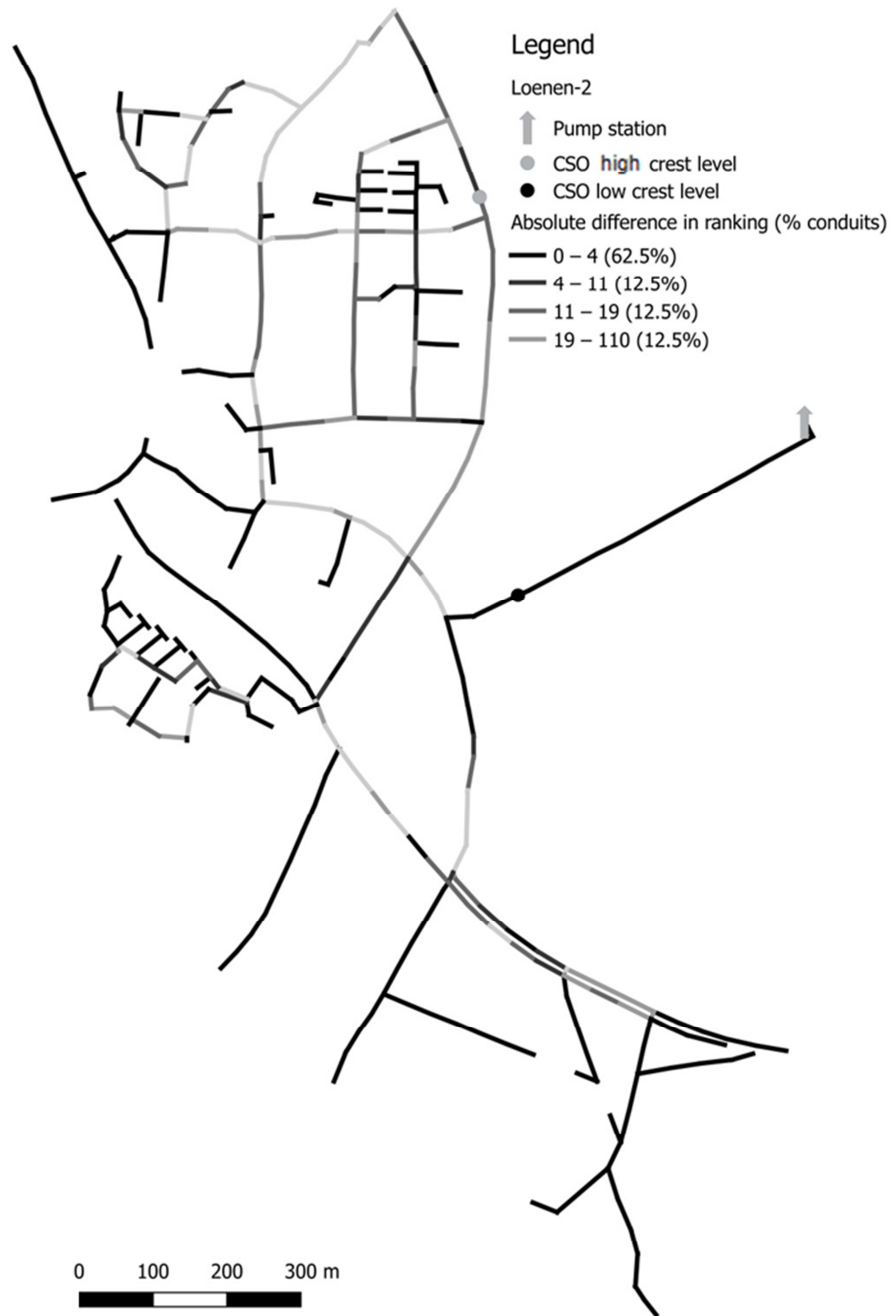
Figure 4.18: Difference in criticality rank between the HMM and the GTM for 'Loenen-2'.

Figure 4.19: Difference in criticality rank between the HMM and the GTM for 'Tuindorp'. The classification of the groups is based on the equal count method.

4.4   Conclusions and perspective

In this chapter, the GTM is presented as a means to identify the most critical elements in a network with respect to malfunctioning of the system as a whole. The method is objective and independent of the type of storm event and requires limited computational effort. The degree of criticality of the conduits is compared with the HMM (Achilles approach). There is a high correlation (Kendall's $\tau_b > 0.72$) between GTM and HMM results.

The degree of criticality based on the HMM depends strongly on the used storm event. In the HMM the degree of criticality is determined by removing each conduit individually from the network. The links are ranked based on the total increase in flood volume and the increase of water level in the sewer system. The use of different storm events leads to a different ranking of the elements. Important elements become less important and vice versa. That means it is impossible to define one rank of the degree of criticality for different rainfall intensities by removing each conduit individually from the network.

99

The criticality for the partly-branched mildly-sloping catchment of 'Loenen' has a stronger correlation with the results of a hydraulic model than the results of the looped, flat 'Tuindorp' catchment. Nevertheless, it was shown that for both catchments it is possible to identify the 30-40% most critical conduits in a robust manner, compared to other methods as applied in practice.

For sewer systems, the degree of criticality based on the GTM depends on three parameters: the discharge, the water level and the difference between crest levels of overflow structures. The outcomes of the GTM are not sensitive for the exact value of the variables as long as the variables have values that result in dynamic and static costs of the same order of magnitude. The importance of the dynamic part of the costs of the conduits is limited for sewer systems in (mildly) sloped areas where the overflow is situated in the lower part of the system.

Apart from the influence of the storm event, there are two main causes for the differences in the results of the degree of criticality based on the HMM and the GTM. The first cause is that, in the GTM, the same discharge is used for all conduits, also when one of the conduits in the system is blocked. The second cause is that, in the GTM, each increase in costs is equally important. In the HMM, an increase in water level that causes a flooding is weighted as more important than a comparable increase in water level without flooding.

The degree of criticality can be used to prioritize the sensitivity of individual sewer conduits for flooding at network level. In addition, the methodology provides input for the design of monitoring networks meant for 'hydraulic fingerprinting' as mentioned in chapter 2.

5 Quantitative impact assessment of sewer condition on health risk

5.1 Introduction

Exposure to urban pluvial flooding may pose a health risk to humans, since floodwater may contain a variety of contaminants depending on its origin. During the past years, there has been an increased interest in microbial impacts through pluvial flooding (see e.g. Fewtrell et al., 2008; Lau et al., 2010; Fewtrell et al., 2011; Cann et al., 2013; De Man et al., 2014; Hashimoto et al., 2014; Andersen, 2015; Mark et al., 2015; Hammond et al., 2015) and CSO spills (Harder-Lauridsen et al., 2013), as well as economic, social and psychological impacts of urban flooding (Stephenson et al., 2014). The latter are expressed as stressors on communities due to repeated flood events.

Originating from rainfall-generated surface runoff, pluvial flooding may be contaminated by dirt from paved surfaces (e.g. dog faeces and bird droppings). From combined sewer systems, it will be contaminated with wastewater and from storm sewers due to illicit connections. The contaminations include human enteric pathogens (e.g. norovirus and enterovirus) from urban wastewater (Lodder and De Roda Husman, 2005), and *Campylobacter*, *Giardia* and *Cryptosporidium* from both animal faeces and human wastewater (Schets et al., 2008; Koenraad et al., 1994). According to De Wit et al. (2001) and Mead et al. (1999), these pathogens account for the majority of gastrointestinal illnesses in the Netherlands and the US. Harder-Lauridsen et al. (2013) demonstrated that the risk of illness from water intake by physically fit, long distance swimmers when swimming in sea water shortly after an extreme rainfall event is considerably larger than from non-polluted water.

In-sewer defects affect the hydraulic performance of a sewer system and may cause increased pluvial flooding. Possible defects include sedimentation, root intrusion, surface damage, attached deposits, settled deposits, corrosion, protruding objects, joint eccentricity and subsidence (see e.g. Stanić, 2014; Bennis et al., 2003). Chapter 2 demonstrated the impact of defects on flooding using data from visual inspections and Monte Carlo simulations for a full hydrodynamic model. The studied defects are sedimentation, root intrusion, surface damage and attached/settled deposits. The results show that in-sewer defects significantly affect flooding with sedimentation as the predominant factor.

Health risks of exposure to pluvial flooding from urban drainage, including combined sewers, were quantified by De Man et al. (2014) using Quantitative Microbial Risk Assessment (QMRA). This requires information on the concentration of pathogens in the water or on the correlation between indicator bacteria and pathogens in the water, the exposure of people to these pathogens, and dose-response relations for different pathogens.

This chapter addresses the impact of in-sewer defects on urban pluvial flooding and, subsequently, on health risks to humans. The analysis is based on flooding frequencies from Monte Carlo simulations as described in chapter 2 and infection probabilities due to ingestion of urban floodwater as presented by De Man et al. (2014).

5.2   Materials and methods

An overview of the data utilised and analysed in this study is shown in Figure 5.1. The catchments of 'Tuindorp' and 'Loenen' have been analysed accordingly. A detailed description is given in sections 5.2.1–5.2.7. The impact of sewer condition on urban flooding has been quantified using Monte Carlo simulations accounting for in-sewer defects, in particular sedimentation. Based on the simulation results, the summed frequency of threshold exceedances has been calculated for each manhole. From this result, the catchment-wide average infection probability per year has been calculated using infection probabilities from De Man et al. (2014).

(1) PIPE BLOCKAGE   *Monte Carlo simulation as described in chapter 2*

sediment growth described with Beta distribution for pipe diameter classes based on CCTV inspections   **5.2.2**

hydrodynamic model of sewer system without in-sewer defects   **5.2.1**

value for sediment depth drawn from Beta distribution for each sewer   **5.2.2**

750 x

Monte Carlo simulation with hydrodynamic model of sewer system with in-sewer defects   **5.2.5**

(2) FLOODING FREQUENCY   *Assessment of water level above threshold*

calculated water levels from models with in-sewer defects (n = 750)

$A_{flooded} = 50m^2$

number of exceedances of threshold level at each manhole   **5.2.6**

summed frequency of exceedances at each manhole per system state per year   **5.2.6**

$A_{flooded} = 75m^2$

number of exceedances of threshold level at each manhole   **5.2.6**

summed frequency of exceedances at each manhole per system state per year   **5.2.6**

$A_{flooded} = 100m^2$

number of exceedances of threshold level at each manhole   **5.2.6**

summed frequency of exceedances at each manhole per system state per year   **5.2.6**

(3) INFECTION PROBABILITY   *Assessment of average catchment-wide probability*

$A_{flooded} = 50m^2$

infection probability per year at each manhole based on values from De Man et al. (2014)   **5.2.7**

average catchment-wide infection probability per year accounting for number of inhabitants per manhole   **5.2.7**

$A_{flooded} = 75m^2$

infection probability per year at each manhole based on values from De Man et al. (2014)   **5.2.7**

average catchment-wide infection probability per year accounting for number of inhabitants per manhole   **5.2.7**

$A_{flooded} = 100m^2$

infection probability per year at each manhole based on values from De Man et al. (2014)   **5.2.7**

average catchment-wide infection probability per year accounting for number of inhabitants per manhole   **5.2.7**
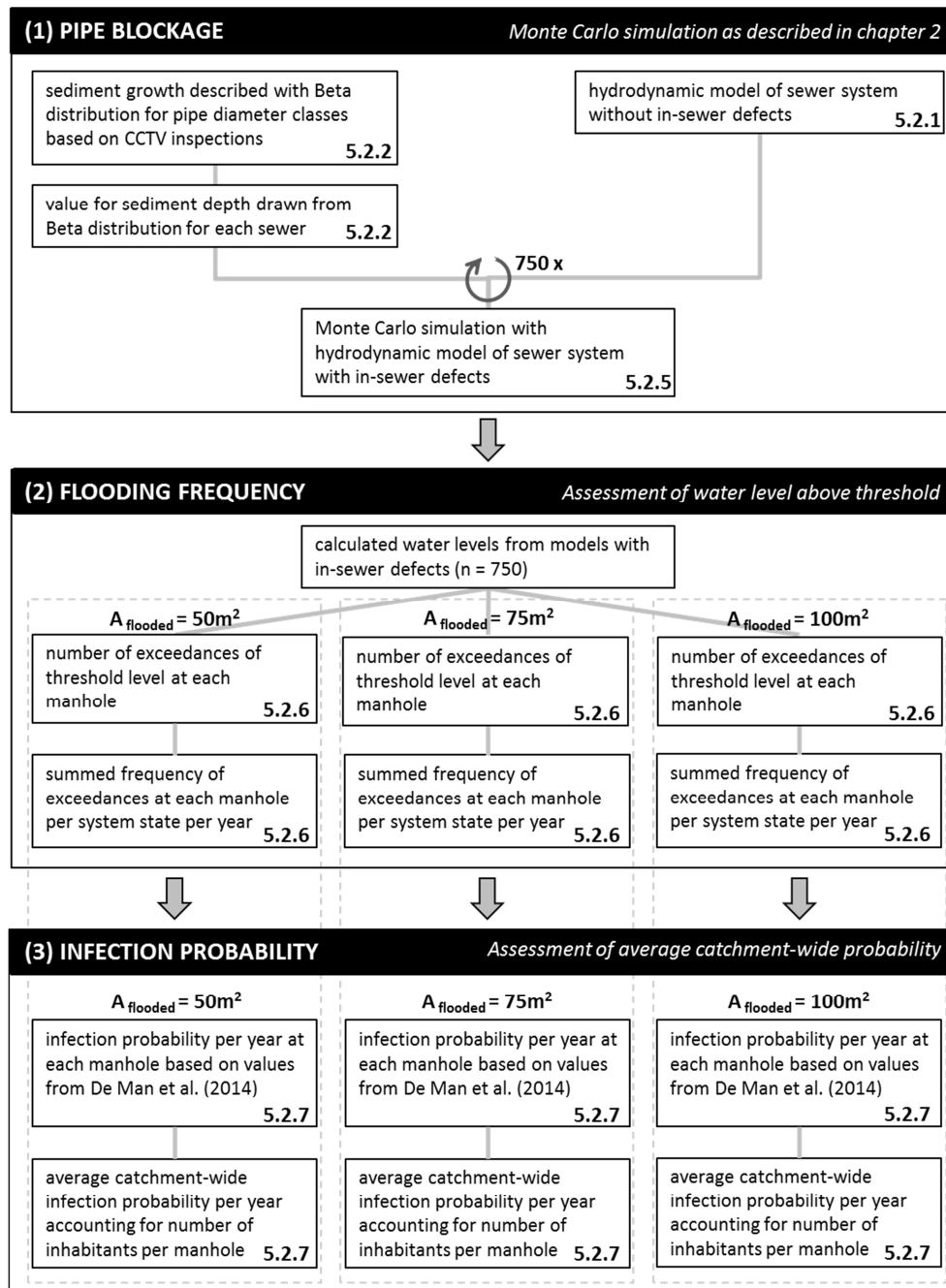
Figure 5.1:   Procedure for calculating average catchment-wide infection probabilities. The numbers refer to the corresponding chapter and paragraph.

5.2.1   Research catchments

The two Dutch combined sewer systems 'Tuindorp' and 'Loenen' are studied. The 'Tuindorp' catchment area is a combined sewer system constructed in the 1970s as a looped gravity flow system. The catchment is relatively flat. It comprises a range of contributing areas in terms of types of roofs and types of pavement. The collected sewage is transported to the pumping station in the southern part of the catchment. The sewer system contains five CSO structures. One of the CSOs discharges into a storage-settling tank. There are no discharges and inflows from adjacent systems into the catchment.

The 'Loenen' catchment is also a combined sewer system. It has been constructed as a partly-branched gravity system and the catchment is mildly-sloping. The sewer system is equipped with one pumping station and two CSO structures. One of these CSO structures discharges into a large pond. There is a relatively large average dry weather flow per inhabitant because of several industrial discharges and an inflow from an adjacent catchment.

The characteristics of both catchments are summarised in Table 1.1. The layout of the sewer systems is presented in Figure 1.6. For more information about both sewer catchments see section 1.6.

5.2.2   Description of in-sewer defects

Observed sediment depths (chapter 2) were used to include sediment deposition in the hydrodynamic model. Crabtree (1989) describes five categories of sediment deposits, based on observations of the provenance, nature, and location of the deposits within the sewer system. Sediment deposits in the Netherlands can typically be classified as type C: mobile, fine grained deposits found in slack flow zones. In this study, sediments are defined as type C deposits, which can be removed from a pipe by means of jetting. In Utrecht, sediment depths are registered by cleaning engineers before jetting individual pipes while carrying out the annual cleaning program. Attached deposits that have to be removed by other techniques can only be detected by detailed visual inspection of sewer pipes. Sediment depths are classified according to the percentage of obstructed pipe height. The accuracy of observed sediment depths depends on cleaning engineers' experience and opinion (Dirksen and Clemens, 2007; Korving, 2004). Before jetting an individual pipe, the cleaning engineer makes an estimation of the sediment depth as can be seen from ground level after opening the manhole. After jetting the pipe, the removed amount of sediment for each pipe is also estimated. Sediment depths are registered as a relative depth (ratio of observed sediment depth and conduit height).

Observed depths were translated into model parameters accounting for conduit shape (circular, egg) and conduit height (250-1,250 mm). For that purpose, a beta distribution function was fitted on observed sediment depths (chapter 2) in order to statistically describe sediment depth for each conduit category (combinations of shape and height). In the hydrodynamic model simulations, the relative sediment depths in the conduits were randomly drawn from the corresponding distribution.

5.2.3   Model set-up

InfoWorks© (version 8.5) was used for the hydraulic calculations. The InfoWorks© models of both sewer systems have been validated but not calibrated. The validation aims at removal of systematic errors from the model. This is done according to the method described in Van Mameren and Clemens (1997), Clemens (2001a) and Stichting RIONED (2004). This implies that system data on structural and geometrical data, ground levels, pumping capacities, etc., are verified in the field and that a comparison is made between call data on flooding events and locations where the model predicts flooding (see section 5.2.4).

Chapter 3 showed for the 'Tuindorp' system that calibrated model parameters based on different storm events vary considerably. Since the calibration parameter set predominantly contains runoff parameters, which change between different rainfall events because the values also incorporate the antecedent condition of the catchment area, it is practically impossible to find one single parameter value set which can be used for a long time series. In addition, the values of calibrated model parameters and their correlations are affected by the presence of the in-sewer defects because these defects are local obstructions to the flow and cannot be included as uniquely identifiable calibration parameters. As a result, the presence of defects will affect the values of the calibrated parameters values which are mainly related to runoff. Considering that the characteristics of the network (i.e. the system state) in the Monte Carlo simulations change each run due to defects at randomly chosen locations, it is nearly impossible to use a set of calibrated parameters derived from a single model state with defects at different locations.

An integrated 1D/1D model has been applied to describe the interaction between the underground sewer network and surface flooding. This modelling approach is sufficient for flat catchments. Leandro et al. (2009) showed, for a relatively flat catchment, that a validated 1D/1D model is able to replicate the 1D/2D maximum flood extent. This is a safe assumption, as the gradient of the catchment presented in Leandro et al. (2009) as a case study, is larger than in the 'Tuindorp' and 'Loenen' catchments ('Tuindorp' factor 10 and

'Loenen' factor 2). Furthermore, the calculation time in the case of a 1D/2D model in combination with long-term rainfall series would not be within acceptable limits.

5.2.4   Model validation

For the model validation, a comparison between call data on flooded streets and simulated flood locations was made for the rainfall event on 4 November 2013. This event was chosen because in 2012, the whole 'Tuindorp' sewer system was cleaned, and between January and July 2013, observed defects were removed, except for root intrusions in the central part of the sewer system. Following these actions, the sewer system was considered "clean" and suitable for validating the InfoWorks© model.

Reported incidents from the call data of the municipality supplemented with interviews with residents were compared with model results. For the storm event on 4 November 2013, this comparison is shown in Figure 5.2. Most of the locations that suffered from flooding in reality coincide with the model results, although some reported incidents in the northern part of the catchment are not present in the simulations. This may be caused by call data systematically underestimating the extent of flooding due to underreporting (Spekkers et al., 2015).
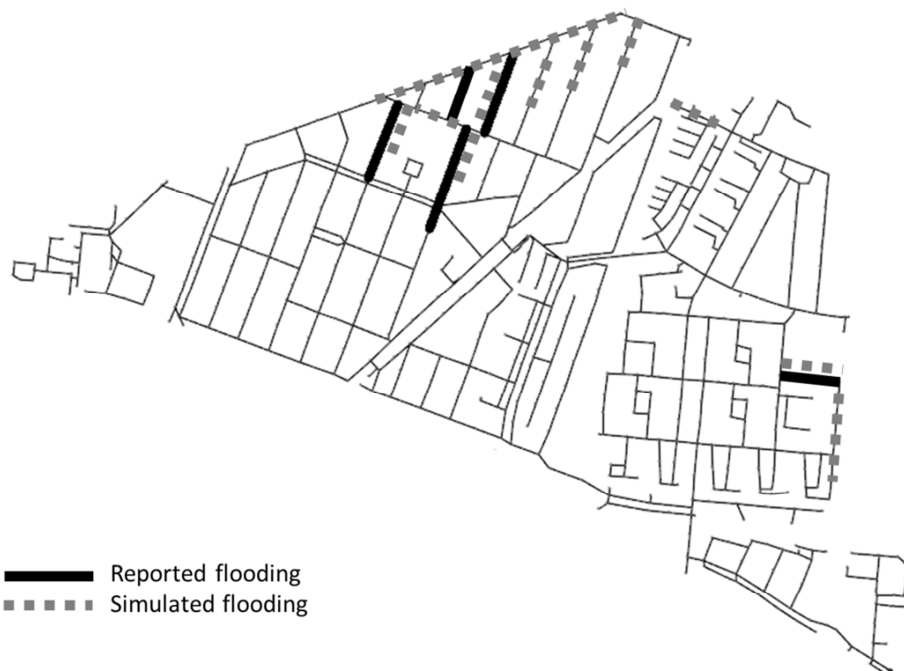
Figure 5.2: Comparison of reported and simulated flood areas in the 'Tuindorp' catchment during the rainfall event on 4 November 2013 in order to validate the InfoWorks© model.

106

5.2.5 **Monte Carlo simulations**

Monte Carlo simulations were used to evaluate the impact of in-sewer defects on flooding frequencies at each manhole. Detailed InfoWorks© models were used for the simulations. Because of the random changes in the characteristics of the network (i.e. system state) in each run during the Monte Carlo procedure, it is impossible to predict beforehand which storm events will cause flooding. Therefore, in the Monte Carlo simulations, long-term rainfall series were used. This series was observed by the Royal Dutch Meteorological Institute in De Bilt (the Netherlands) during the period 1955-1964. This series comprises continuous series of rainfall volumes in De Bilt, as observed with an interval of 15 minutes (Figure 5.3). This time series is generally used in the Netherlands to evaluate the design performance of sewer systems (Stichting RIONED, 2004). In the case of the 'Tuindorp' catchment, 322 independent storm events were filtered from the 10-year time series. This filter is based on in-sewer storage volume, pumping capacity, and required length of dry periods between storm events. For the 'Loenen' catchment, 572 events remained after filtering. The rain volume and the time in between storms are such that the system has returned to a stable dry weather flow configuration. As a result, the initial conditions are the same for each storm so as to prevent interdependence between storm events.
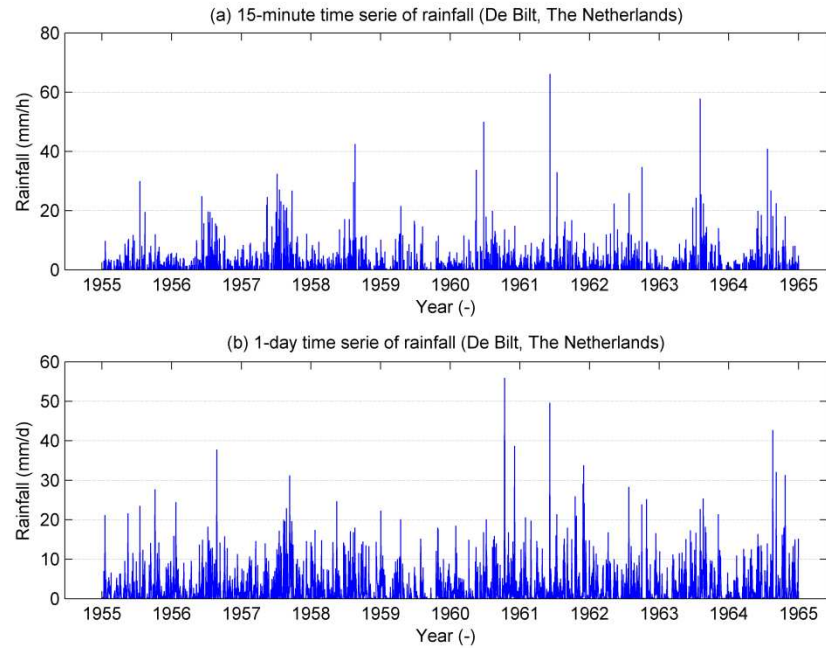
Figure 5.3: Long-term rainfall series of De Bilt (the Netherlands) Observed rainfall volumes (by the Royal Dutch Meteorological Institute) during the period 1955-1964. 15-minute time series of rainfall (top) and 1-day time series of rainfall (bottom).

A single run in the Monte Carlo procedure is defined as the hydrodynamic simulation of the complete collection of the selected (and independent) storm events for a single system state. In each Monte Carlo run, the relative sediment depth of each pipe was randomly drawn from the beta distributions describing the presence of sediments. As a result, the network will have a different configuration in each Monte Carlo run. For reliable estimates of flooding frequencies, 750 Monte Carlo runs were performed. This number of runs is sufficient because the mean and standard deviation of the average infection probability per year become stable after approximately 600 runs (Figure 5.4).
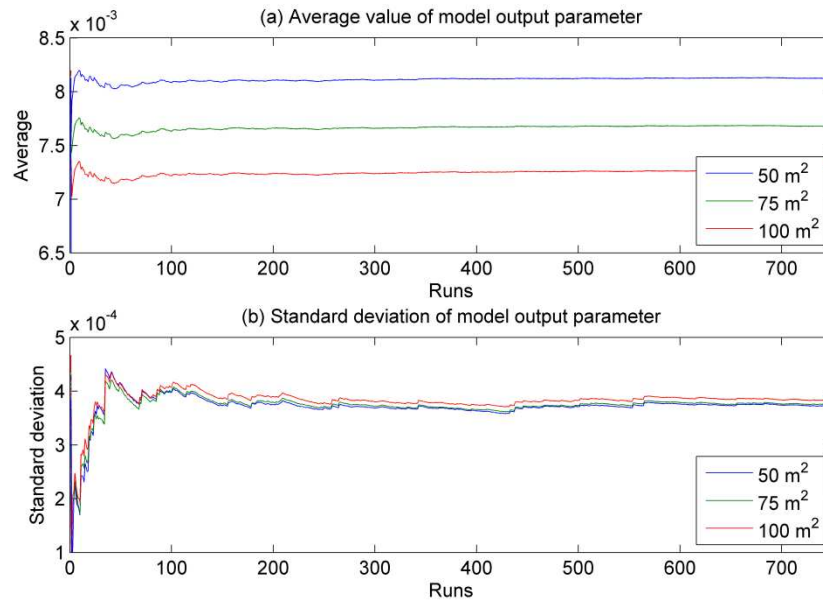
Figure 5.4:   Average (top) and standard deviation (bottom) of relevant model output parameter (i.e. average infection probability per year).

The sediment depth at the conduit bottom, reduces the hydraulic capacity of the conduit. The sediment is modelled as permanent sediment deposits in the InfoWorks© model. Erosion or deposition of sediment and transport of sediment through the system are not accounted for in the applied model approach.

5.2.6 Quantification flooding frequencies

Calculated water levels exceeding manhole cover levels are considered as flooding. Since overland flow is not considered in the 1D/1D approach chosen for this study, the storage of floodwater is included in the model by adding a 'cone' on top of the manhole. In modelling terms, this floodwater is stored above ground in a flood cone. The volume of water held by the cone will be discharged into the sewer system as the water level drops again. The shape of the flood cone is sketched in Figure 5.5. The floodable area ($A_{floodable}$) is the total area available for the storage of floodwater at a specific node. As a result, it is the sum of the contributing areas draining to this node. The shape of the flood cone (Figure 5.5) determines the relationship between flood volume and water level above street. Flood volume is defined as the calculated water volume on street level due to a flooding event at a specific manhole. The part of the flood cone below 0.1 m represents the contributing areas of streets and adjacent pavements (Figure 5.5). This equals approximately 50% of the total floodable area at each node, which corresponds to the average value of contributing impervious and semi-pervious areas of all nodes. The second part runs from 0.1 m to 0.5 m, with a linear increase in floodable area from 50% to 100%. Above 0.5 m, the floodable area remains 100% (Figure 5.5). This implies that, with flood depths below 0.1 m, the flooded area stays between the sidewalks, whereas for larger depths, the flooded area spreads across the entire contributing area of a node.
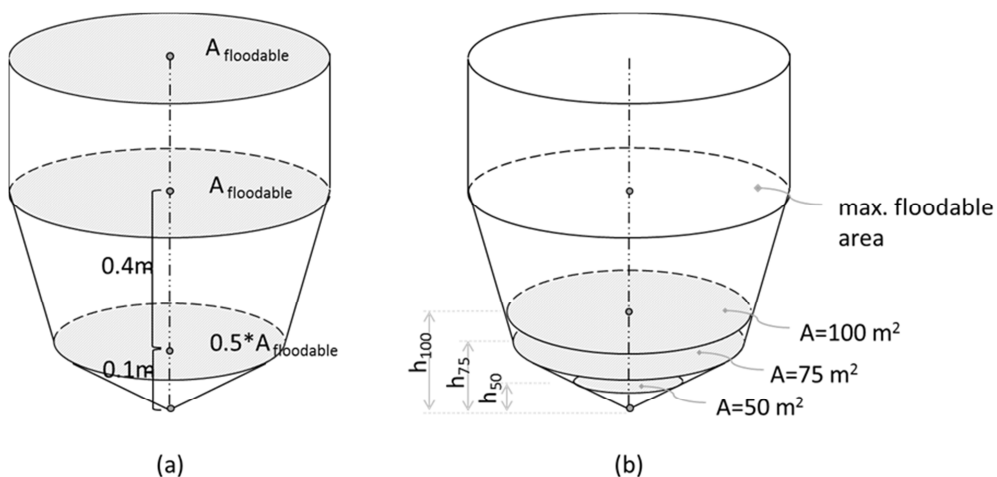

Figure 5.5: Flood cone on top of a manhole in the hydrodynamic model storing water above street level. The relationship between flood volume and water level above the street (left). Three threshold areas 50, 75, and 100 m^2, including the corresponding threshold water levels h_{50}, h_{75}, and h_{100} for assessing the sensitivity of the results (right).

The severity of exposure to floodwater depends on the amount of floodwater and the duration of the flooding event. De Man et al. (2014) took samples of pluvial flooding if the flooded area was larger than 100 m^2. In order to assess the sensitivity of the results for the flooded area, next to this value, threshold values for the flooded area of 50 and 75 m^2 are applied as well. For each threshold area, a corresponding threshold water level is calculated given the shape of the flood cone (Figure 5.5). The maximum threshold level for the flood depth is limited to 0.15 m in order to avoid levels above the sidewalks and to exclude the part of the flood cone representing flat and inclining roofs. This limitation is only necessary at locations with very small contributing areas.

For each manhole, the number of exceedances of threshold water levels is calculated from the 10-year rainfall series. An exceedance is defined as an event in which the calculated flood depth in the sewer system exceeds the threshold water levels corresponding with a specific threshold value of the flooded area at an individual manhole. Consequently, exceedance of a threshold at two different manholes during the same time step is counted as two separate threshold exceedances. Finally, the summed frequency of exceedances at each manhole per system state per year is calculated.

5.2.7 Quantification of health risks

Due to backflow from combined sewer systems, pluvial flooding may contain high amounts of pathogenic micro-organisms (Alderman et al., 2012). Consequently, exposure to this floodwater entails a risk for public health. In De Man et al. (2014), infection risks from exposure to urban pluvial flooding were assessed using QMRA. Urban floodwater was sampled to quantify the presence of waterborne pathogens *Campylobacter*, *Cryptosporidium*, *Giardia*, norovirus, and enterovirus. Samples of approximately 20 L were taken during flood incidents in the Netherlands and the concentrations of the pathogens were analysed according to ISO standards (De Man et al., 2014). Questionnaires were used for an estimation of the volume of floodwater ingested by people during exposure. Based on pathogen data and exposure data, the probability of infection due to flooding from combined sewers, storm sewers, and rainfall generated surface runoff was quantified.

A distinction was made between children and adults in terms of infection probabilities because of the higher ingestion probability for children. For adults, the average probability of infection equals 3.9 % per event. For children, this probability is almost ten times higher and amounts to 33 %.

De Man et al. (2014) applied dose-response relationships for the quantification of the probability of infection per exposure event (P_{event}) for the different pathogens *Campylobacter*, *Cryptosporidium*, *Giardia*, norovirus and enterovirus. It is assumed that, except for enteroviruses, all waterborne pathogens are infectious. This can be justified because by the fact that the different pathogens lead to similar complaints concerning public health and that one pathogen was likely to prevail to cause a gastrointestinal infection. As a result, the overall probability of infection per exposure event ($P_{infection/event}$) is quantified by summation of the values for each pathogen.

The infection probability per year is calculated from the overall probability of infection per exposure event ($P_{infection/event}$) and the frequency of exposure events to flooding per year (*n*). The latter is the number of events where flooding occurred during the 10-year rainfall series in the Monte Carlo simulations (i.e. exceedances of defined thresholds values of floodable area). The set exposure events (*n*) are represented in Figure 5.6 as rectangle S, whereas the sub-set of exposure events that actually results in infection are represented by region A. In addition, the complement Ā (shaded part of rectangle S) of A is the subset of S that contains all the exposure events that does not lead to infection ($1 - P_{\text{infection/event}}$). The infection probability per year is calculated by application of the rule of multiplication for probabilities.
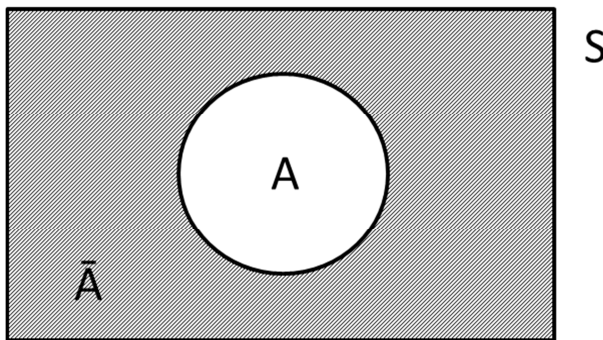

Figure 5.6: Venn diagram representing all exposure events as the rectangle S. Region A shows the exposure events that actually lead to infection. The complement Ā (shaded part of rectangle S) of A is the subset of S that contains all the exposure events that does not lead to infection ($1-P_{infection/event}$).

112

5. Quantitative impact assessment of sewer condition on health risk

In addition, the infection probability per year is calculated from the overall probability of infection per exposure event and the frequency of flooding events (i.e. exceedances of defined thresholds values of floodable area), as follows:

$$P_{\text{infection/year}} = 1 - \prod_{i=1}^{n} (1 - P_{\text{infection/event}}) = 1 - (1 - P_{\text{infection/event}})^n \qquad (5.1)$$

where n is the frequency of exposure events to flooding per year. The uppercase pi ($\prod$) represents the product over ($1 - P_{\text{infection/event}}$) from $i = 1$ to $i = n$. Using equation (5.1), the infection probability per year at each manhole is calculated. Based on these probabilities the average infection probability per year was determined as a weighted average based on the number of inhabitants per manhole:

$$P_{average\_\text{infection/year}} = \frac{\sum_{i=1}^{y} n_i P_{infection/year}(manhole\_i)}{n_{total}} \qquad (5.2)$$

where y is the total number of manholes, n_i is the number of inhabitants for manhole i and n_{total} is the total number of inhabitants in the catchment area.

Next to frequency, the impact of exposure to floodwater depends on the duration of flooding. It can be expected that the infection probability is also related to the duration of flooding. However, flood duration is not incorporated in equations (5.1) and (5.2). The knowledge on the relation between flood duration and infection probabilities is still very limited as literature in methods quantifying infection risks (De Man et al., 2014; Fewtrell et al., 2011 and Andersen, 2015) does not include flood duration.

5.3 Results and discussion

5.3.1 Results 'Tuindorp' catchment

5.3.1.1 Frequency of flooding

Exposure to floodwater is influenced by the frequency of flooding (De Man et al., 2015; Hashizume et al., 2008). De Man et al. (2015) showed that floodwater-associated diseases occur in urban areas after flood events due to extreme rainfall. The total number of people visiting the general practitioner for gastrointestinal, influenza-like illness, and dermatological complaints increased by 13% compared to a situation without flooding. Flooding frequency varies across the 'Tuindorp' catchment (Figure 5.7). This Figure shows the average number of flooding events per manhole in the catchment, which is calculated from the results of the 750 Monte Carlo runs. Spatial differences indicate the sensitivity to flooding of a location or area. The eastern and north-western parts of the catchment are more sensitive to flooding. The eastern part is more sensitive because it is a sub-catchment with a very limited number of direct connections to CSO structures.
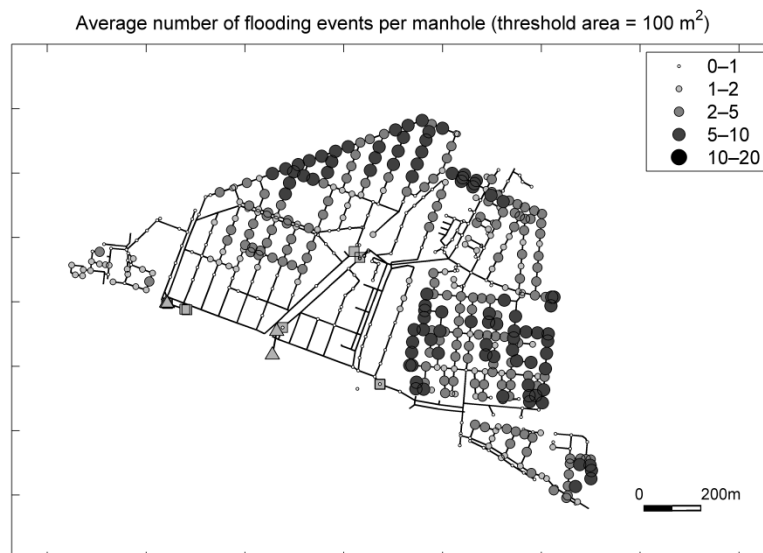
Figure 5.7: Average number of flooding events per manhole based on the Monte Carlo simulations for the 'Tuindorp' catchment.

114

5.3.1.2   Duration of flooding

Next to frequency, the impact of exposure to floodwater depends on the duration of flooding. This also varies across the catchment (Figure 5.8). This Figure shows the maximum flood duration per manhole for different thresholds. Starting at the top left figure, the threshold of the maximum duration per manhole increases clock-wise (30 minutes, one hour, two hours, and four hours respectively).

Manholes showing extended flood durations (> 2 hours) are concentrated in the eastern part of the catchment. Flood durations over four hours occur at a limited number of top ends in the sewer system. Based on a comparison of Figures 5.7 and 5.8, it is concluded that in the eastern part of the catchment, flooding events occur more often and last longer relative to the rest of the catchment area. The coincidence of higher frequencies and longer durations increases infection probabilities in this sub-catchment.

Table 5.1 presents the summary statistics for the duration of flooding events in the 'Tuindorp' catchment. Both mean values and 95% uncertainty intervals of average, minimum, and maximum event duration (in minutes) are displayed for three different threshold area dimensions. An event is defined as a combination of a rainfall event and a system state (i.e. 322 × 750 events). The mean value of the average flood duration per event is limited to approximately 20 minutes. However, the spread is relatively large (1–64 minutes), with a long tail towards the higher values. The mean of the maximum flood duration per event is approximately 37 minutes, also exhibiting a large spread (1–127 minutes).

Table 5.1 also demonstrates that the selected rainfall events are independent with respect to flood impacts. The upper value of the 95% interval of the maximum flood duration per event (approximately two hours) is much smaller than the total duration of the rainfall events (12 hours and more).
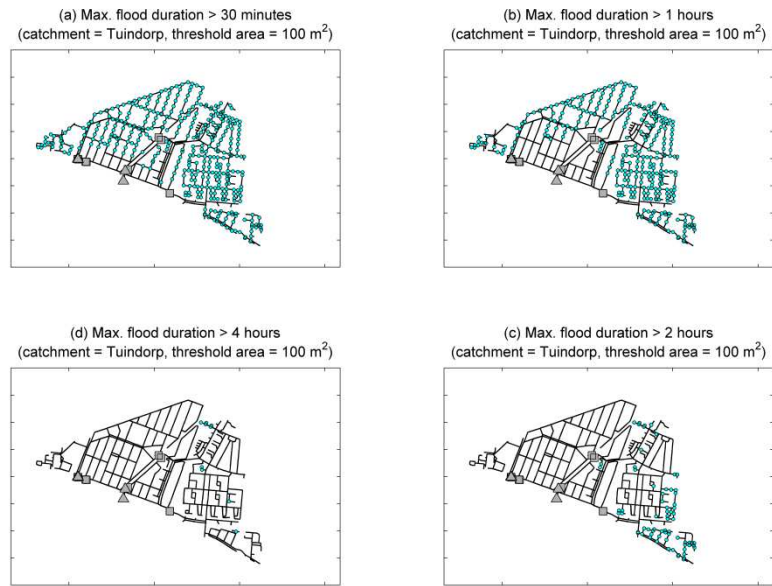
Figure 5.8: Manholes in the 'Tuindorp' catchment with an increasing maximum flood duration (clockwise): larger than 30 minutes (top, left), larger than 1 hour (top, right), larger than 2 hours (bottom, right) and larger than 4 hours (bottom, left).

Table 5.1: Summary statistics of duration (in minutes) of flooding events in the 'Tuindorp' catchment.

		flooded area		
		50 m^2	75 m^2	100 m^2
average event duration (min)	mean	19.60	19.32	19.05
	95%-interval	2 - 64.08	1.67 - 63.98	1 - 63.62
min. event duration (min)	mean	4.23	4.17	4.02
	95%-interval	1 - 36	1 - 33	1 - 31
max. event duration (min)	mean	37	36.77	36.49
	95%-interval	3 - 127	3 - 127	1 - 127

5.3.1.3   **Probability of infection**

Overall for 'Tuindorp', the average infection probability for adults increases (Figure 5.9). This figure shows the catchment-wide density function of infection probabilities for three different threshold area dimensions. The density function is calculated using kernel smoothing based on an Epanechnikov kernel (Wand and Jones, 1995). This kernel has the

shape of the positive part of a parabola (i.e. has no long tails). The selected bandwidth performs well for normal distributions.
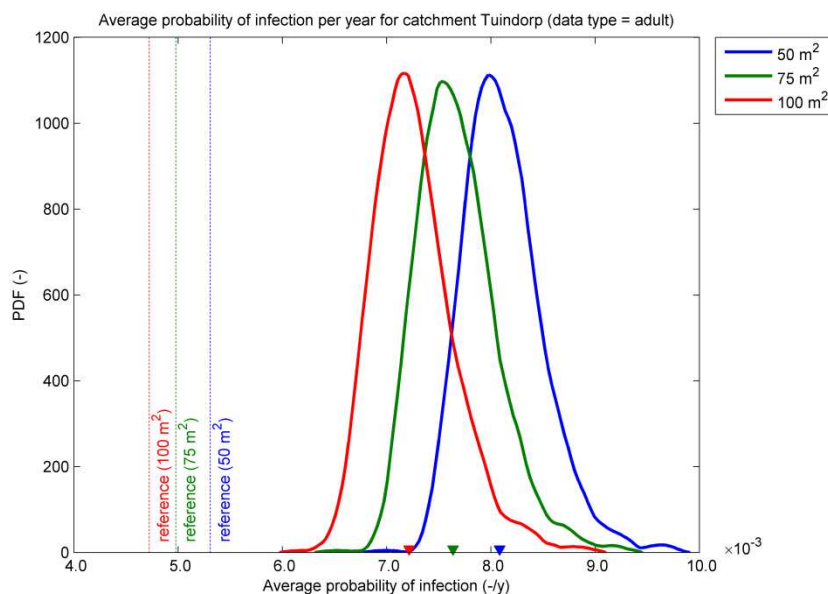

Figure 5.9:   Infection probability for adults per year in the 'Tuindorp' catchment.

The median value of the infection probability decreases with increasing threshold area. This simply means that the probability of a smaller flooded area is larger and, as a result, the infection probability is also larger. The spread is due to the different system states in the Monte Carlo sample.

There is a shift in infection probabilities due to sedimentation. This shift equals an approximate factor of 1.5 (Table 5.2). This table shows the summary statistics for adults in the 'Tuindorp' catchment.

Table 5.2:   Summary statistics of probability of infection per year for adults in the 'Tuindorp' catchment.

flooded area	reference ($\times 10^{-3}$) (no sedimentation)	median ($\times 10^{-3}$) (MC simulation)	shift[*] ($\times 10^{-3}$)	95% ($\times 10^{-3}$)
50 m^2	5.3	8.1	2.8	1.4
75 m^2	5.0	7.6	2.7	1.5
100 m^2	4.7	7.2	2.5	1.5

*) shift = median - reference

117

The shift from the reference to the median of the Monte Carlo simulations is statistically significant. The significance is tested for each threshold area dimension (50, 75 and 100 m^2) using a *t*-test. The test statistic for the t-test is calculated as follows. The difference between the reference value and the median of distribution function is divided by the standard error of the distribution function. This standard error equals the standard deviation of the distribution function divided by the square root of the sample size (i.e. the number of Monte Carlo runs). The corresponding *p*-value of the test statistic is calculated using the cumulative distribution function of the Students' t-distribution with 1 degree of freedom for a one-tailed *p*-value. The calculated *p*-value is compared with a significance level of 0.5%. Since the distribution functions are not Gaussian and, therefore, violate *t*-test assumptions, the data are transformed prior to significance testing. For 'Tuindorp' the transformation equals $1/x^3$.

For children in the 'Tuindorp' catchment the infection probability increases as well due to sediment deposits. Summary statistics are shown in Table 5.3. The calculated probability accounts for the non-homogeneous distribution of children in the catchment area as shown in Figure 5.10.

Table 5.3:   Summary statistics of probability of infection per year for children in the 'Tuindorp' catchment.

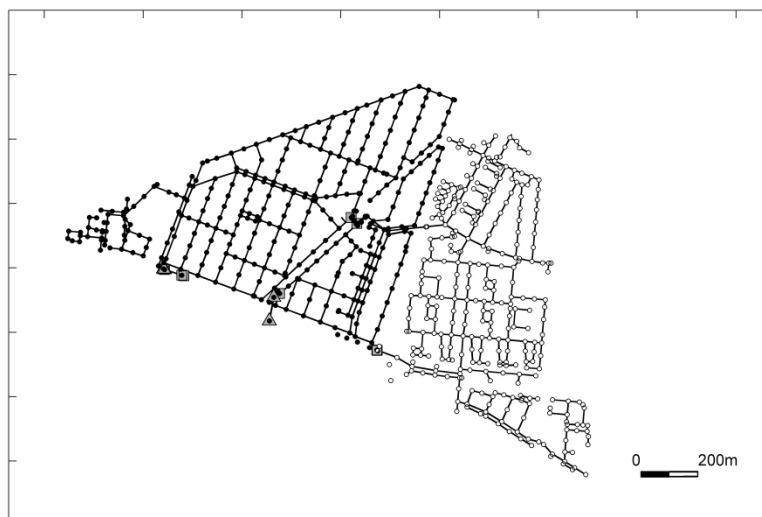| flooded area	reference (×10^{-2}) (no sedimentation)	median (×10^{-2}) (MC simulation)	shift[*] (×10^{-2})	95% (×10^{-2})
50 m^2	5.1	7.5	2.5	1.2
75 m^2	4.8	7.1	2.4	1.3
100 m^2	4.5	6.8	2.2	1.3

*) shift = median - reference

Figure 5.10: Spatial distribution of children in the 'Tuindorp' catchment: black dots (21 % of population) and white dots (12 % of population) (CBS, 2017).

Although the infection probability per event is 10 times higher for children compared to adults, the average infection probability per year only increases by a factor of 9.6. This is due to the afore-mentioned distribution of percentages of children (CBS, 2017). Comparison of figures 5.7 and 5.10 shows that the frequency of flooding events is higher in the area with a lower proportion of children (12% of population) and lower in the area with a higher proportion (21% of population).

The spatial distribution of infection probabilities per manhole per year for children in the 'Tuindorp' catchment for one system state (i.e. one Monte Carlo run) and a threshold area of 100 m^2 is illustrated in Figure 5.11. This figure shows that the impact of sedimentation on infection probability varies within the catchment.

Probability of infection per year per manhole (data type = child, system state = 178, threshold area = 100 m^2)

Figure 5.11: Example of spatial distribution of infection probability for children per year per manhole for a specific system state (i.e. Monte Carlo run) of 'Tuindorp' catchment.

5.3.2 Results 'Loenen' catchment

5.3.2.1 Frequency of flooding

In the partly-branched 'Loenen' catchment, the average number of flooding events per manhole is more or less evenly distributed over the catchment area. The number of more sensitive sewers is limited (Figure 5.12).
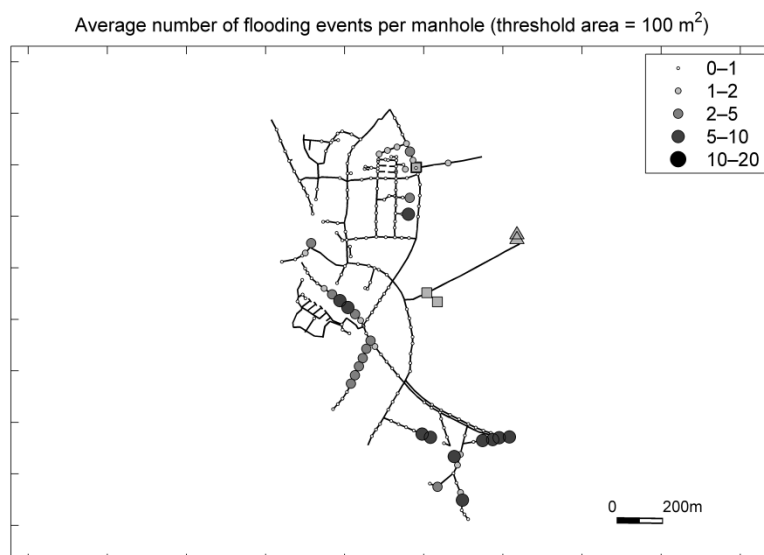
Figure 5.12: Average number of flooding events per manhole based on the Monte Carlo simulations for the 'Loenen' catchment.

5.3.2.2 Probability of infection

The impact of in-sewer defects on infection probabilities for adults in the 'Loenen' catchment is shown in Figure 5.13. As for 'Tuindorp', the density functions are calculated using kernel smoothing. The figure shows that the infection probability increases for adults due to sedimentation. Again, the calculated median probability for the different threshold area dimensions decreases with increasing flooded areas.

For adults, the median of the probability distribution of the system with sediment deposits is almost four times larger than the reference (Table 5.4). This shift from the reference to the median of the Monte Carlo simulations is statistically significant. This was tested using a *t*-test. In order to avoid violations of *t*-test assumptions, the data are transformed to normal with a factor of $1/x$.
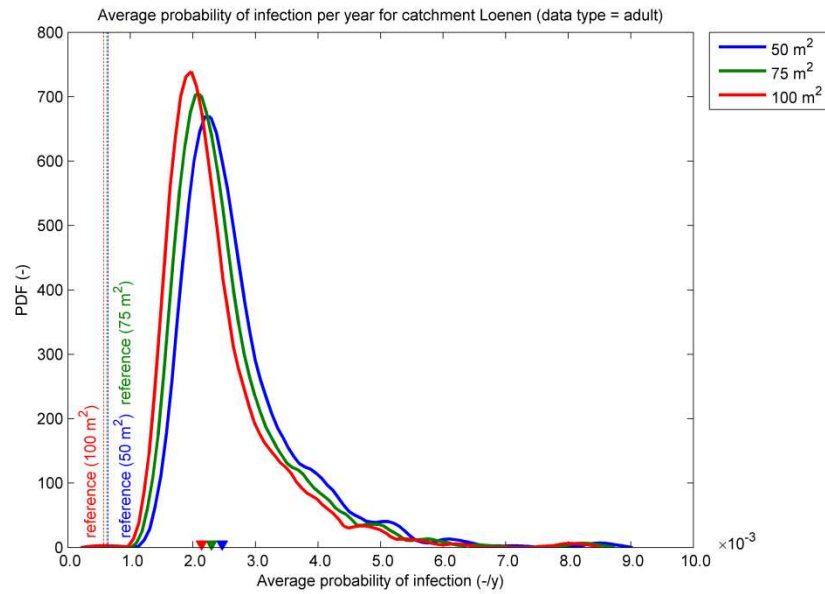

Figure 5.13: Infection probability for adults per year in the 'Loenen' catchment.

Table 5.4: Summary statistics of probability of infection per year for adults in the 'Loenen' catchment.

flooded area	reference (×10⁻³) (no sedimentation)	median (×10⁻³) (MC simulation)	shift* (×10⁻³)	95% (×10⁻³)
50 m²	0.64	2.5	1.8	3.6
75 m²	0.62	2.3	1.7	3.5
100 m²	0.58	2.1	1.6	3.4

*) shift = median - reference

5.3.3 Discussion

A comparison of the results for both catchments in this chapter shows that the impact of sediment deposits on infection probabilities is system-dependent. One difference is that the tail of the distribution functions for the infection probability for 'Loenen' is much longer than for 'Tuindorp'. This can most probably be explained by the partly-branched character of the sewer system and the steeper catchment area in 'Loenen'. As a result, the impact of sediment deposits in a relatively limited set of sewer pipes most important for draining the area spreads out over a relatively large part of the catchment. Another difference is that the distance between the median values of the probability distributions for the three threshold area dimensions is larger for 'Tuindorp' than for 'Loenen'. This relates to the looped character of the sewer system and the flatter catchment area in 'Tuindorp'.

The average infection probability per year is determined from the overall probability of infection per exposure event and the frequency of flooding events. Flood duration is not incorporated in this approach. However, the results demonstrate that flood duration may vary considerably over the catchment, possibly affecting infection probabilities. Despite recent developments in methods to quantify infection risks (Fewtrell et al., 2011; De Man et al., 2014 and Andersen, 2015), knowledge on the impact of flood duration on infection probability is still very limited. Moreover, none of the methods take the timing of the flooding event (time of the day, time of the year) into account, although it can be expected that the infection probability is also strongly related to this. Consequently, further research is needed on the impact of duration and timing on infection probabilities.

In this study, flood cones are applied for estimating flooding levels above a street instead of a 2D overland flow model (as in e.g. Mark et al., 2015). The use of flood cones significantly accelerates calculations, which is useful for the Monte Carlo simulations. Compared to other situations, in which a 2D overland flow model has been used, the hydraulic gradient of the catchment in 'Tuindorp' and 'Loenen' is smaller than the catchments used in Leandro et al. (2009) and Mark et al. (2015). Consequently, a 2D overland flow model is not considered crucial for obtaining realistic results in 'Tuindorp' and 'Loenen'.

Call data of the municipality have been used to validate model results. This shows that not all locations at which the model indicates flooding coincide with registered calls. The registration of calls was not sufficient for correctly analysing reported flood events. For example, information on the location of the flooding, the duration and the total affected area is not present or understandable.

Chapter 2 demonstrates that the return period of flooding, number of flooded locations, and flooded volumes are substantially affected by in-sewer defects. This increases the possibility of exposure to pluvial flooding and its high amounts of pathogens. In order to reduce risks of exposure, it is recommended that proactive maintenance strategies are developed to optimize hydraulic performance. If the importance of an element for the total network is known, maintenance can be adjusted accordingly instead of maintaining all elements to the same quality level. Methods to determine the importance of individual elements in relation to the total network are described in Arthur et al. (2008), Arthur and Crow (2007), Mair et al. (2012), Möderl et al. (2009), Möderl and Rauch (2011), and Meijer et al. (2018). When the critical elements are known, hydraulic properties of the sewer system at these locations can be monitored to safeguard performance (see chapter 3). If no monitoring equipment is available, rapid and cost-effective inspection methods, such as the manhole-zoom camera and the SewerBatt™ instrument, can be used to examine the sewer condition more often and to determine whether maintenance is necessary (Plihal et al. 2016).

The methods presented here may serve to further rationalise decision making in sewer asset management. As shown by van Riel et al. (2017), decision making in sewer asset management is largely based on intuition and economic considerations, while the original motivation for constructing sewer systems was protection from infectious diseases. Using the methods presented here, designers and sewer managers have a tool to quantify health effects of design and/or maintenance activities on the actual protection level offered by a sewer system and take these into account in their decision making.

5.4 Conclusion

Exposure to urban pluvial flooding can cause health risks for humans because floodwater may contain a variety of contaminants. The contaminations depend on the origin of the floodwater. These include human enteric pathogens from urban wastewater and *Campylobacter*, *Giardia*, and *Cryptosporidium* from both animal faeces and human wastewater.

5. Quantitative impact assessment of sewer condition on health risk

In-sewer defects affect the hydraulic performance of a sewer system and may cause increased pluvial flooding. This chapter shows that the occurrence of flooding, and therefore the infection probability, are significantly enlarged due to sediment deposits, thus providing input for risk-informed sewer asset management actions such as proactive maintenance strategies to preserve hydraulic performance. The average catchment-wide infection probability is calculated using Quantitative Microbial Risk Assessment (QMRA) and flooding frequencies from Monte Carlo simulations with a hydrodynamic model.

The impact of sediment deposits on the infection probabilities is significant and depends on sewer systems characteristics. The overall picture for the flat and looped 'Tuindorp' catchment is that the catchment-wide average infection probability increases due to sedimentation, both for adults and children. In comparison with a sewer system without sediment deposits, the median of the probability distribution of the system with sediment deposits is approximately 1.5 times larger. This shift is statistically significant. The average infection probability for children is almost 10 times larger than for adults. For the partly-branched and mildly-sloping 'Loenen' catchment, it can be concluded that the median of the average infection probability distribution is approximately four times larger due to sedimentation compared to the reference. The shift in Loenen is also significant.

The results in this chapter demonstrate that flood duration may vary considerably over the catchment, possibly affecting infection probabilities. However, flood duration is not incorporated in QMRA approaches for urban flooding presented in literature. In order to account for flood duration in catchment-wide infection probabilities, further research is needed.

Municipalities should inform inhabitants that floodwater is contaminated with pathogens and that exposure to this floodwater has to be avoided. Furthermore, special attention is needed for avoiding contamination of precipitation with pathogens in rehabilitation projects, reconstruction works, and the design and construction of new drainage systems (Fletcher et al., 2015).

6 Discussion, conclusions and recommendations

This thesis deals with the influence of the structural condition of sewer assets on the hydraulic performance of sewer systems (maintenance condition). Hydrodynamic model simulations taking into account the effects of in-sewer defects are used to assess this influence. The defects' characteristics are based on field observations. Model calibration is applied to enable detections of changes in hydraulic system behaviour. To this end, an extensive monitoring network has been installed. The outcomes provide input for risk-informed sewer maintenance strategies in order to preserve hydraulic performance of sewer systems. Moreover, the results can be used to improve the protection of public health by reducing urban pluvial flooding and, subsequently, the infection probability.

The next sections present the final discussion, followed by the conclusions and recommendations for further research.

6.1 Discussion

In day-to-day practice structural in-sewer defects are normally not incorporated in model-based assessments of pluvial flooding due to lack of knowledge and data. In order to address the impact of in-sewer defects on hydraulic performance on network level, Monte Carlo simulations are applied. The variation of flooding impacts (frequencies and volumes) due to in-sewer defects has been analysed. The input ranges of the model parameter sediment in the simulations are based on the results of observed sediment depths. Because of the lack of knowledge on sediment transport in sewer systems, observed sediment depths have been used to predict the presence of sediment in the conduits of the sewer catchment during each 'system state' in the Monte Carlo runs. The model parameter sediment depth is characterised with a beta probability distribution. For each conduit shape and dimension class, a distribution function is fitted on the observed sediment depths. It is assumed that the sediment depth for a specific conduit shape and dimension can be described with the fitted distribution function on the observed values. This is assumed to be sufficient to answer the main question of the Monte Carlo

127

simulations: does the maintenance condition of a sewer system affect hydraulic performance?

Model calibration showed that a change in residuals after calibration is an indication for local changes in system behaviour. To this end, an extended monitoring network has been installed in the combined 'Tuindorp' system in Utrecht (the Netherlands). To a certain extent, the minimal design of the monitoring network is crucial for accurate results in other sewer catchments. The design of the monitoring concerning the measurement locations and the total amount of measurements needs to be done properly. In the Netherlands there has been an increase in the number of monitoring networks in sewer systems to get more knowledge on the functioning of the systems during rainfall. The monitoring networks typically mainly consist of sensors at the CSO constructions and pumping stations. An extension of those networks with a couple of sensors at locations that are important for the hydraulic performance will be useful. Those sensors provide necessary information to perform model calibration and, consequently, to detect system changes as mentioned in this thesis. In the 'Tuindorp' sewer catchment the high within-cluster correlation that can be seen at the locations suffering from in-sewer defects such as root intrusion, does not depend on the sensor that is chosen within each cluster. Hence, it is not necessary to have monitoring equipment exactly upstream and downstream of an obstruction, as is the case for the 'Tuindorp' catchment, in order to observe changing system behaviour due to in-sewer defects using model calibration.

Determining the degree of criticality applying the Graph-theory method can be useful input for choosing monitoring locations. In this thesis the method is tested on relatively small sewer catchments ('Loenen' 23.4 ha and 'Tuindorp' 56.9 ha). The results need to be validated for larger looped systems in flat areas and the extension of the method for other network systems (e.g. gas and water supply networks and district heating networks) may be explored in the future.

A comparison of the results for both catchments in this thesis shows that the impact of sediment deposits on infection probabilities is system-dependent. One difference is that the tail of the distribution functions for the infection probability for 'Loenen' is much longer than for 'Tuindorp'. This can be explained most likely from the partly-branched character of the sewer system and the steeper catchment area in 'Loenen'. As a result, the impact of sediment deposits spreads out over a relatively large part of the catchment area because a very limited set of sewer pipes is most important for draining the upstream area. For other sewer catchments it is possible that specific sub-sewer catchments are more sensitive to flooding than others. Another difference is that the distance between the median values of the probability distributions for the three threshold area dimensions

is larger for 'Tuindorp' than for 'Loenen'. This relates to the looped character of the sewer system and the flatter catchment area in 'Tuindorp'. This means that system structure and surface slope of the catchment area are important parameters for the outcomes of the Monte Carlo simulations. Consequently, applying the simulations to other sewer catchments will most probably result in other results depending on the differences in catchment area structure and surface slope. Nevertheless, this thesis shows that in-sewer defects affect urban pluvial flooding.

The average infection probability per year in this thesis is determined from the overall probability of infection per exposure event and the frequency of flooding events. Flood duration is not incorporated in this approach. However, the results in chapter 5 demonstrate that flood duration may vary considerably over the catchment possibly affecting infection probabilities. The knowledge on the impact of flood duration on infection probability is still very limited. Moreover, none of the methods takes the timing of the flooding event (time of the day, time of the year) into account, although it can be expected that the infection probability is also strongly related to this. Consequently, further research is needed on the impact of duration and timing on infection probabilities.

In this thesis flood cones are applied for estimating flooding levels above street instead of a 2D overland flow model. The use of flood cones significantly accelerates calculations, which is useful for the Monte Carlo simulations. Compared to other situations, in which a 2D overland flow model has been used, the hydraulic gradient of the catchment in 'Tuindorp' and 'Loenen' is smaller than the catchments used in Leandro et al. (2009) and Mark et al. (2015). Consequently, a 2D overland flow model is not considered crucial for obtaining realistic results in 'Tuindorp' and 'Loenen'.

For the model validation in chapter 5, a comparison between call data on flooded streets and simulated flood locations was made for the rainfall event on November 4, 2013. To this end, model validation has to be done comparing the clean sewer system with registered flood locations. The registration of calls was not sufficient for correctly analysing reported flood events. For example, information on the location of the flooding, the duration and the total affected area is not present or understandable. For a better understanding of call data, further research is needed on the psychological background of calls. The 4 November 2013 event was chosen in this thesis because in 2012 the whole 'Tuindorp' sewer system was cleaned and between January and July 2013 observed defects were removed, except for root intrusions in the central part of the sewer system. After these actions, the sewer system is considered "clean" and suitable for validating the theoretical sewer model.

Without data processing and validation, monitoring results in data sets with an unknown quality. Validation not only provides information on the functioning of the measuring equipment, but also enhances the accessibility of the data. In addition, data validation increases the reliability of model calibration results. Attention to automatic data validation is necessary. Obtaining high quality data requires monitoring networks in which sensors are installed and operate according to predefined standards and protocols.

6.2 Conclusions

In the Netherlands, 1,5 billion euro is spent annually to maintain and operate sewer systems. Increasingly, risk-based sewer asset management is being advocated to balance the required budget and the provided service to society. A prerequisite for risk-based sewer asset management is to be able to relate the condition of the infrastructure with infrastructure performance and consequently, the provided service level.

Nowadays, sewer maintenance activities are mainly based on the observed condition of individual assets and simulation results of calculations using as-built data. Assessing actual sewer hydraulic performance and directing maintenance actions requires more information on the relation between the actual maintenance condition of an asset versus influence it has on sewer network level. This thesis focusses on the impact of in-sewer defects on urban pluvial flooding and, subsequently, on infection probabilities for humans. The objective of this thesis is to develop methods to assess and quantify the effect of in-sewer defects on sewer performance. The influence of sewer condition on the hydraulic performance is studied and model calibration is applied to identify in-sewer defects which affect hydraulic performance.

Structural in-sewer defects are normally not incorporated in model-based assessments of pluvial flooding due to lack of knowledge and lack of data. In order to address the impact of in-sewer defects on hydraulic performance on network level, two research catchments are studied. The variation of flooding impacts (frequencies and volumes) due to in-sewer defects are systematically studied. The studied in-sewer defects include root intrusion, surface damage, attached deposits and settled deposits and sedimentation. The analysis is based on Monte Carlo simulations with a full hydrodynamic model of the sewer system using a series of 10 years observed precipitation. Ranges for the inputs of in-sewer defects in the simulations are based on the results of observed defects. The analysis of simulation results shows that in-sewer defects significantly affect calculated return periods, flood volumes and threshold exceedances. A comparison with calculated flooding without in-sewer defects shows that the protection level with respect to urban pluvial flooding

130

drastically deteriorates. The impact of in-sewer defects and sedimentation in the flat 'Tuindorp' area with the looped sewer system, is larger than in the mildly-sloping 'Loenen' area with the partly-branched sewer system. This mainly results from the flatness of the catchment. In the partly-branched system, for sedimentation, the variance of all flooding characteristics is larger in comparison with the looped system.

In-sewer defects are normally classified and rated based on visual inspections (mostly using CCTV footage). As the inspection frequency is typically once per decade, the sewer asset manager has to rely on relatively sparse, and to a certain extent incorrect, data on in-sewer defects. Hydraulic monitoring provides long-term, high-frequency data on the hydraulics. Therefore, the added value of model calibration to obtain information on in-sewer defects from hydraulic monitoring data either without or in-between periodic inspections is examined. It is concluded that model calibration is able to demonstrate changes in the hydraulic properties of the sewer system and can be used to optimise sewer asset management and especially operation and maintenance actions. This can be done by means of 'hydraulic fingerprinting', where the fingerprint is defined by the model parameters and the residuals after calibration. Model calibration showed that, given a chosen calibration parameter set which predominantly contains runoff parameters, a change in residuals after calibration is an indication for local changes in system behaviour (i.e. root intrusions and sediment deposits). To this end, the combined 'Tuindorp' system in Utrecht (the Netherlands) was first monitored to obtain the hydraulic performance with known defects in the system. After this first monitoring period, the sewer system was cleaned and monitored continuously to obtain a calibrated model that functions as a reference 'hydraulic fingerprint'.

A method to identify critical elements for hydraulic performance of sewer systems, required to design monitoring networks, is proposed. Knowledge on the impact of in-sewer defects on network level provides information for maintenance activities reducing flooding and, subsequently, decreasing infection probabilities for humans. Sewer systems are networks consisting of many elements. The performance on network level depends on the performance of the individual elements. The importance of an element in the total network depends on the characteristics of the element and its position in the network. If the degree of criticality of the elements in a network is known, the maintenance and rehabilitation can be adjusted accordingly to the degree of criticality instead on maintaining all elements to the same quality level. The degree of criticality can be used as a basis for risk-informed asset management. It can be used to choose monitoring locations in monitoring networks applied for model calibration to detect changes in system behaviour. In this thesis, the Graph-theory method is proposed as an approach towards identifying the criticality of individual pipes in sewer systems. This method is independent

of the load on the system and is not computationaly demanding. The degree of criticality based on the Graph-theory method depends on three parameters: the discharge, the water level and the difference between crest levels of overflow structures. It was shown that for both research catchments 'Tuindorp' and 'Loenen' it is possible to identify the 30-40% most critical pipes in a robust manner.

Exposure to urban pluvial flooding may pose a health risk to humans. Pluvial flooding may be contaminated by dirt from paved surfaces (e.g. dog faeces and bird droppings), by wastewater from combined sewer systems and by wastewater from storm sewers due to illicit connections. The contaminations include human enteric pathogens (e.g. norovirus and enterovirus) from urban wastewater, and *Campylobacter*, *Giardia* and *Cryptosporidium* from both animal faeces and human wastewater. The occurrence of flooding, and therefore the infection probability, are significantly enlarged due to sediment deposits in the sewer. The average catchment-wide infection probability is calculated using Quantitative Microbial Risk Assessment (QMRA) and flooding frequencies from Monte Carlo simulations with a hydrodynamic model. The impact of sediment deposits on the infection probabilities is significant and depends on sewer system characteristics. The overall picture for the flat and looped 'Tuindorp' catchment is that the catchment-wide average infection probability increases due to sedimentation both for adults and children. In comparison with a sewer system without sediment deposits, the median of the probability distribution of the system with sediment deposits is approximately 1.5 times larger. For the partly-branched and mildly-sloping 'Loenen' catchment it can be concluded that the median of the average infection probability distribution is approximately 4 times larger due to sedimentation compared to the reference. By designing a sewer system using a certain design standard a certain infection probability is implicitly accepted. A lack of maintenance will increase the infection probability.

In this thesis, a new method has been developed to identify in sewer defects by using advanced model calibration. In addition, it is demonstrated that currently, there is a big gap between theoretical system performance and system performance in reality due to the condition of the sewers. Consequently, the return period for urban flooding can decrease from 2 years to 1 year on average with as a negative side effect an increase in the infection probability. Improved sewer maintenance or more robust sewer design could be applied to circumvent this issue. The results show that risk-based sewer asset management should focus more on risks and performance rather than on cost savings.

6.3 Recommendations

The application of the proposed model calibration methodology shows very promising results when applied to the 'Tuindorp' sewer system. Given the background of the methodology, i.e. detecting changes in system behaviour based on changes in characteristics of residuals, it is expected that it will also work for other systems. This is supported by results of earlier work on the calibration of hydrodynamic models. The work described in this thesis shows that model calibration can be used not only to detect errors in the structural properties of a sewer model, but also to detect changes in system behaviour due to changes of system properties over time. In addition, the quality of the database of the structural sewer properties and the quality of the monitoring data is crucial with respect to the calibration results. Therefore, it is recommended to apply this method in other sewer catchments as well taking into account the following steps:

> (1) model validation;
> (2) calibration parameter selection;
> (3) selection of storm event for calibration;
> (4) monitoring data validation;
> (5) reduced parameter set for calibration;
> (6) model calibration;
> (7) residual analysis.

Data validation increases the reliability of model calibration results. For practical feasibility automatic data validation needs to be applied. A further development of such tools, accessible and applicable for practitioners, is recommended.

The Graph-theory method is applicable to determine critical assets in sewer networks and choose the monitoring locations which provide the correct information that can be used in the model calibration technique. Designing monitoring networks by using the Graph-theory method needs to be investigated in other sewer areas as well.

133

The results of visual inspections determine whether rehabilitation or replacement is needed for different assets. Furthermore, the structural condition of sewers should not hamper the required system performance regarding flow. Currently, in the Netherlands, visual inspection of all sewers within a municipality is done repeatedly every 10 years. The hydraulic condition of a sewer system changes over time in a much shorter period (6 months) in comparison with the structural condition (10 years). Therefore, to maintain the defined service of sewer systems regarding hydraulic performance an inspection frequency of once every 2 years is recommended. To this end, other different rapid and cost-effective inspection methods instead of CCTV are available, e.g. the manhole-zoom camera and the SewerBatt™ instrument.

References

Alderman, K., Turner, L.R., and Tong, S. (2012). Floods and human health: a systematic review. Environment International, 47: 37-47, doi:10.1016/j.envint.2012.06.003.

Anbari, M.J., Tabesh, M., Roozbahani, A. (2017). Risk assessment model to prioritize sewer pipes inspection in wastewater collection networks. *Journal of Environmental Management*, 190, 91–101, https://doi.org/10.1016/j.jenvman.2016.12.052.

Andersen, S.T. (2015). *Urban flooding and health risk analysis by use of quantitative microbial risk assessment - Limitations and Improvements*. PhD thesis, DTU Environment, Department of Environmental Engineering.

Arthur, S. and Crow, H. (2007). Prioritising sewerage maintenance using serviceability criteria. *Water Management*, 160: 189–194. doi:10.1680/wama.2007.160.3.189.

Arthur, S., Crow, H., Pedezert, L., and Karikas, N. (2008). Using serviceability to prioritise proactive sewer maintenance. In: *Proceedings of 11th International Conference on Urban Drainage*, Edinburgh, Scotland, UK.

Ashley, R.M., Fraser, A., Burrows, R., and Blanksby, J. (2000). The management of sediment in combined sewers. *Urban Water*, 2(4): 263-275.

Ashley, R.M., Bertrand-Krajewski, J.-L., Hvitved-Jacobsen, T., and Verbanck, M. (2004). Solids in Sewers. IWA, London. *Scientific and Technical Report*, No. 14.

Baah, K., Dubey, B., Harvey, R., and McBean, E. (2015). A risk-based approach to sanitary sewer pipe asset management. *Science of The Total Environment*, 505: 1011–1017, doi:10.1016/j.scitotenv.2014.10.040.

Barreto, W., Vojinovic, Z., Price, R.K., and Solomatine, D.P. (2008). Multi-tier modelling of urban drainage systems: Multi-objective optimization and parallel computing. In: *Proceedings of 11th International Conference on Urban Drainage*, Edinburgh, Scotland.

135

Bennis, S., Bengassem, J., and Lamarre, P. (2003). Hydraulic performance index of a sewer network. *Journal of hydraulic engineering*, 129(7): 504-510.

Bertrand-Krajewski, J.-L. (2007). Storm water pollutant loads modelling: Epistemological aspects and case studies on the influence of field data sets on calibration and verification. *Water Science and Technology, 55*(4): 1–17.

Bonneux, L. (2010). Kindersterfte in de wereld. *DEMOS*, 26(2): 1-3.

Burger, G., Fach, S., Kinzel, H., and Rauch, W. (2010). Parallel computing in conceptual sewer simulations. *Water Science and Technology*, 61(2): 283-291.

Butler D. and Davies J.W. (2004). *Urban Drainage.* 2nd Edition. E&FN Spon, London, UK.

Camenen, B., Bayram, A., and Larson, M. (2006). Equivalent roughness height for plane bed under steady flow. *Journal of hydraulic engineering*, 132(11): 1146-1158, 51010.1061/(ASCE)0733-9429(2006)132:11(1146).

Cann, K.F., Thomas, D.R., Salmon, R.L., Wyn-Jones, A.P., and Kay, D. (2013). Extreme water-related weather events and waterborne disease. *Epidemiology & Infection*, 141 (4), 671–686.

Carrera, J. and Neuman, S. P. (1986a). Estimation of aquifer parameters under transient and steady state conditions: 1. Maximum likelihood method incorporating prior information. *Water Resources Research, 22*: 199–210.

Carrera, J. and Neuman, S. P. (1986b). Estimation of aquifer parameters under transient and steady state conditions: 2. Uniqueness, stability, and solution algorithms. *Water Resources Research, 22*: 211–227.

CBS (2016). http://statline.cbs.nl/. Last accessed on October 2017.

CBS (2017). http://www.cbsinuwbuurt.nl/#buurten2016_perc_personen_tot_15_jaar. Last accessed on 26 September 2017.

Clemens, F. H. L. R. (2001a). *Hydrodynamic models in urban drainage: Application and calibration*. PhD thesis. Delft University of Technology, Delft, the Netherlands.

Clemens, F. H. L. R. (2001b). A design method for monitoring networks in urban drainage. In: *Urban drainage modelling. Proceedings of the specialty symposium held in conjunction with the World Water and Environmental Resources Congress*, Orlando, FL, USA.

References

Clemens, F. H. L. R. (2001c). Calibration and verification of hydrodynamic models in urban drainage. In: *Urban drainage modelling. Proceedings of the specialty symposium held in conjunction with the World Water and Environmental Resources Congress*, Orlando, FL, USA.

Conover, W. J. (1999). *Practical nonparametric statistics*. New York, NY: Wiley, 3rd edition: 443–447.

Crabtree, R. (1989). Sediments in Sewers. *Water and Environment Journal*, 3(6), 569–578, https://doi.org/10.1111/j.1747-6593.1989.tb01437.x.

De Man, H., Van den Berg, H.H.J.L., Leenen, E.J.T.M., Schijven, J.F., Schets, F.M., Van der Vliet, J.C. Van Knapen, and F. De Roda Husman, A.M. (2014). Quantitative assessment of infection risk from exposure to waterborne pathogens in urban floodwater. *Water Research*, 48, 90-99.

De Man, H., Mughini Gras, L., Schimmer, B., Friesema, I.H., De Roda Husman, A.M., Van Pelt, W. (2015). Gastrointestinal, influenza-like illness and dermatological complaints following exposure to floodwater: A cross-sectional survey in The Netherlands. *Epidemiology & Infection*, 144(7), 1445–1454, Epub 11 November 2015, doi: 10.1017/S0950268815002654.

De Wit, M.A.S., Koopmans, M.P.G., Kortbeek, L.M., Van Leeuwen, N.J., Bartelds, A.I.M., and Van Duynhoven, Y.T.H.P. (2001). Gastroenteritis in sentinel general practices, the Netherlands. *Emerging Infectuous Diseases*, 7(1): 82-91.

Desbordes, M. (1978). Urban runoff and design modelling. In: *Proceedings of International Conference on Urban Storm Drainage*, Southampton, UK, 353-361.

Dietz, E.J. and Killeen, T.J. (2006). A non parametric multivariate test for monotone trend with pharmaceutical applications. *Journal of the American Statistic Association*, 76: 169-174.

Dijkstra, E.W. (1959). A note on two problems in connexion with graphs. *Numerische Mathematiek*, 1: 269–271.

Dirksen, J. and Clemens, F.H.L.R. (2007). The role of uncertainties in urban drainage decisions: uncertainty in inspection data and their impact on rehabilitation decisions. In: *Proceedings of 2nd Leading Edge Conference on Strategic Asset Management*, Lisbon, Portugal, October 2007.

137

Dirksen, J., Clemens, F., Korving, H., Cherqui, F., Le Gauffre, P., Ertl, T., Plihal, H., Müller, K., and Snaterse, C. (2013). The consistency of visual sewer inspection data. *Structure and Infrastructure Engineering*, 9(3): 214-228, first published on: 07 February 2011 (iFirst).

Dirkzwager, A.H. (1997). Sustainable development: new ways of thinking about 'water in urban areas'. *European Water Pollution Control*, 7(1): 28-40.

Doherty, J. (2005). PEST model-independent parameter estimation user manual. Watermark Numerical Computing, 5th edition, retrieved from http://www.pesthomepage.org/Downloads.php.

Dotto, C. B. S., Kleidorfer, M., McCarthy, D. T., Deletic, A., Rauch, W., and Fletcher, T. D. (2010). Towards global assessment of modelling errors. In: *Proceedings of 6th International Conference on Sewer Processes and Networks*, Surfers Paradise, Gold Coast, Australia.

Draper, N. and Smith, H. (1981). *Applied regression analysis*. Second edition. Wiley, New York.

Fewtrell, L., Kay, D., and Ashley, R. (2008). Flooding and health - an evaluation of the health impacts of urban pluvial flooding in the UK. *In: Health Impact Assessment for Sustainable Water Management. IWA Publishing*, 121–154.

Fewtrell, L., Kay, D., Watkins, J., Davies C., and Francis, C. (2011). The microbiology of urban UK floodwaters and a quantitative microbial risk assessment of flooding and gastrointestinal illness. *Journal of Flood Risk Management*, 4, 77-87.

Fletcher, T.D., Shuster, W., Hunt, W.F., Ashley, R., Butler, D., Arthur, S., Trowsdale, S., Barraud, S., Semadeni-Davies, A., Bertrand-Krajewski, J.L., Mikkelsen, P.S., Rivard, G., Uhl, M., Dagenais, D., and Viklander, M. (2015). SUDS, LID, BMPs, WSUD and more - The evolution and application of terminology surrounding urban drainage. *Urban Water Journal*, 12:7, 525-542, doi: http://dx.doi.org/10.1080/1573062X.2014.916314.

Fuchs, L. (1998). Hydrologic modelling of urban catchments. In: *Hydroinformatics tools for planning, design, operation and rehabilitation of sewer systems* (pp. 189–208), Kluwer Academic, Dordrecht.

Gérard, C. and Chocat, B. (1999). Prediction of sediment build-up from analysis of physical network data. *Water Science and Technology*, 39(9): 185-192.

Hagberg, A.A., Schult, D.A., Swart, P.J. (2008). Exploring Network Structure, Dynamics, and Function using NetworkX. In: *Proceedings of the 7th Python in Science Conference (SciPy2008)*, Pasadena, CA, USA, 19–24 August 2008, pp. 11–15.

References

Hager, W. H. (2010). *Wastewater Hydraulics: Theory and Practice*. 2nd edition, Springer Berlin Heidelberg, pp. 1-652, doi: 10.1007/978-3-642-11383-3.

Hammond, M.J., Chen, A.S., Djordjević, S., Butler, D., and Mark O. (2015). Urban flood impact assessment: A state-of-the-art review. *Urban Water Journal*, doi: 10.1080/1573062X.2013. 857421.

Harder-Lauridsen, N.M., Kuhn, K.G., Erichsen, A.C., Mølbak, K., and Ethelberg, S. (2013). Gastrointestinal illness among triathletes swimming in non-polluted versus polluted seawater affected by heavy rainfall, Denmark, 2010-2011. *PLoS ONE*, 8(11): e78371. doi:10.1371/journal.pone.0078371.

Harju, T. (2011). *Lecture Notes on Graph Theory*.

Hashimoto, M., Suetsugi, T., Ichikawa, Y., Sunada, K., Nishida, K., Kondo, N., and Ishidaira, H. (2014). Assessing the relationship between inundation and diarrhoeal cases by flood simulations in low-income communities of Dhaka City, Bangladesh. *Hydrological Research Letters*, 8 (3): 96–102.

Hashizume, M., Armstrong, B., Hajat, S., Wagatsuma, Y., Faruque, A., Hayashi, T., Sack, D. (2008). The Effect of Rainfall on the Incidence of Cholera in Bangladesh. *Epidemiology*, 19(1), 103-110, doi: 10.1097/EDE.0b013e31815c09ea.

Hemker, C. J. (1996). The reliability of parameters in automatic calibration (in Dutch). In *Modelkalibratie: Het automatisch ijken van grondwatermodellen*, The Dutch Hydrological Association, NHV, Special Issue 2: 39–51.

Henrichs, M., Vosswinkel, N., and Uhl, M. (2008). Influence of uncertainties on calibration results of a hydrological model. In: *11th International Conference on Urban Drainage*, Edinburgh, Scotland, UK, 1-10.

Hirsch, R.M. and Slack, R.J. (1984). A non parametric trend test for seasonal data with serial dependence. *Water Resources Research*, 20(6): 727-732.

Holland, J. H. (1975). *Adaptation in natural and artificial systems*. Ann Harbor, MI: The University of Michigan Press.

Hunter, J.D. (2007). Matplotlib: A 2D Graphics Environment. *Computing in Science & Engineering*, 9(3), 90–95, doi:10.1109/MCSE.2007.55.

Horton, R. E. (1940). An approach towards a physical interpretation of infiltration capacity. Soil Science Society of America, 5: 399–417.

Hurley, R. (1994). Urban sewerage rehabilitation in the UK. *Water and Environment Journal*, 8(4): 425-431, doi://dx.doi.org/10.1111/j.1747-6593.1994.tb01127.x.

Idelchik, I.E. (2007). *Handbook of Hydraulic resistance*. Begell House Publishers Inc.,U.S., 4th edition.

Innovyze Software. (2012). InfoWorks CS documentation. *On-line documentation* (Version 13.0.6), Broomfield.

ISO (1992b). Standard 6817:1992. *Measurement of conductive liquid flow in closed conduits - Method using electromagnetic flowmeters*.

Jacobs, C., Elbers, J., Moors, E., and Van Hove, B. (2015). How much water is the city evaporating? Edition H2O. *Water Matters, Knowledge Journal for Water Professionals,* Edition 2/2015: 34–37.

Jacobson, E. (1985). *A statistical parameter estimation method using singular value decomposition with application to Avra Valley in southern Arizona*. PhD thesis, University of Arizona, Tucson, AZ, USA.

Jones, E., Oliphant, T., Peterson, P., Others, A. (2018). SciPy: Open Source Scientific Tools for Python. http://www.scipy.org. Last accessed on 30 January 2018.

Kendall, M.G. (1945). The treatment of ties in ranking problems. *Biometrika*, 33(3): 239–251.

Kleijwegt, R.A. (1992). *On sediment transport in circular sewers with non-cohesive deposits*. PhD thesis. Delft University of Technology, Delft, the Netherlands.

Koenraad, P.M.F.J., Hazeleger, W.C., Vanderlaan, T., Beumer, R.R., and Rombouts, F.M. (1994). Survey of Campylobacter spp in sewage plants in the Netherlands. *Food Microbiology*, 11(1): 65-75.

König, D. (1936). *Theorie der endlichen und unendlichen Graphen: Kombinatorische topologie der streckenkomplexe*.

Korving, H. (2004). *Probabilistic assessment of the performance of combined sewer systems*. PhD thesis. Delft University of Technology, Delft, the Netherlands.

Laakso, T., Ahopelto, S., Lampola, T., Kokkonen, T., Vahala, R. (2017). Estimating water and wastewater pipe failure consequences and the most detrimental failure modes. *Water Science and Technology*, Water Supply, ws2017164, doi: 10.2166/ws.2017.164.

References

Langeveld, J. G. (2004). *Interactions within wastewater systems*. PhD thesis, Delft University of Technology, Delft, the Netherlands.

Lau, C.L., Smythe, L.D., Craig, S.B., and Weinstein, P. (2010). Climate change, flooding, urbanisation and leptospirosis: fuelling the fire? *Transactions of the Royal Society of Tropical Medicine and Hygiene*, 104 (10), 613–8.

Leandro, J., Chen, A.S., Djordjević, S., Savić, D.A. (2009). Comparison of 1D/1D and 1D/2D Coupled (Sewer/Surface) Hydraulic Models for Urban Flood Simulation. Journal of Hydraulic Engineering, 135(6), 495-504, DOI: 10.1061/(ASCE)HY.1943-7900.0000037.

Le Gauffre, P., Joannis, C., Vasconcelos, E., Breysse, D., Gibello, C., and Desmulliez, J. (2007). Performance indicators and multicriteria decision support for sewer asset management. *Journal of Infrastructure Systems*, 13(2): 105-114, doi://dx.doi.org/10.1061/(ASCE)1076-0342(2007)13:2(105).

Lodder, W.J. and De Roda Husman, A.M. (2005). Presence of noroviruses and other enteric viruses in sewage and surface waters in The Netherlands. *Applied Environmental Microbiology*, 71(3): 1453-1461.

Lukas, A. and Merrill, M. (2006). *Scraps: an expert system for prioritizing sewer inspections*. Water Environment Research Foundation.

Mair, M., Sitzenfrei, R., Kleidorfer, M., Möderl, M., and Rauch, W. (2012). GIS-based applications of sensitivity analysis for sewer models. *Water Science and Technology*, 65: 1215–1222, doi:10.2166/wst.2012.954.

Mancuso, A., Compare, M., Salo, A., Zio, E., Laakso, T. (2016). Risk-based optimization of pipe inspections in large underground networks with imprecise information. *Reliability. Engineering & System Safety*, 152, 228–238, https://doi.org/10.1016/j.ress.2016.03.011.

Mark, O., Jørgensen, C., Hammond, M., Khan, D., Tjener, R., Erichsen, A., and Helwigh B. (2015). A new methodology for modelling of health risk from urban flooding exemplified by cholera - Case Dhaka, Bangladesh. *Journal of Flood Risk Management*, September 2015. DOI: 10.1111/jfr3.12182.

Marquardt, D. W. (1963). An algorithm for least-squares estimation of nonlinear parameters. *Journal of the Society for Industrial and Applied Mathematics, 11*: 431-441.

McDonald, S. and Zhao, J. (2001). Condition assessment and rehabilitation of large sewers. In: *Proceedings International Conference on Underground Infrastructure Research*, University of Waterloo, Waterloo, Ontario, 361-369.

McKinney, W. (2010). Data Structures for Statistical Computing in Python. In: *Proceedings of the 9th Python in Science Conference (SCIPY 2010)*, Austin, TX, USA, 28 June–3 July 2010, pp. 51–56.

Mead, P.S., Slutsker, L., Dietz, V., McCaig, L.F., Bresee, J.S., Shapiro, C., Griffin, P.M., and Tauxe, R.V. (1999). Food-related illness and death in the United States. *Emerging Infectuous Diseases*, 5(5): 607-625.

Meijer, D., Van Bijnen, M., Langeveld, J., Korving, H., Post, P., Clemens, F. (2018) Identifying Critical Elements in Sewer Networks Using Graph-Theory. *Water*, 10(2), 136, doi:10.3390/w10020136.

Möderl, M., Kleidorfer, M., Sitzenfrei, R., and Rauch, W. (2009). Identifying weak points of urban drainage systems by means of VulNetUD. *Water Science and Technology*, 60:2507-2513, doi:10.2166/wst.2009.664.

Möderl, M. and Rauch, W. (2011). Spatial risk assessment for critical network infrastructure using sensitivity analysis. *Frontiers of Earth Science*, 5: 414–420, doi:10.1007/s11707-011-0202-1.

Mourad, M. and Bertrand-Krajewski, J.-L. (2002). A method for automatic validation of long time series of data in urban hydrology. *Water Science and Technology*, 45(4-5): 263–270.

Nash, J. E. and Sutcliffe, J. V. (1970). River flow forecasting through conceptual models part I - A discussion of principles. *Journal of Hydrology, 10*:282–290.

NEN 3399 (2004). *Sewerage systems outside buildings - Classification system for visual inspection of objects*. January 2004, Stichting Nederlands Normalisatie-instituut, Delft.

NEN-EN 752:2017 (2017). *Drain and sewer systems outside buildings - Sewer system management.* Stichting Nederlands Normalisatie-instituut, Delft.

NEN-EN 13508-2 (2003). *Conditions of drain and sewer systems outside buildings - Part 2: Visual inspection coding system*. August 2003, Stichting Nederlands Normalisatie-instituut, Delft.

Nikuradse, J. (1933). Strömungsgesetze in rauhen Rohren. In: *Ver. Deut. Ing. Forschungsheft,* 361.

Pedersen, F. B. and Mark, O. (1990). Head losses in storm sewer manholes: Submerged jet theory. *Journal of Hydraulic Engineering*, 116(11): 1317-1328.

References

Penman, H. L. (1948). Natural evaporation from open water, bare soil and grass. In: *Proceedings of the Royal Society A: Mathematical, Physical and Engineering Sciences, 193:* 120–145.

Pienaar, M. (2013). Outcomes from a sewer maintenance backlog investigation. In: *Institute of Municipal Engineering of South Africa (IMESA) Conference 2013*, 11.

Plihal, H., Kretschmer, F., Bin Ali, M.T., See, C.H., Romanova, A., Horoshenkov, K.V., and Ertl, Th. (2016). A novel method for rapid inspection of sewer networks: combining acoustic and optical means. *Urban Water Journal*, 13(1): 3-14, doi://dx.doi.org/10.1080/1573062X.2015.1076857.

Post, J.A.B., Langeveld, J.G., and Clemens, F.H.L.R. (2016). Analysing spatial patterns in lateral house connection blockages to support management strategies. *Structure and Infrastructure Engineering*, doi://dx.doi.org/10.1080/15732479.2016.1245761.

Preston, S.H. and Van de Walle, E. (1978). Urban French mortality in the nineteenth century. *Population studies*, 32(2):275-297, doi://dx.doi.org/10.1080/00324728.1978.10410715.

Price, R. K. and Osborne, M. P. (1986). Verification of sewer simulation models. In: *Proceedings of International Symposium on comparison of urban drainage models with real catchment data.* UDM 1986, Pergamon Press, Dubrovnik, Yugoslavia.

Rauch, W. and Harremoës, P. (1999a). On the potential of genetic algorithms in urban drainage modelling. *Urban Water, 1*: 79–89.

Rauch, W., and Harremoës, P. (1999b). Genetic algorithms in real time control applied to minimize transient pollution from urban wastewater systems. *Water Research, 33*: 1265–1277.

Rodrigue, J.-P., Comtois, P., and Slack, B. (2017). *The geography of transport systems*. 4th edition, New York.

Rosen, C., Röttorp, J., and Jeppsson, U. (2003). Multivariate on-line monitoring: Challenges and solutions for modern wastewater treatment operation. *Water Science and Technology, 47(2):* 171–179.

Saegrov, S. (2006). CARE-S. Computer aided rehabilitation of sewer and storm water networks. *IWA Publishing*. London.

Schellart, A. (2007). *Analysis of uncertainty in the sewer sediment transport predictions used for sewer management purposes*. PhD thesis. The University of Sheffield, Sheffield, UK.

Schets, F.M., Van Wijnen, J.H., Schijven, J.F., Schoon, H., and De Roda Husman, A.M. (2008). Monitoring of waterborne pathogens in surface waters in Amsterdam, the Netherlands, and the potential health risk associated with exposure to Cryptosporidium and Giardia in these waters. *Applied Environmental Microbiology*, 74 (7): 2069-2078.

Schilperoort, R. P. S., Dirksen, J., and Clemens, F. H. L. R. (2008). Practical aspects for long-term monitoring campaigns: Pitfalls to avoid to maximize data yield. In: *Proceedings of the 10th ICUD conference*, Edinburgh, Scotland, UK.

Schilperoort, R.P.S. (2011). *Monitoring as a tool for the assessment of wastewater quality dynamics.* (PhD thesis). Delft University of Technology, Delft, The Netherlands.

Sitzenfrei, R., Mair, M., Möderl, M., and Rauch, W. (2011). Cascade vulnerability for risk analysis of water infrastructure. *Water Science and Technology*, 64 (9): 1885-1891, doi: 10.2166/wst.2011.813.

Snow, J. (1854). *On the Mode of Communication of Cholera.* Second extended edition. John Churchill, New Burlington Street, London.

Spekkers, M.H., Clemens, F.H.L.R., and Ten Veldhuis, J.A.E. (2015). On the occurrence of rainstorm damage based on home insurance and weather data. *Natural Hazards and Earth System Sciences*, 15(2): 261-272.

Stanić, N., Langeveld, J.G. and Clemens, F.H.L.R. (2014). HAZard and OPerability (HAZOP) analysis for identification of information requirements for sewer asset management. *Structure and Infrastructure Engineering*, 10(11):1345-1356, doi://dx.doi.org/10.1080/15732479.2013.807845.

Stanić, N., Clemens, F.H.L.R. and Langeveld, J.G. (2017). Estimation of Hydraulic Roughness of Concrete Sewer Pipes by Laser Scanning. *Journal of Hydraulic Engineering*, 143(2): 1-12, doi://doi.org/10.1061/(ASCE)HY.1943-7900.0001223.

Stegeman, B. (2012). *Model calibration as a tool to identify sewer maintenance*. Msc thesis. Delft University of Technology, Delft, the Netherlands.

Stephenson, J., Vaganay, M., Cameron, R., and Joseph, P. (2014). The long-term health impacts of repeated flood events. *WIT Transactions on Ecology and The Environment*, Vol 184, WIT Press, www.witpress.com, ISSN 1743-3541 (on-line), doi:10.2495/FRIAR140171.

References

Stichting RIONED (2004). Module C2100: Rioleringsberekeningen, hydraulisch functioneren (in Dutch). In: *Leidraad Riolering*, pages 1-100.

Stichting RIONED (2016). Het nut van stedelijk waterbeheer.

Thissen, W. and Oomens, A. (1991). Systems Engineering for Sewer Management. In: *IEEE International Conference on Systems, Man, and Cybernetics, 'Decision Aiding for Complex Systems'*, 13-16 October, pages 473-478.

Tscheikner-Gratl, F., Sitzenfrei, R., Rauch, W., Kleidorfer, M. (2016). Integrated rehabilitation planning of urban infrastructure systems using a street section priority model. *Urban Water Journal*, 13, 28–40, https://doi.org/10.1080/1573062X.2015.1057174.

Van Bijnen, M. and Korving, H. (2008). Application and results of automatic validation of sewer monitoring data. In: *Proceedings of 11th International Conference on Urban Drainage*, Edinburgh, Scotland, UK.

Van der Walt, S., Colbert, S.C., Varoquaux, G. (2011). The NumPy Array: A Structure for Efficient Numerical Computation. *Computing in Science & Engineering*, 13(2), 22–30, doi: 10.1109/MCSE.2011.37.

Van Luijtelaar, H. and Rebergen, E. W. (1997). Guidelines for hydrodynamic calculations on urban drainage in the Netherlands: Backgrounds and examples. *Water Science and Technology, 36(8-9):* 253–258.

Van Mameren, H.J. and Clemens, F.H.L.R. (1997). Dutch guidelines for hydrodynamic design, overview and principles. *Water Science and Technology*, 36(8-9): 247-252.

Van Riel, W., Langeveld, J.G., Herder, P.M., and Clemens, F.H.L.R. (2014). Intuition and information in decision-making for sewer asset management. *Urban Water Journal*, 11(6):506-518.

Van Riel, W., Langeveld, J., Van Bueren, E., Herder, P., and Clemens, F. (2016). Decision-making for sewer asset management: Theory and practice. *Urban Water Journal*, 13(1):57-68.

Van Riel, W. (2017). *On Decision-Making for Sewer Replacement*. PhD thesis. Delft University of Technology, Delft, the Netherlands.

Van Zon, H. (1986). *Een zeer onfrisse geschiedenis: studies over niet-industriële verontreiniging in Nederland 1850-1920.* Staatsuitgeverij, 's-Gravenhage, the Netherlands.

145

Wallingford Software (2007). InfoWorks CS Documentation. *On-line documentation*. Version 8.5.

Wand, M.P. and Jones, M.C. (1995). Kernel Smoothing. *Monographs on Statistics and Applied Probability*. Chapman & Hall.

Wirahadikusumah, R., Abraham, D.M., and Iseley, T. (2001). Challenging issues in modeling deterioration of combined sewers. *Journal of infrastructure systems*, 7(2):77-84, doi://dx.doi.org/110.1061/(ASCE)1076-0342(2001)7:2(77).

Yen, C.B. (1987). Urban drainage hydraulics and hydrology; from art to science. *In proceedings of 4th ICUSD*, Lausanne, Switzerland.

Yoo, C.K., Villez, K., Lee, I.B., Van Hulle, S. and Vanrolleghem, P.A. (2006). Sensor validation and reconciliation for a partial nitrification process. *Water Science and Technology*, 53(4-5), 513-521.

A Description of the monitoring network in the 'Tuindorp' catchment

This appendix represents a full overview of the monitoring network in the 'Tuindorp' sewer catchment. To obtain data on the hydraulic performance of the sewer system and to understand the impact of in-sewer defects on hydrodynamic system behaviour, a total of 30 sensors have been installed (Figure A.1). Water level measurements (Lev1 to Lev27) are performed at four CSO locations (two of them including surface water level behind the CSO), the internal and external weir of a storage tank (including surface water level at the external weir), the pumping station and nineteen sewer manholes. In addition, rainfall is registered at two locations (R1 and R2) in the catchment. All the sensors are read out manually and all parameters are measured at a five-minute time step. A description of the monitoring locations and sensors is presented in Table A.1. The table contains the location code, location name, measured parameter, unit, sensor name sensors are described. The 'Tuindorp' system was monitored during the period January 2010 - September 2015. The results of the data quality assessment as described in section 1.7 is presented in appendix B.

Water level sensors are of type DCX-22-AA of manufacturer Keller (Switzerland). Measuring water levels is realized in relation to the ambient pressure (the pressure on the surface). The water level and the fluctuations thereof are determined on site by measuring the pressure at a defined depth beneath the surface level of the water (hydrostatic pressure). Because the density of the water is assumed to be 1000 kg/m^3 the measured pressure (mbar) can be converted to a water level (e.g. for water: 100 mbar ≈ 100 cm water column). The device is equipped with a second absolute pressure sensor integrated in the read-out unit (which acts as a barometer) and automatically calculates the difference between the two measuring values to compensate barometric pressure. This enables a direct read-out of the water level. This makes the measurement independent of air pressure fluctuations acting upon the surface of the water. In order to configure the device and read out the measured values that are stored in the data logger, the sensor can be connected to a laptop on site using a data cable.
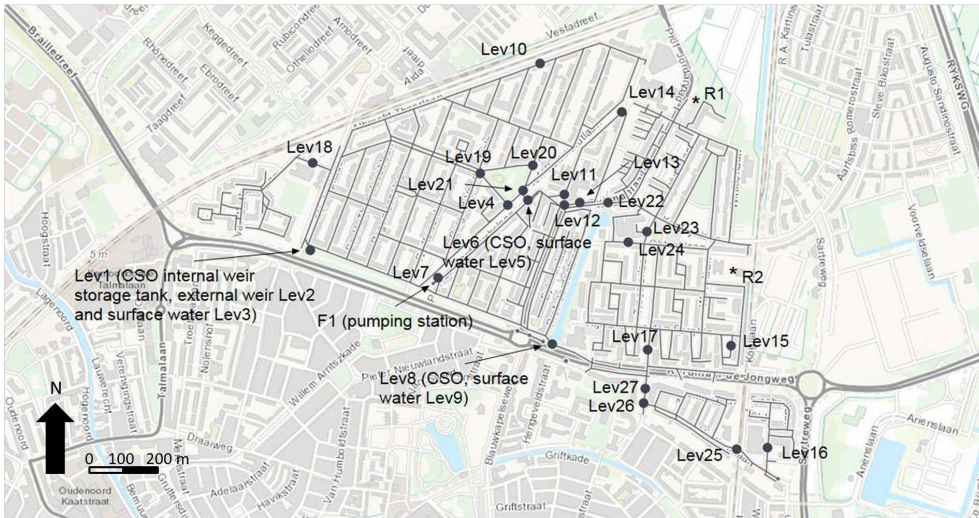
Figure A.1: Overview monitoring network 'Tuindorp' sewer catchment. Rainfall (R1 and R2), flow measurement pumping station (F1), water level measurements at CSOs, surface water and storage tank (Lev1 to Lev27).

Tipping-bucket rain gauges have been selected to monitor rainfall. The gauges are of type OMC-210 of manufacturer Observator Instruments BV (the Netherlands). The gauge consists of a catchment funnel with an inside diameter of 22.57 cm (400 cm^2). It funnels rainwater to a bucket, which accumulates the rainfall water. When the bucket is full, it tips over and empties. When the bucket tips, a reed contact mounted beside the bucket is activated by a magnet and generates a signal. The bucket tips when a precise amount of water has been collected, in this case the bucket size is 0.2 mm. No heating option was available. Figure A.2 presents the location of both tipping-buckets in the 'Tuindorp' catchment.

Figure A.2: Locations rain gauges R1 'Q8 petrol station'(left) and R2 'Primary school De Regenboog' (right) in the 'Tuindorp' sewer catchment. Installation of the gauges followed the guidelines. There are no obstructions affecting the measurements.

A. Description of the monitoring network in the 'Tuindorp' catchment

The pumping station (F1) transports the collected wastewater to a downstream catchment area, from where the wastewater is transported by a gravity sewer to the wastewater treatment plant Utrecht. An electromagnetic flow sensor has been installed to monitor the amounts of water passing the pumping station (Figure A.3). The flow sensor is of type OPTIFLUX 2000 of manufacturer KROHNE (the Netherlands). For information on the principles of flow sensing using electromagnetic induction see ISO (1992b).

Figure A.3:   Flow sensor (electromagnetic flow sensor OPTIFLUX 2000) at the pumping station in the 'Tuindorp' sewer catchment (Professor Leonard Fuchslaan). Installation of the flow sensor followed the standard EN 287/EN ISO 15614 (Welding) and has been calibrated against a fixed-volume tank.

Table A.1: Description of the monitoring locations and sensors in the 'Tuindorp' sewer catchment. Location code, location name, measured parameter and unit are described.

code	name	parameter	unit
Lev1	Meester Sickeszlaan internal weir storage tank 09.0248	water level	m AD
Lev2	Meester Sickeszlaan external weir storage tank 09.0248	water level	m AD
Lev3	Meester Sickeszlaan surface water behind storage tank 09.0248	water level	m AD
Lev4	Professor Reinwardtlaan sewer manhole 09.0203	water level	m AD
Lev5	Professor Leonard Fuchslaan surface water behind CSO Professor Leonard Fuchslaan Lev6	water level	m AD
Lev6	Professor Leonard Fuchslaan CSO 09.0219	water level	m AD
Lev7	Professor Leonard Fuchslaan sewer manhole 09.0280 nearby pumping station 09.0279 and CSO Professor Leonard Fuchslaan Lev6	water level	m AD
Lev8	Kardinaal de Jongweg CSO 09.0546	water level	m AD
Lev9	Kardinaal de Jongweg surface water behind CSO Kardinaal de Jongweg Lev8	water level	m AD
Lev10	Albrecht Thaerlaan sewer manhole 09.0028	water level	m AD
Lev11	Ornsteinsingel sewer manhole 09.0410	water level	m AD
Lev12	Eykmanlaan sewer manhole 09.0417	water level	m AD
Lev13	Eykmanlaan sewer manhole 09.0418	water level	m AD
Lev14	Professor Reinwardtlaan sewer manhole 09.0352	water level	m AD
Lev15	Fruinplantsoen sewer manhole 09.0607	water level	m AD
Lev16	Smijerslaan sewer manhole 09.0680	water level	m AD
Lev17	Van Everdingenlaan sewer manhole 09.0576	water level	m AD
Lev18	Christiaan Krammlaan sewer manhole 09.0037	water level	m AD
Lev19	Professor Melchior Treublaan sewer manhole 09.0200	water level	m AD
Lev20	H. Copijnlaan sewer manhole 09.0110	water level	m AD
Lev21	Professor Reinwardtlaan sewer manhole 09.0214 nearby CSO Professor Reinwardtlaan 09.0213	water level	m AD
Lev22	Eykmanlaan sewer manhole 09.0430	water level	m AD
Lev23	Troosterlaan sewer manhole 09.0442	water level	m AD
Lev24	Obbinklaan sewer manhole 09.0487	water level	m AD
Lev25	Huizingalaan sewer manhole 09.0654	water level	m AD
Lev26	Jan van Galenstraat sewer manhole 09.0622	water level	m AD
Lev27	Jan van Galenstraat sewer manhole 09.0623	water level	m AD
F1	Professor Leonard Fuchslaan pumping station 09.0279 with flow sensor directly after the pumps in the outgoing pipe	Flow	m^3/s
R1	Eykmanlaan petrol station Q8, rainfall on roof building	rainfall	mm
R2	Wevelaan primary school De Regenboog, rainall on roof school	rainfall	mm

B Results of monitoring data quality assessment

The quality of the collected data as measured by the sensors at the different monitoring locations is assessed (see section 1.7) before the data sets are used for comparing measured and modelled water levels and for model calibration. This appendix describes the process of data validation and provides an overview of the results of the data quality assessments in the Tables B.1 to B.6. The legend is presented in Figure B.2. The recorded storm events that have been used in this research to demonstrate the impacts of observed in-sewer defects on simulation and calibration results are drawn as a dotted line in the Tables.

The validation procedure is organized as depicted in Figure B.1. It comprises several general standard checks independent of the type of sensor and a more site specific control model depending on the type of instrument (water level, flow or rainfall). The validation tool automatically diagnoses the quality of measurements (correct, uncertain and incorrect), if possible, by separately validating all measurements of one sensor. This data validation answers the following questions about the data to be used in this research:
- is the sensor working?
- are the measurements reliable?
- can the measurements be used for comparing measured and modelled system behaviour?
- can the measurements be used for calibration of the hydrodynamic model?
- which measurements have to be investigated in more detail?
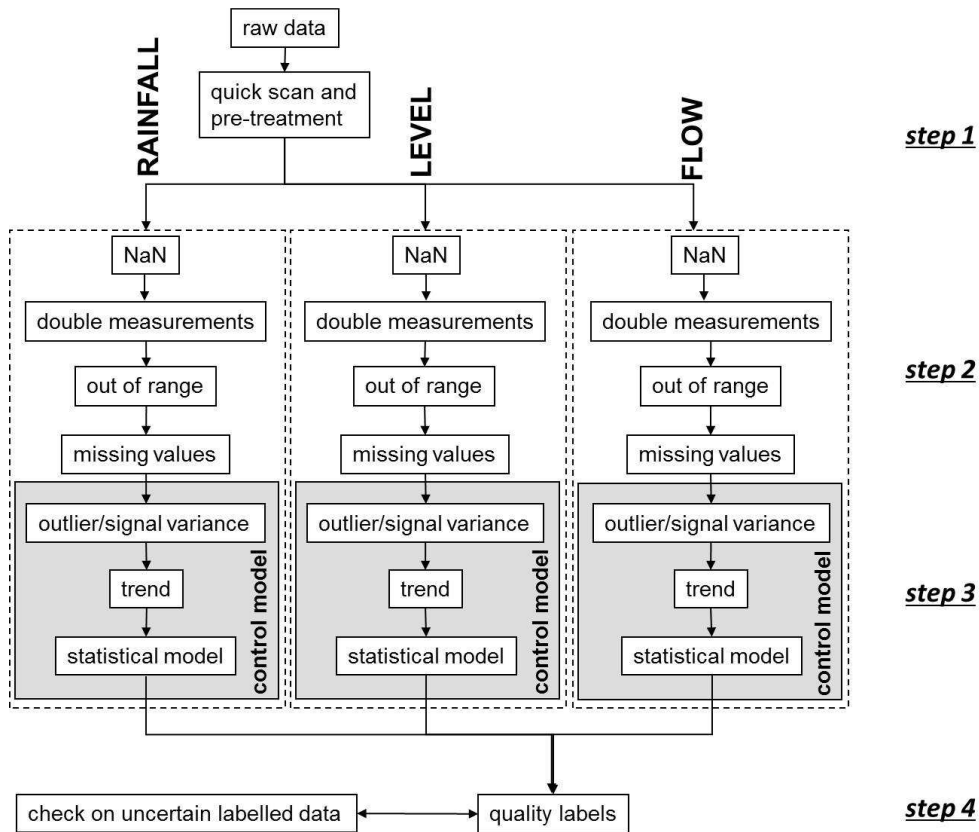
Figure B.1: Flow chart of validation procedure.

Prior to validation (see step 1 in Figure B.1), pre-treatment can be necessary, e.g. in case of a mismatch between measuring frequency and sampling time. This requires a synchronisation of intervals between subsequent measurements to, for example, 5 minutes. Another example of pre-treatment is filling gaps due to missing data. Both routines are based on interpolation. Level measurements are suitable for interpolation, because of their nearly continuous character. Furthermore, aggregation of data can be necessary because of low correlation between values at the original time scale. This often results from fast variations in process dynamics. For example the correlation between precipitation and water level is low at a sampling frequency of 5 minutes due to the time needed for run off. Aggregation to hourly values increases correlation. A disadvantage of aggregation is that measurements cannot be validated individually at the original time scale. However, it enables a more reliable assessment at a larger time scale.

B. Results of monitoring data quality assessment

Step 2 (Figure B.1) comprises several general standard checks (double measurements, out of range measurements, NaN and missing values) independent of the type of sensor. Double measurements are measurements that occur more than once in the data set with the same date and time labels but with a different observed value. Incorrect programming of readout software can cause such errors. Measurements exceeding the maximum and minimum limits of the sensor or the physical range (e.g. below manhole bottom) are labelled as out of range. Furthermore, the value is checked if it is a numeric value. Finally, missing values (e.g. because of incorrectly programmed sampling intervals, loss of data as a result from limited storage capacity in the data logger, problems with telemetry, loss of power supply or malfunctioning of equipment).

Depending on the type of instrument (water level, flow or rainfall), one or more statistical models are used to automatically diagnose the quality of measurements (see step 3 in Figure B.1). This site specific control model is based on the correlation between sensors. The control model consists of relatively simple regression models and the cluster of sensors is re-calibrated during each validation round using stepwise regression (Draper and Smith, 1981). The main advantage of this approach is that malfunctioning sensors are automatically left out. It results in a regression model in which the most significant parameters are included. If an already included location appears to be not significant enough, it is removed again. In the statistical model the time series are also checked for linear and sudden trends. Trends can be indicative of drift of the sensor as well of gradual changes in the system itself. Most classical trend tests, however cannot properly deal with signals with a large auto correlation and fast fluctuations of sewer processes. As a result, the applied trend test has to account for both aspects. A seasonal Kendall test with correction for covariance of the signal is most appropriate for detecting a linear trend (Hirsch and Slack, 1984; Dietz and Killeen, 2006). A step (sudden) trend can be detected by comparing local variance with the variance of the complete time series. When a cause for a detected trend is found, measurements are labelled as correct (e.g. because of the impact of reconstruction works on system performance). Otherwise, jumps in the measurements due to auto-calibration of the sensor results in the label 'sudden trend' because the measurements are unsuitable for further application.

The results of the control steps 1 to 3 are combined in an overall assessment of the measurement values. A quality label (correct, uncertain and incorrect) is attached to each individual measurement (see step 4 in Figure B.1). The incorrect labels are made more specific (e.g. linear trend, sudden trend, outlier, no signal variance, double measurement, NaN or out of range) when possible. In order to prevent erroneous labelling of measurements, e.g. due to construction works in the sewer system, consultation of the sewer manager or other people with relevant knowledge on how the system is functioning is needed. Those measurements are labelled as uncertain and further investigation is required, because no possible cause is found for those measurements.

Legend
- Correct data
- Linear trend
- Outlier
- No signal variance
- Out of range
- Sudden trend
- Double measurement
- Uncertain data
- NaN
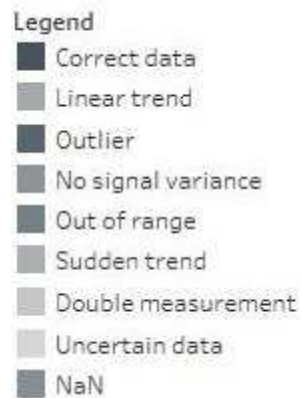
Figure B.2:   Legend results of automatic data quality assessment sensors as shown in the Tables B.1 to B.6.

B. Results of monitoring data quality assessment

Table B.1: Results of automatic data quality assessment sensors in 2010. Correct data (dark grey), data gaps (white) and anomalous data (lighter grey). The legend is shown in Figure B.2.
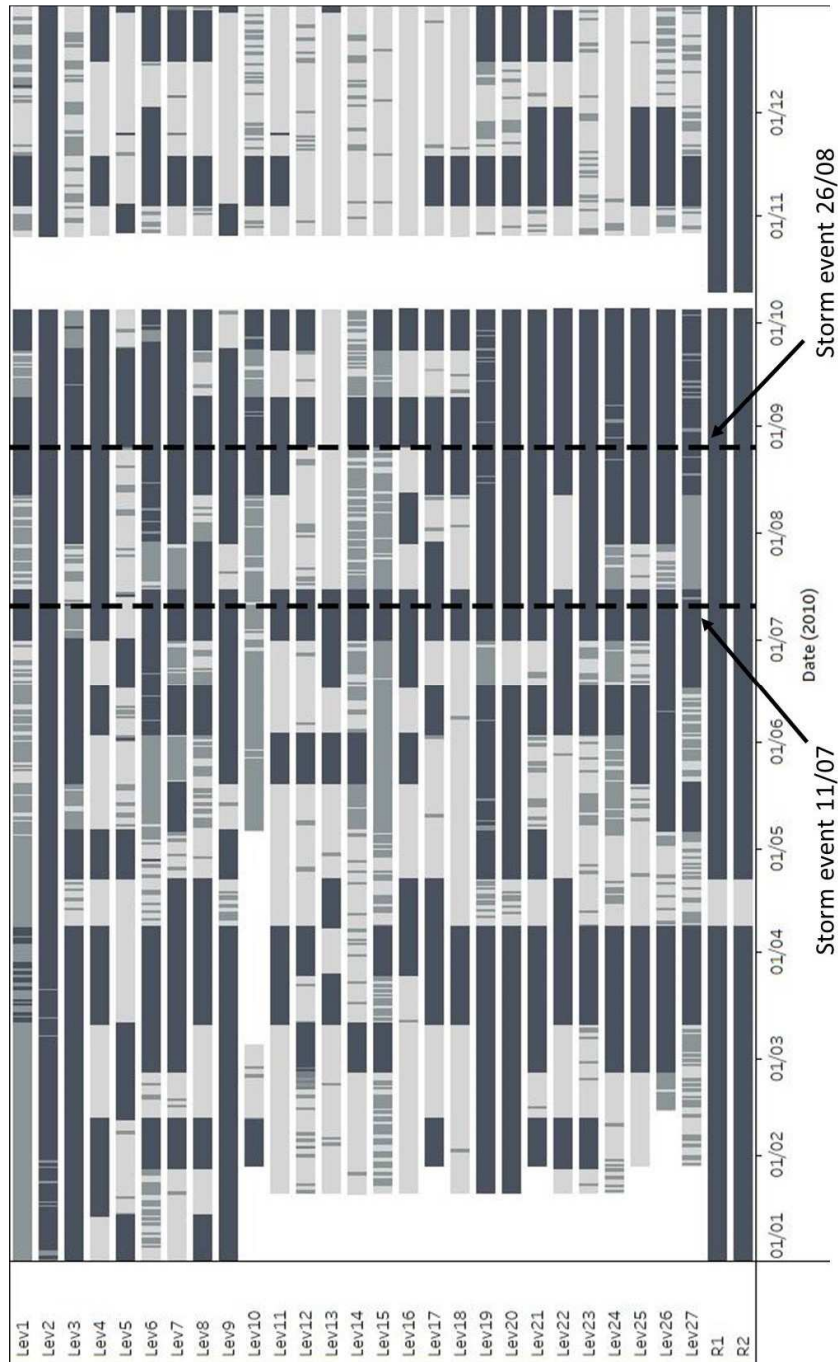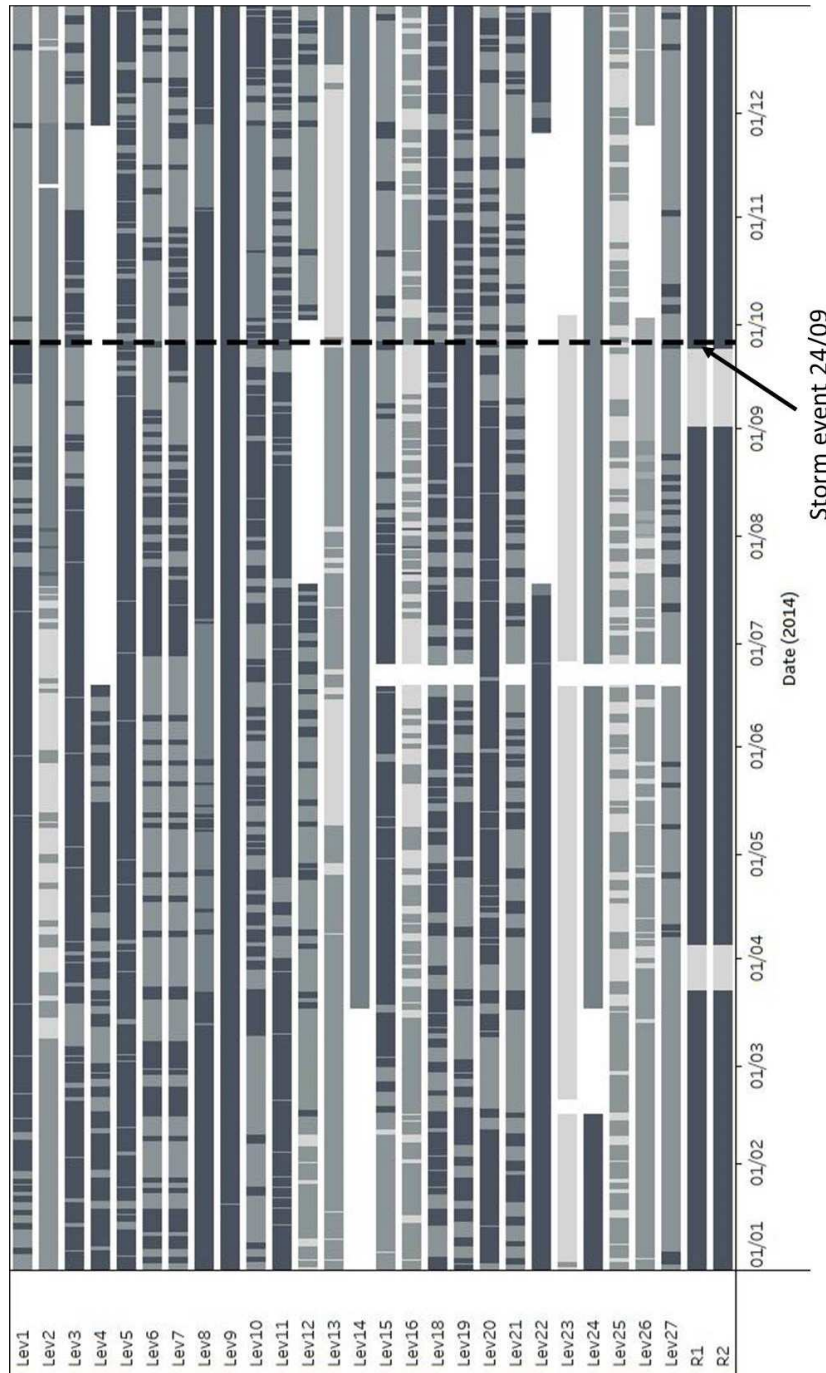
Table B.2: Results of automatic data quality assessment sensors in 2011. Correct data (dark grey), data gaps (white) and anomalous data (lighter grey). The legend is shown in Figure B.2.

156
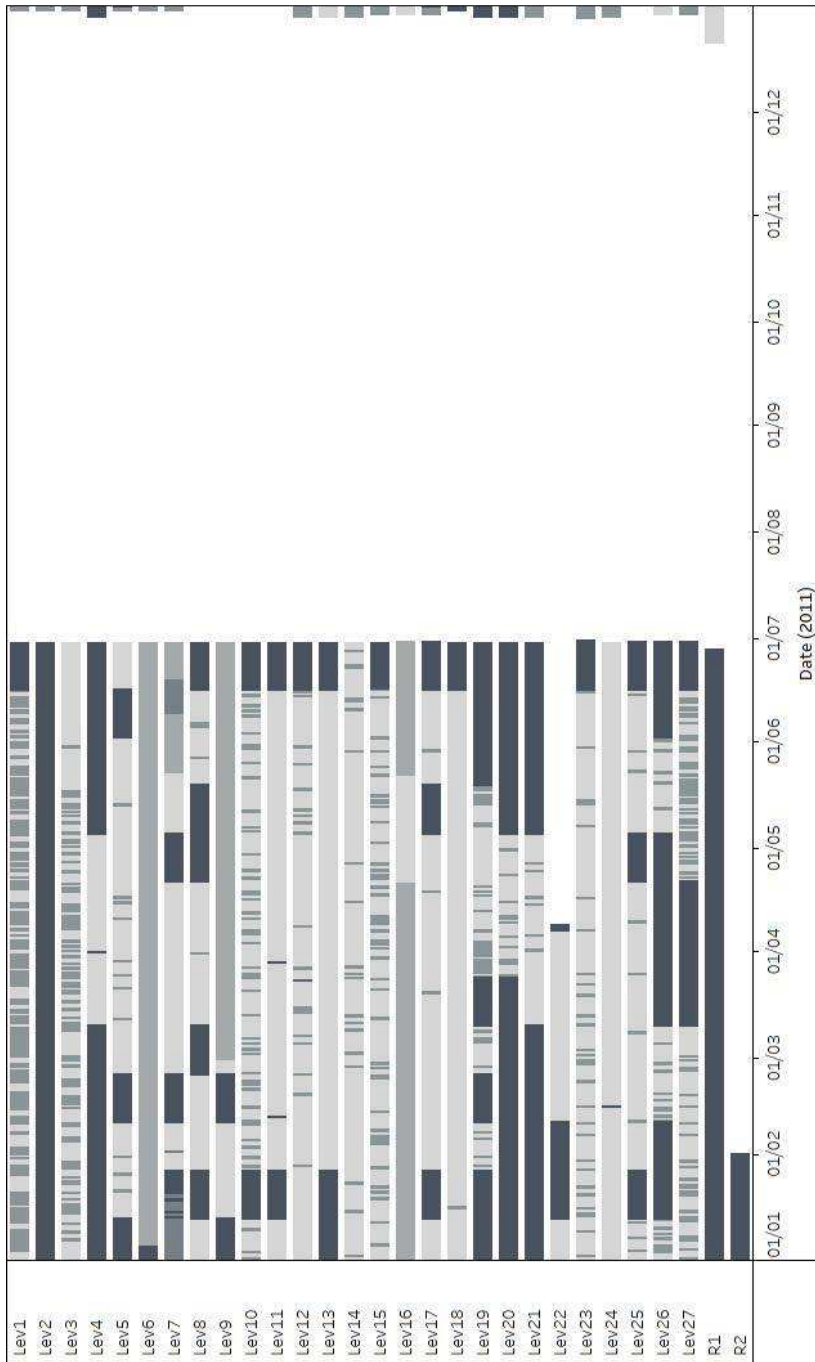
B. Results of monitoring data quality assessment

Table B.3: Results of automatic data quality assessment sensors in 2012. Correct data (dark grey), data gaps (white) and anomalous data (lighter grey). The legend is shown in Figure B.2.
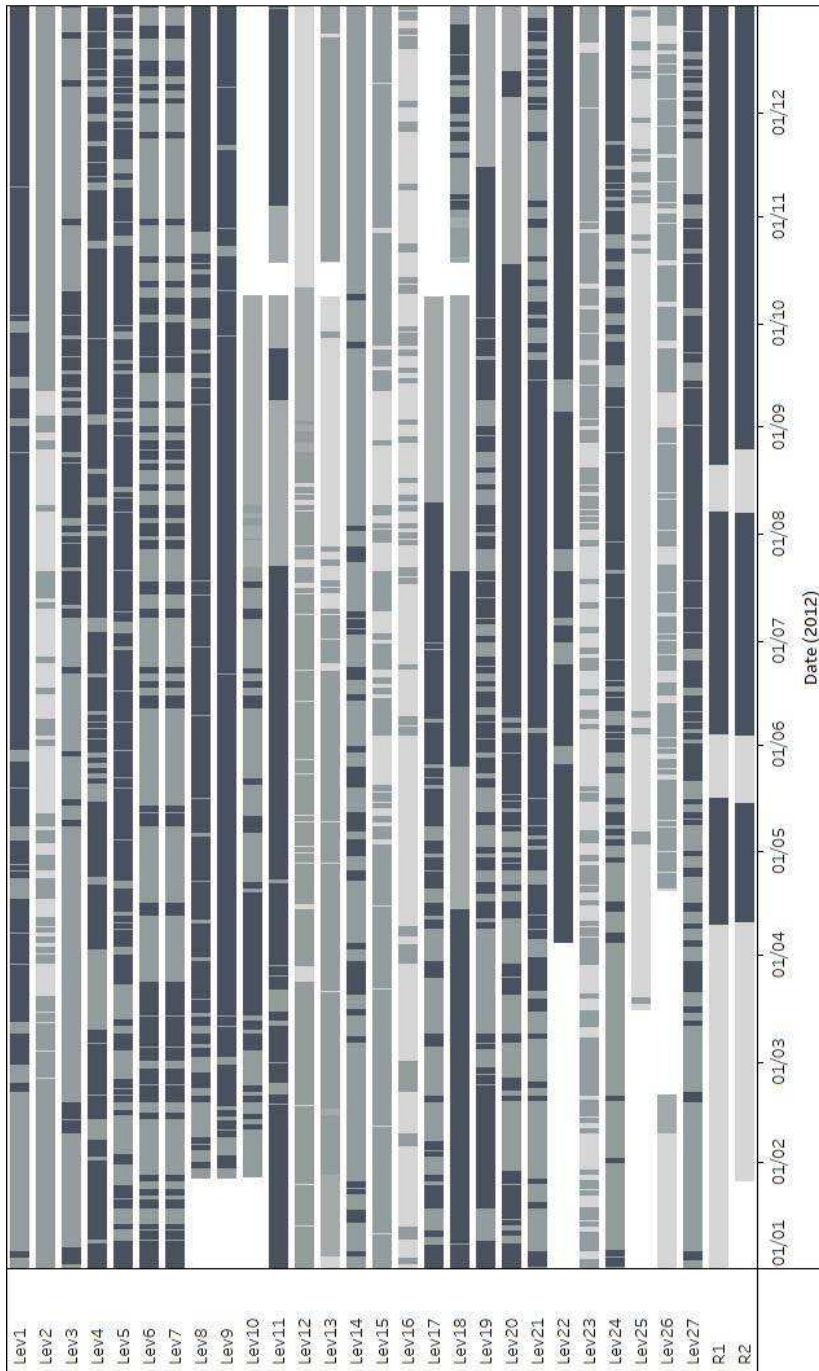
Table B.4: Results of automatic data quality assessment sensors in 2013. Correct data (dark grey), data gaps (white) and anomalous data (lighter grey). The legend is shown in Figure B.2.
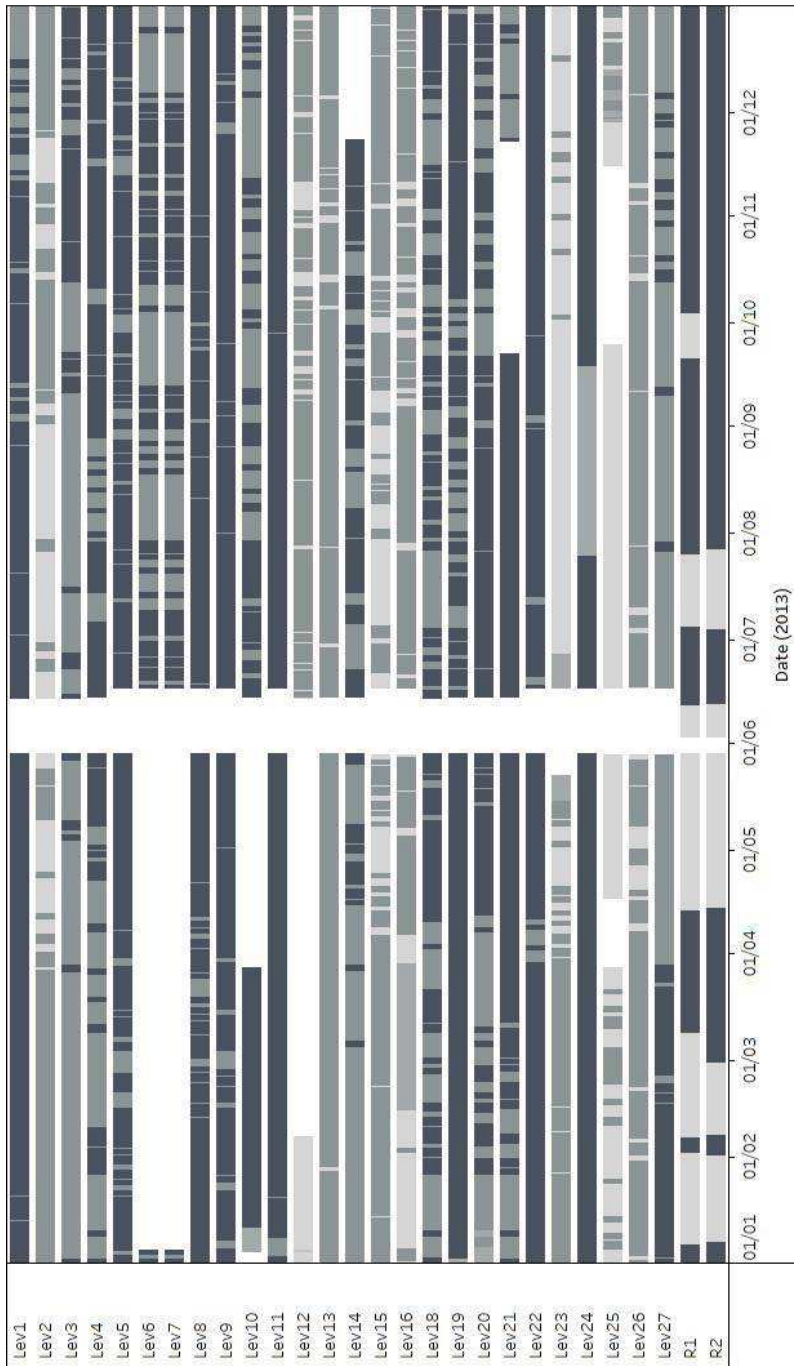
B. Results of monitoring data quality assessment

Table B.5: Results of automatic data quality assessment sensors in 2014. Correct data (dark grey), data gaps (white) and anomalous data (lighter grey). The legend is shown in Figure B.2.

159

Table B.6: Results of automatic data quality assessment sensors in 2015. Correct data (dark grey), data gaps (white) and anomalous data (lighter grey). The legend is shown in Figure B.2.

160
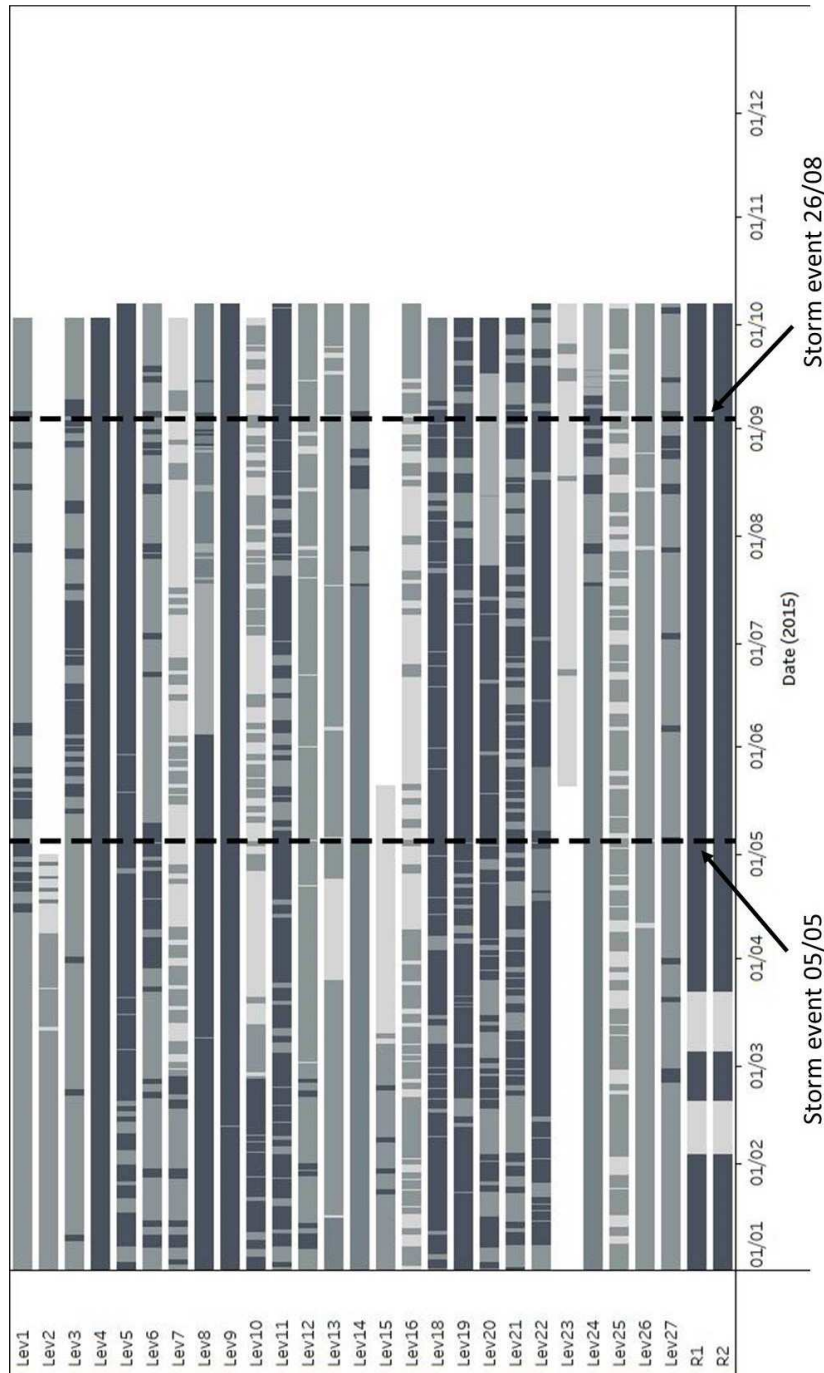
C Comparison between simulated and measured system behaviour

This appendix addresses a comparison of simulated and measured system behaviour in the 'Tuindorp' sewer system) accounting for in-sewer defects. The 'Tuindorp' sewer system is described in section 1.6 of this thesis. First, the applied methodology for the analysis of system behaviour is described. Additional to the available monitoring data, information from the complaint register has been used for comparing simulated and measured behaviour. Subsequently, the results of the analysis are presented. Finally, the impact of in-sewer defects on system performance is illustrated and some practical aspects are highlighted.

This part of the research focuses on a more detailed comparison of monitoring and model results. Both during different storm events and at two different monitoring locations in the catchment area in order to further enlarge knowledge on system behaviour. The results of this comparison are used as input to find out if it is possible to obtain a "hydraulic fingerprint" of a clean sewer system as a measure for the necessity of maintenance, based on hydraulic monitoring (see chapter 3). To this end, the 'Tuindorp' system was monitored during a period of 1 year to obtain the hydraulic characteristics with known defects in the system. After that system has been cleaned and is being monitored to obtain a calibrated model of the clean system that can function as a reference as described in chapter 3.

Methodology

Research catchment

In this research, the 'Tuindorp' sewer system (Utrecht, the Netherlands) is studied. The characteristics of this catchment area are summarised in Table 1.1 in section 1.6 of this thesis. The layout of the sewer system is presented in Figure 1.6.

Analysis of system behaviour

The analysis of simulated and measured behaviour of the 'Tuindorp' sewer system catchment regarding pluvial flooding comprises the following steps:

- Selection of characteristic storm events. Two storm events have been selected accounting for both total rainfall volume of the event and number of reported incidents in the catchment area during the event.
- Calculation of system behaviour for the selected storm events. Simulations have been performed with a detailed InfoWorks© model. The model has been validated as described in Van Mameren and Clemens (1997) and Clemens (2001a).
- Validation of monitoring data. Prior to the analysis of system behaviour, inconsistencies, errors and outliers have been removed from the monitoring data. The validation algorithms are described in Van Bijnen and Korving (2008) and in section 1.7 of this thesis.
- Comparison of simulated and observed system behaviour. For two locations where defects were observed, simulated and observed water levels in the sewer system around these locations have been compared.

Field observations in-sewer defects

In order to collect information on in-sewer defects, visual inspections (CCTV, closed circuit television) were carried out in the sewer system. The observations were recorded using a uniform classification system (NEN-EN 13508-2, 2003; NEN 3399, 2004). In total, 28% (7.6 km) of the system has been inspected. Approximately 34% of inspected conduits showed in-sewer defects. Figure 1.6 in chapter 1 of this thesis presents an overview of the inspected conduits (bold lines). In Figure C.1 observed defects, including root intrusion, surface damage, other obstacles and attached and settled deposits are shown.
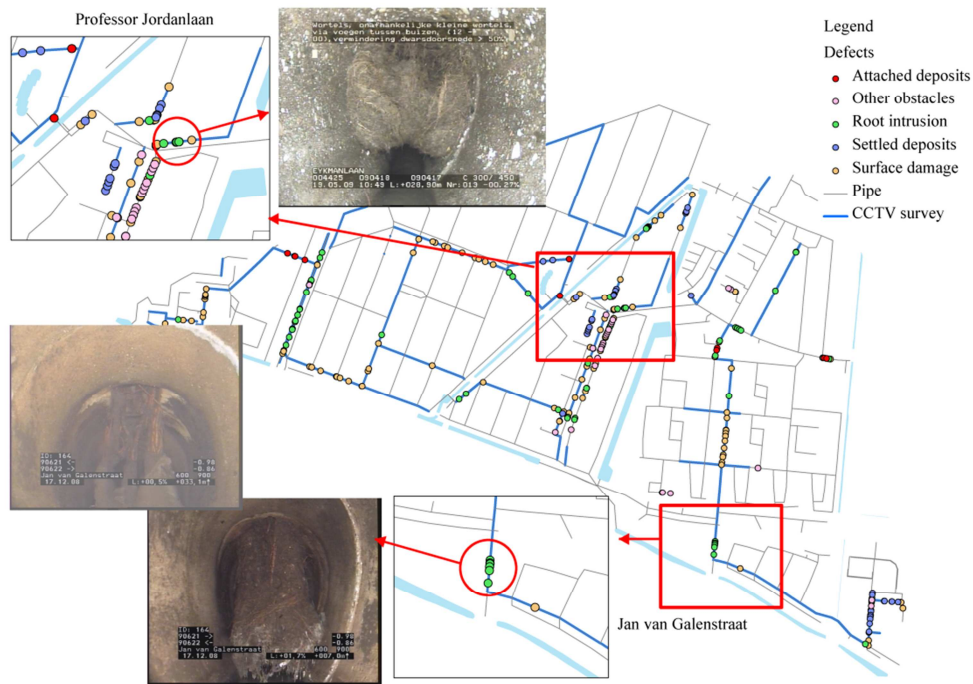
Figure C.1: Observed defects 'Tuindorp' sewer catchment.

The analysis of simulated and measured behaviour focuses on two locations with defect 'root intrusion' (code BBA according to NEN-EN 13508-2, 2003). The defects were classified as class 5 (most severe). The locations are situated in the south and centre of the 'Tuindorp' catchment (see pictures in Figure C.1).

Measurement data

A monitoring network (32 sensors) has been installed to obtain data on the hydraulic performance of the sewer system and understand the impact of in-sewer defects on hydrodynamic system behaviour. Flows (F1), water levels (Lev1, Lev2,…, Lev27) and rainfall (R1 and R2) are monitored at several locations in the catchment area (Figure 1.6 in section 1.6). Network design is based on a combination of hydraulic simulations, reported incidents and observed in-sewer defects. For example, several water level sensors are installed in the manholes just upstream and downstream of an observed defect. Two tipping bucket rain gauges (R1 and R2) have been used to measure rainfall in the 'Tuindorp' catchment.

In order to ensure high data quality and enable condition based maintenance of sensors, monitoring data have been validated using automatic algorithms as described in Van Bijnen and Korving (2008). These (statistical) tools account for outliers, (linear) trend, signal variance and spatial correlations. Depending on the type of instrument (water level, flow or rainfall), a combination of algorithms is used to determine whether a measurement is correct. The validation tool automatically diagnoses the quality of measurements ('correct', 'uncertain' and 'incorrect'), if possible, by validating individual measurements of each sensor. The results of the data quality assessment are presented in appendix B.

Hydraulic simulations

Simulations have been performed with a detailed InfoWorks© model of the sewer system. The model has been validated to eliminate systematic errors in the model according to the method described by Van Mameren and Clemens (1997) and Clemens (2001a). This implies that structural and geometrical data, ground levels, etc. are verified in the field. In addition, a comparison has been made between reported incidents and locations where the hydraulic model predicts flooding.

Two recorded storm events (10/07/2010 and 25/08/2010) have been studied with respect to impacts of observed in-sewer defects on water levels in the sewer system (Table C.1). The first storm event represents a short but heavy storm, the second event a storm with low rainfall intensities and relatively long duration. These events have been chosen because afterwards flooding at a number of locations was reported to the call centre by several residents. Only the first event (10/07/2010) also caused flooding in the model simulation.

Table C.1:   Observed storm events.

date	rain depth R1 (mm)	rain depth R2 (mm)	flooding in model simulation	reported flooding in catchment
10/07/2010-11/07/2010	32.2	33.0	Yes	yes
25/08/2010-27/08/2010	66.0	60.0	No	yes

Results and discussion

For the two storm events in Table C.1, simulated and measured hydraulic performance have been compared at two locations close to observed defects (Figure C.1): Jan van Galenstraat and Professor Jordanlaan. At the first location, Jan van Galenstraat, root intrusion (class 5) at two locations in the same sewer pipe has been observed. At the second location, Professor Jordanlaan, at one location root intrusion (class 5) has been observed.

Location Jan van Galenstraat

Around the root intrusion at the Jan van Galenstraat, 4 water level sensors are analysed. The locations include Lev16, Lev25, Lev26 and Lev27 (see Figure C.1 and Figure 1.6 in section 1.6). The observed root intrusions are located between Lev26 and Lev27. The reference levels of these sensors are -0.52 m AD and -0.58 m AD respectively, and the levels of the pipe bottom are -0.86 m AD and -0.98 m AD respectively. The other two sensors (Lev16 and Lev25) are located more upstream in the system.

Figure C.2 presents the comparison of measured and modelled water levels at these locations during the storm event of 10/07/2010. The figure shows that measured levels are substantially lower than modelled levels. This indicates that the inflow of rainfall in the sewer system is smaller than expected. Probably, the contributing area of the sewer system is smaller. In addition, the inflow of rainfall is faster in reality as is shown by the earlier arrival of the peaks at the different locations. These differences relate to the rainfall runoff model and will most probably be reduced when calibrating the model.

The impact of the root intrusion is expressed in the much larger difference between the measured water level at Lev26 (upstream of defect) and Lev27 (downstream of defect) in the monitoring data compared to the model results. This difference is present in the first as well as the second peak. This also holds for the difference between Lev16 and Lev25 which can be an indication of an obstruction in the connecting sewers. However, this sewer was not inspected.
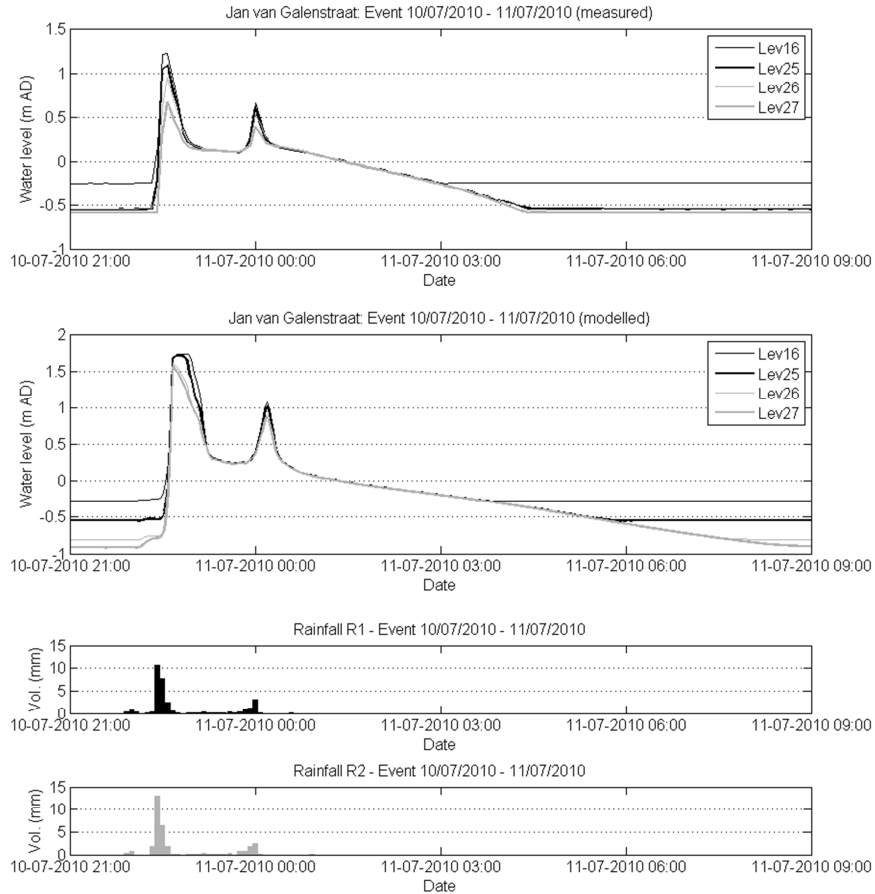
165

Figure C.2: Jan van Galenstraat measured and modelled water levels during event 10/07/2010.

The storm event of 25/08/2010 also causes higher calculated than measured water levels (Figure C.3). Again, the impact of the root intrusion on the water level difference upstream and downstream of the defect is clearly visible. The second peak (26/08/2010 15:00), however, does not enlarge the water level difference between Lev26 and Lev27. Figure C.4 (top right) shows that the hydraulic impact of the root intrusion starts at approximately 0.15 m AD. This level is not reached during the second peak of this storm event. Consequently, the root intrusion has no impact on the water level in the second peak.
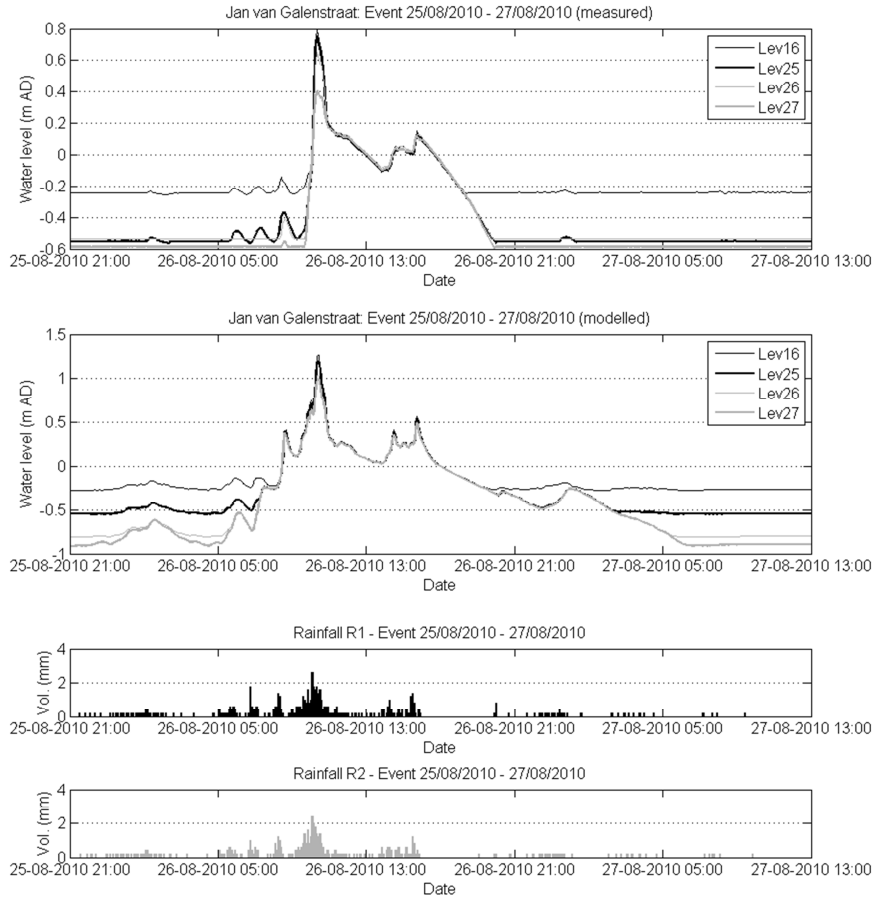
Figure C.3:   Jan van Galenstraat measured and modelled water levels during event 25/08/2010.

The level of approx. 0.15 m AD at which the difference between the water levels upstream and downstream of the defect increases substantially (Figure C.4 (top left and right)), is slightly higher than the pipe soffit (-0.86 m AD + 900 mm pipe height). Overall the increase in water level difference is up to 15 times larger in the monitoring data compared to the model calculations. The impact of the short but heavy storm event on 10/07/2010 is comparable to the longer storm event with lower intensities on 25/08/2010. At the start of one of the two storm events, there is no additional backwater effect due to the roots.

The water level differences around the reference levels of Lev26 (-0.52 m AD) can be explained from the difference between the reference levels of Lev 26 and Lev 27. This difference is 6 cm. Both reference levels are above the maximum water level during dry weather flow (DWF). When the water level starts rising, the sensor at Lev26 is immersed earlier than the sensor at Lev27. This causes a substantial water level difference at low upstream water levels. The largest water level difference occurs at the beginning of the largest peaks.
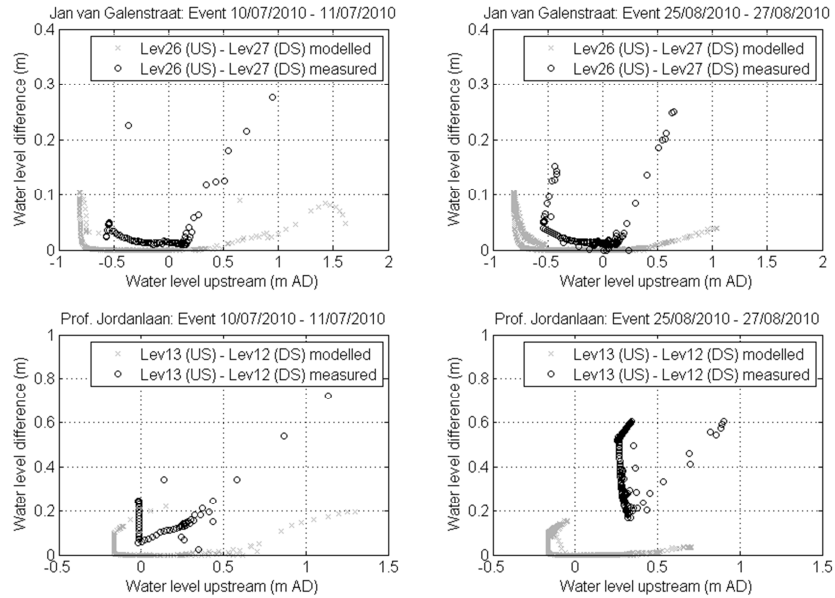
Figure C.4:   Water level difference between manholes just upstream (US) and downstream (DS) of the defect root intrusion.

Analysis has shown that sensor Lev26 suffers from an offset error of 2-4 cm depending on the storm event. In between the events, the sensor has been removed from the manhole for cleaning. This resulted in a slightly different height of the sensor head. However, this offset error does not affect our conclusion because the increase in water level difference is at least 6 times larger than the error.

Location Professor Jordanlaan

At the other location with observed root intrusion, Professor Jordanlaan, 5 water level sensors are part of the analysis. The locations include Lev11, Lev12, Lev13, Lev14 and Lev22 (see Figure C.1 and Figure 1.6 in section 1.6). The observed roots are located in the pipe between Lev12 and Lev13. The reference levels of these sensors are -0.24 m AD and +0.00 m AD respectively. The levels of the pipe bottom are -0.31 m AD and -0.19 m AD respectively. Sensor Lev14 is located more upstream in the sewer system and the other two sensors (Lev11 and Lev22) are located more downstream in the system.

In Figure C.5 measured and modelled water levels during the storm event of 10/07/2010 are compared. The figure shows that, except for the first peak at Lev13, measured levels are substantially lower than modelled. Again this indicates that the inflow of rainfall in the sewer system is smaller than expected. In addition, the inflow of rainfall is faster in reality as is shown by the earlier arrival of the peaks at the different locations. This corresponds with location Jan van Galenstraat.

In general, the impact of the root intrusion at the Professor Jordanlaan is larger than at the Jan van Galenstraat. Due to the root intrusion the difference between the water level at Lev13 (upstream of defect) and Lev12 (downstream of defect) in the monitoring data is much larger compared to the model results. This difference is present in the first as well as the second peak. Compared to the model results, in reality the water flows in the opposite direction: from Lev13 to Lev 14 and then to Lev11 (Figure C.5). This directly results from the obstruction due to the roots. In case of a branched sewer system this would probably led to flooding much earlier in reality.
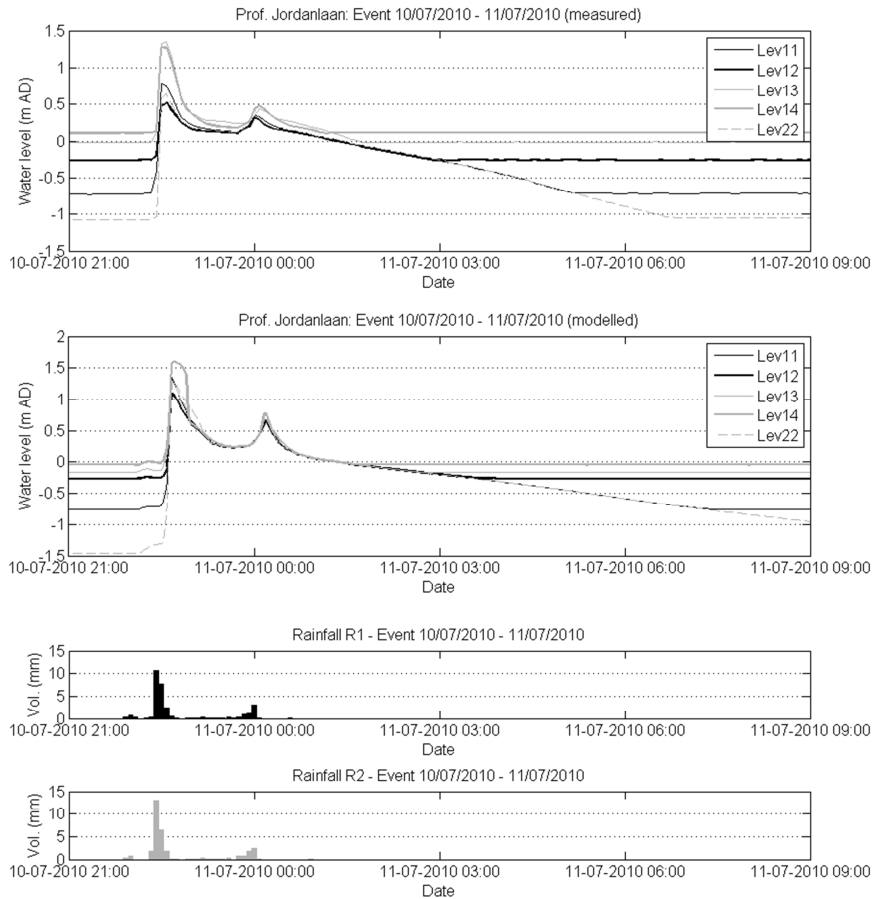
Figure C.5: Professor Jordanlaan measured and modelled water levels during event 10/07/2010.

The impact of the storm event of 25/08/2010 is different from the previous one (Figure C.6). At the beginning of the event, the measured water level at Lev13 is substantially larger than the initial water level of the 10/07/2010 event. This is most probably caused by dirt that sticks to the roots in the sewer and obstructs the hole at the pipe bottom resulting in increased backwater (see Figure C.1, top). The obstruction is only temporary, since the initial water level returns to its lower level during later storm events. During the event the system behaviour is as follows. The measured water levels at Lev14 and Lev13 are higher than the model results, at the other locations the measured levels are lower. Note that the sensor at location Lev13 also suffers from an offset error of approximately 1.5 cm. Similar to the 10/07/2010 event, the flow direction switches to the opposite direction.
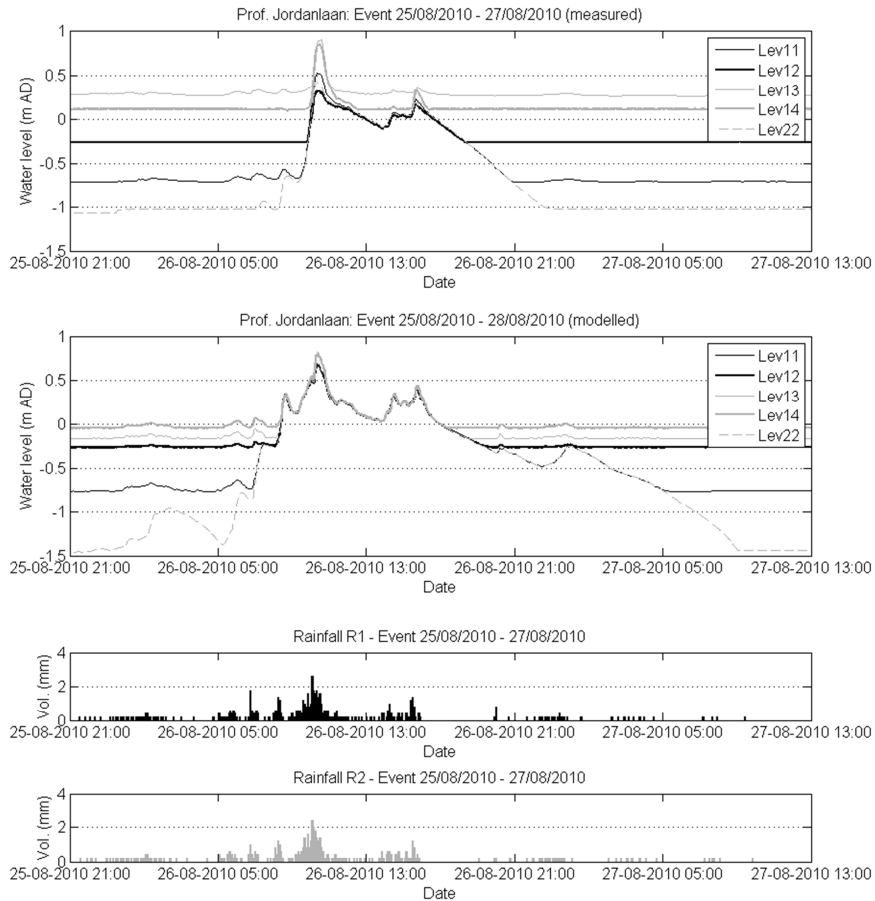
Figure C.6:   Professor Jordanlaan measured and modelled water levels during event 25/08/2010.

Figure C.4 (bottom left and right) shows that during both storm events the difference between the water levels upstream and downstream of the defect increases substantially when the upstream level becomes a bit higher than the pipe soffit (-0.19 m AD + 450 mm pipe height). The higher upstream water level at the start of the 25/08/2010 event can be recognised in Figure C.4 (bottom right). Overall the increase in water level differences is up to 20 times larger in the monitoring data compared to the model results. The explanation of the shape of the curves is comparable to the location Jan van Galenstraat.

The head loss initiated by the roots has been quantified using the measuring data. An example of this is shown in Figure C.7 for the location Professor Jordanlaan. This figure presents head loss as a function of upstream water level,

$$\Delta H = 0.60495 H^{1.1926} \quad \text{for } H > 0.20\text{m} \tag{C.1}$$

This suggests that root intrusions in branched sewer systems can be modelled as an orifice. A difficulty encountered here is that calibration for different storm events leads to different parameter values in this function. This is an indication that the geometry of the obstacle changes over time. Overall, this knowledge can be used to better quantify the impact of root intrusion on hydraulic behaviour of sewer systems.
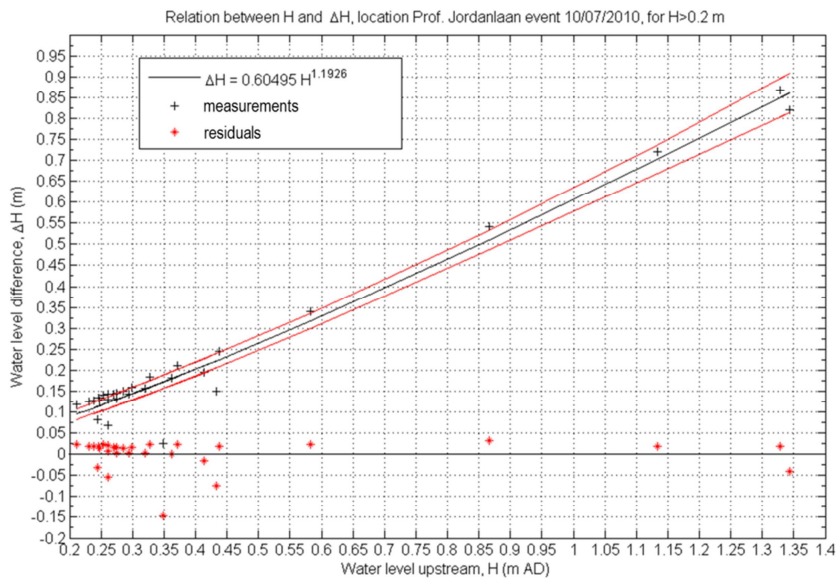

Figure C.7: Relation between water level H and head loss ΔH initiated by the observed root intrusion, location Professor Jordanlaan. Event 10/07/2010.

Conclusions

The objective of this appendix is to describe the impact of in-sewer defects on sewer system behaviour and to compare simulated and measured system behaviour in the 'Tuindorp' sewer system (Utrecht, the Netherlands) accounting for in-sewer defects. Performance has been assessed using hydraulic models, customer complaints, monitoring data and CCTV inspections.

The comparison of simulated and observed system behaviour at two locations in the sewer system where root intrusions have been observed during inspection shows that:

- Root intrusions substantially enlarge the difference between the water levels upstream and downstream of the defects in reality compared to model results.
- In reality, the water levels start rising much faster than in the model calculations above a certain offset level which is approximately at the soffit level of the pipe in the manhole upstream of the defect.
- The increase in water level differences due to the defects is up to 15-20 times larger in the monitoring data compared to the model calculations, this discrepancy is probably due to the fact that the exact hydraulic characteristic of the root intrusions found are unknown and prove hard to be caught in a model.

Specifically, at location Professor Jordanlaan the following conclusions can be drawn:

- The flow direction changes due to root intrusion. The impact of such a defect would have been much larger in a branched instead of a looped system, in branched systems reversal of flow is not possible without direct causing flooding.
- The initial backwater effect upstream of the defect differs between the two storm events. This probably results from dirt that sticks to the roots and obstructs the hole at the pipe bottom (see Figure C.1, top).

In general, the results show that monitoring data provide key information on the behaviour of a sewer system which suffers from defects such as root intrusions. Consequently, it is very useful for determining the necessary sewer management. In addition, this knowledge on system behaviour is used as input for the research in chapter 3 of this thesis.

List of publications

Peer-reviewed journals

Van Bijnen, M., Korving, J.L., and Clemens, F.H.L.R. (2012). Impact of sewer condition on urban flooding: an uncertainty analysis based on field observations and Monte Carlo simulations on full hydrodynamic models. *Water Science and Technology*, 65(12): 2219-2227, http://dx.doi.org/10.2166/wst.2012.134.

Van Bijnen, M., Korving, J.L., Langeveld, J.G., and Clemens, F.H.L.R. (2016). Calibration of hydrodynamic model-driven sewer maintenance. *Structure and Infrastructure Engineering*, 13(9): 1167-1185. http://dx.doi.org/10.1080/15732479.2016.1247287.

Meijer, D., Van Bijnen, M., Langeveld, J., Korving, H., Post, P., Clemens, F. (2018) Identifying Critical Elements in Sewer Networks Using Graph-Theory. *Water*, 10(2), 136, doi:10.3390/w10020136.

Van Bijnen, M., Korving, J.L., Langeveld, J.G., and Clemens, F.H.L.R. (2018). Quantitative assessment of impacts of sewer condition on health risk. Water, 10(3), 245, doi:10.3390/w10030245.

Conference papers

Van Bijnen, M. and Korving, H. (2008). Application and results of automatic validation of sewer monitoring data. In: *Proceedings of 11th International Conference on Urban Drainage*. Edinburgh, Scotland, UK.

Van Bijnen, M., Korving, H., and Clemens F. (2011). Impact of sewer condition on urban flooding: a sensitivity analysis based on Monte Carlo simulations on full hydrodynamic models. In: *Proceedings 12th International Conference on Urban Drainage*. Porto Alegre, Brazil.

Van Bijnen, M., Korving, H., and Clemens F. (2012). Impact of sewer condition on urban flooding: a comparison between simulated and measured system behaviour. In: *Proceedings of 12th International Conference on Urban Drainage*. Belgrade, Serbia.

National publications

Van Bijnen, M. (2002). Gemeente Bergeijk "per spoor" naar inzicht in rioolstelsel. *Vakblad Riolering*, 9(4): 25-27.

Van Bijnen, M. (2005). Meten in de riolering. Wat komt er op mijn pad? *Vakblad Riolering*, 12(8/9): 43-47.

Van Bijnen, M. en Moens, M. (2005). Gemeente Utrecht meet werking van riooloverstorten. *Land + Water*, 45(9): 20-21.

Korving, H. en Van Bijnen, M. (2007). Datavalidatie als onderdeel van een goed en effectief rioleringsbeheer. *Rioleringswetenschap*, 7(28): 15-29.

Henckens, G., Bos, R., Van Bijnen, M., en Meijer, D. (2008). Meten in de riolering (deel 1). Van aanleiding naar meetprogramma. *Vakblad Riolering*, 15(1): 19-20.

Henckens, G., Van Bijnen, M., Bos, R., en Meijer, D. (2008). Meten in de riolering (deel 2). Van meetplan naar bestek. *Vakblad Riolering*, 15(2): 18-19.

Meijer, D., Van Bijnen, M., Bos, R., en Henckens, G. (2008). Meten in de riolering (deel 3). Van bestek naar uitvoering. *Vakblad Riolering*, 15(3): 18-19.

Meijer, D., Bos, R., Van Bijnen, M., en Henckens, G. (2008). Meten in de riolering (deel 4). Van uitvoering naar bruikbare data. *Vakblad Riolering*, 15(4): 11-13.

Meijer, D., Van Bijnen, M., Bos, R., en Henckens, G. (2008). Meten in de riolering (deel 5). Van data naar informatie. *Vakblad Riolering*, 15(5): 11-13.

Van Bijnen, M. (2010). Utrecht richt aandacht op validatie meetgegevens. *Land + Water*, 50(9/10).

Van Bijnen, M., Korving, H., en Clemens F. (2011). Invloed toestand van de riolering op 'water op straat': een onzekerheidsanalyse gebaseerd op praktijkwaarnemingen en Monte Carlo simulatie met een hydrodynamisch model. *WT-Afvalwater*,12(2): 155-165.

Korving, H., Admiraal, N., Veurink, J., en Van Bijnen, M. (2012). Rioolvreemd water efficiënt opsporen en effectief aanpakken. *H2O*, 2: 35-37.

Vleeshouwers, K., Venderbos, J., Paredis, E., en Van Bijnen, M. (2016). Uitwerking hemelwaterzorgplicht gemeente Cranendonck. *Vakblad Riolering*, 23(3).

About the author

Marco van Bijnen was born on 8 October 1970 in Drunen, the Netherlands. He followed his secondary education (MAVO) at "De Bolster" in Vlijmen. After receiving his diploma, he followed an additional secondary education (HAVO) at "d'Oultremontcollege" in Drunen. Marco started the study Civil Engineering at the HTS 's-Hertogenbosch in 1989 and received his B.Sc degree in 1993. After his graduation, Marco joined the Dutch army for nine months for his military service. During the period of May 1994 - December 1999 he was employed at Oranjewoud in Oosterhout, specialising in hydraulic modelling of sewer systems. In January 2000 he started working at ARCADIS consultancy company in 's-Hertogenbosch. At ARCADIS, he focussed on the field of sewer monitoring networks. From November 2002 until January 2015, Marco was employed at the municipality of Utrecht (the Netherlands) as an advisor on urban drainage. In 2008, next to his full-time job, he started as a PhD candidate at Delft University of Technology in the section Sanitary Engineering. The research focussed on the impact of sewer condition on the performance of sewer systems. From January 2015 until January 2016 Marco was employed at TU Delft as a full time PhD student. Since January 2015 Marco has been an independent consultant in the field of urban drainage at M. van Bijnen Advies.